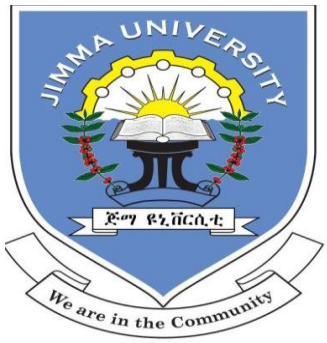

JIMMA UNIVERSITY

SCHOOL OF GRADUATE STUDIES

JIMMA INSTITUTE OF TECHNOLOGY

FACULTY OF CIVIL AND ENVIRONMENTAL ENGINEERING

HIGHWAY ENGINEERING STREAM

SIMULATION ON FLEXIBLE PAVEMENT USING BAGASSE ASHE WITH LIME AS A WEAK SUBGRADE STABLIZER (CASE STUDY ON JIMMA TOWN)

A thesis submitted to the School of Graduate Studies of Jimma University in Partial Fulfillment of the Requirements for the Degree of Master of Science in Civil Engineering (Highway Engineering Stream)

By:

Shimelis Agito

November, 2019

Jimma, Ethiopia

JIMMA UNIVERSITY

SCHOOL OF GRADUATE STUDIES

JIMMA INSTITUTE OF TECHNOLOGY

FACULTY OF CIVIL AND ENVIRONMENTAL ENGINEERING

HIGHWAY ENGINEERING STREAM

SIMULATION ON FLEXIBLE PAVEMENT USING BAGASSE ASHE WITH LIME AS A WEAK SUBGRADE STABLIZER (CASE STUDY ON JIMMA TOWN)

A thesis submitted to the school of Graduate Studies of Jimma University in Partial Fulfillment of the Requirements for the Degree of Master of Science in Civil Engineering (Highway Engineering)

By:

Shimelis Agito

Advisor: Eng'r Elmer C. Agon, Asso.Prof

Co-adviser: Eng'r. Mesfin Dinku (MSc.)

November, 2019

Jimma Ethiopia

Jimma University

Jimma Institute of Technology

School of Post Graduate Studies

Faculty of Civil and Environmental Engineering

Highway Engineering Stream

SIMULATION ON FLEXIBLE PAVEMENT USING BAGASSE ASHE WITH LIME AS A WEAK SUBGRADE STABLIZER (CASE STUDY ON JIMMA TOWN) (CASE STUDY ON JIMMA TOWN)

By

Shimelis Agito

APPROVED BY BOARD OF EXAMINERS

1.	_____	_____	____/_____/____
	External Examiner	Signature	Date
2.	_____	_____	____/_____/____
	Internal Examiner	Signature	Date
3.	_____	_____	____/_____/____
	Chairman of Examiner	Signature	Date
4.	Engr. Elmer C. Agon, Asso. Prof	_____	____/_____/____
	Main Advisor	Signature	Date
5.	Engr. Mesfin Dinku (MSc)	_____	____/_____/____
	Co - Advisor	Signature	Date

DECLARATION

I, the undersigned, declare that this thesis entitled "Simulation on Flexible Pavement Using Bagasse Ashes with lime as a Weak Subgrade Stabilizer." is my original work, and has not been presented by any other person for an award of a degree in this or any other University, and all sources of material used for theses have been duly acknowledged.

Candidate:

Shimelis Agito

Signature_____

As Master research Advisors, we hereby certify that we have read and evaluated this MSc research prepared under our guidance, by **Shimelis Agito** entitled: Simulation on Flexible Pavement Using Bagasse Ashes with lime as a Weak Subgrade Stabilizer

We recommend that it can be submitted as fulfilling the MSc Thesis requirements

Eng'r Elmer C. Agon, Asso.prof	_____	_____
Main Advisor	Signature	Date
Engr. Mesfin Dinku (MSc).	_____	____/_____/____
Co - Advisor	Signature	Date

ACKNOWLEDGEMENT

Firstly, with a grateful heart, I give thanks to ALMIGHTY GOD for HIS love, grace, strength, wisdom, knowledge and understanding. I thank HIM for always being by my side. Without HIM, the completion of this thesis study would not have been possible.

My deepest gratitude goes to my advisor, **Engr. Elmer C. Agon (Asso. Prof)**. I appreciate you for his continuous Support, encouragement and guidance during this term thesis. Furthermore, my gratitude also goes to Engr. **Mesfin Dinku (MSc)** for his guidance and great effort on showing the directions of the term thesis and on sharing his idea on different problems.

Mores so, my deepest appreciation goes to Jimma highway laboratory assistances to their limitless support and guidance to conducting all the necessary laboratory tests.,

Finally, my last but not least appreciation goes to Jimma University, School of Graduate Studies, Jimma Institute of Technology, Civil Engineering Department, and Highway Engineering Stream.

ABSTRACT

The poor performance of flexible pavements results from the use of poor-quality materials, inappropriate stabilization It may have swell and shrinkage distinctiveness and causes significant damage to pavement structures. Expansive clay soil is available in different parts of Ethiopia. However, utilization of such soil in the construction of road is limited due to their substandard qualities. Therefore, it becomes essential to improve the properties of locally available materials with cheaper stabilizer and understanding the behavior of the pavement under loading conditions with cheaper stabilizer to the extent that it can be used in the construction of road. The general objective of this research was to simulate road pavement response model using sugar cane bagasse ashes (SCBA) mixed with Lime as a weak subgrade soil stabilizer. Two types of soils sample with Dry Density, Liquid limit, Plastic limit and CBR test were conducted for by (0%, 1%L+4%SCBA, 2%L+3%SCBA, 3%L+2%SCBA, 4%L+1%SCBA, and 4%SCBA). It was observed that 1% bagasse ashes with 4 % lime content was a good result. The four days soaked CBR value of subgrade Soil – KK and Soil – AC was 1.56 % and 1.72 % respectively, it was increased to 9.58 % and 11.04% respectively with stabilization of 1 % SCBA with 4 % lime content. Due to related properties, of both soil samples the average of stabilized and unstabilized CBR to be determined in order to conduct finite element simulation with 1% SCBA + 4 % lime that means with resilient modulus 110.86 (Mpa) and 17.06 (Mpa) respectively.

The finite element simulation result with (ABAQUS software (version 12.14-1) program showed that, the contours' range of the linear elastic model has horizontal tensile strain ($1.490\times10^{-4)}$ μm) without stabilization and then decreased gradually with the maximum horizontal strain to reach about (1.351×10^{-4} μm) with stabilization at the bottom of HMA layer corresponding to approximately (9.32%) strain reduction with the reinforcement of subgrade and also the vertical compressive strains at the top of subgrade which the contours' range of the linear elastic model shows that the maximum vertical compressive strain (2.555×10^{-4} μm) without stabilization then decreased to (1.446×10^{-4} μm) which is almost 43% strain reduction at the top of subgrade. The increasing and decreasing of vertical strain and horizontal strain indicate that natural subgrade layer in this simulation are about less in stiffness without stabilization than that of the vertical strain with stabilization at the bottom of HMA layer and at the top of subgrade respectively

Keywords: ***ABAQUS; Flexible pavement; finite element; rutting; Stresses; Strains;***

TABLE OF CONTENTS

LIST OF TABLE

LIST OF FIGUR

ACRONYMS

2D	Two Dimensional Element
3D	Three Dimensional Element
ASTM	American Society for Testing and Materials Classification
AASHTO	American Association State Highway Transportation Official
AC	Agricultural Campus
C3D8R	8 Node Solid Continuum Elements with Reduction Integration
C3D20R	20 nodes Solid Continuum Element with Reduction Integration
CBR	California Bearing Ratio
CH	Clay with High Plasticity
ERA	Ethiopian Road Authority
ESAL	Equivalent Single Axle Load
FEM	Finite Element Method
HMA	Hot mix Asphalt
KK	Kochi Keble
LL	Liquid Limit
MDD	Maximum Dry Density
MR	Resilient Modulus
Nf	Number of Load Repetition
OMC	Optimum Moisture Content
OH	High plasticity
SCBA	Sugar Cane Bagasse Ashes

USCS	Unified Soil Classification System
(δ)	Deflection
(ε_t),	Tensile strain
(ε_v),	Vertical strain
v	Poisson's ratio

CHAPTER ONE

INTRODUCTION

1.1. Background of the study

In Ethiopia, there are 101,359 kilometers of road network and numbers of million vehicles, which make all sectors of the economy depend on roads to transport goods. the majority of goods, estimated at 83 percent, are transported by road, and in addition. Considering its significant role in the economic and communication activities of the modern societies, researchers have been searching to attain the most suitable road pavement behavior (Shafabakhsh, et al., 2013), and consequently design and construct safe, stable, cost-effective and environment friendly roads.

With all the attention from researchers, pavement structures experience failure before the desirable design life resulting from the low bearing capacity of soil (Kordi, et al., 2010) and overloading of the pavements, inadequacy in designs and unsuitable design methods used (Kordi, et al., 2010) ; (Shafabakhsh, et al., 2013). Its construction becomes uneconomical most often because of the cost incurred on materials used. With an appropriate method of soil stabilization, the soil's stability may be improved; resulting in stable pavements as well as the cost of construction may be reduced. However, the challenges with respect to the design of pavements remain

With the advent of powerful design software based on different methods such as the Finite Element, Discrete Element, Finite Difference, and Boundary Element Methods, the possibility of design and construction of quality pavement structures is enhanced. Therefore, in this study an attempt is made to simulate the behaviors of the flexible road pavements having bagasse ashes as an alternative soil stabilizer, by using Finite Element Method (FEM)

According to Aminaton, Nima and Houman (2013), stabilizing soil using lime, cement, chemicals, plastics, rice husk ash, millet husk ash, corn cob ash, coconut shell ash, foundry sand, cement kiln dust, granular blast furnace slag (GBS), and sugar cane bagasse ashes increases the soil's resistance, strength and permeability. Furthermore, results and

experience show that lime as a stabilizer yields better results than others, but its use will make pavement structure uneconomical, which in turn makes bagasse ashes as an alternative stabilizer.

Bagasse is often used as a primary fuel source for sugar mills; when burned in quantity, it produces sufficient heat energy to supply all the needs of a typical sugar mill, with energy to spare. To this end, a secondary use for this waste product is in co-generation. The use of a fuel source to provide heat energy, used in the mill, and electricity, which is typically sold to the consumer electricity grid. The combustion yields ashes containing high amounts of unburned matter, Silicon and Aluminum oxides as main components (Paya, et al., 2002). Among other properties, pozzolanic activity is the main property that the researchers seek in industrial waste material of mineral nature. The pozzolanas are materials containing reactive silica and/or alumina, which on their own have little or no binding property, but when mixed with lime in the presence of water will set and harden like a cement (Lea, 1956). Recently, a variety of alternative building materials are available. The use of these new materials may provide better, efficient, durable and cost-effective construction-material resources with reduced degradation of environment. Some of the materials are manufactured by using waste materials, such as fly ash (the ashen byproduct of burning coal), or agricultural waste ash as the raw material for their production (ASTM C 618, 1999).

FEM is a numerical technique for finding approximate solution to boundary value problems for differential equations, also with the ability of handling changes of material properties such as Resilient Modulus and Poisson's Ratio in both vertical and horizontal directions and having successfully been used not only for designing pavement structures, but also for optimizing the design by stimulation (Brooks, Hutapea, Obeid, Bai, and Takkalapelli, 2008; Shafabakhsh et al., 2013a). Additionally, it is suitable for eliminating tensile stresses in granular layers by stress transfer method and also enables pavement designers to predict with some amount of certainty the life of the pavement (Brooks et al. 2008). FEM includes two-dimensional (2D) and three-dimensional (3D) methods, both of which can be employed to capture the structural response of flexible pavements.

1.2 Statement of the problem

The poor performance of flexible pavements results from the use of poor-quality materials, inappropriate stabilization (Paige-Green, 2008). It may have shrinkage and and causes significant damage to pavement structures. Pavement failure in Ethiopia is becoming a common problem and great challenge, consuming a lot of money. According to (Nebro, 2002).Expansive clay soil is available in different parts of Ethiopia. However, utilization of such soil in the construction of road is limited due to their substandard qualities. Especially in urban areas, borrow earthen soil is not easily available which has to be hauled from Long distance. To utilize such expansive soils conventional stabilizing agents commonly used in expensive soil and replacement of the inferior subgrade soils by borrow materials are fairly expensive Therefore, it becomes essential to improve the properties of locally available materials with cheaper stabilizer and understanding the behavior of the pavement under loading conditions with cheaper stabilizer to the extent that it can be used in the construction of roads. Since most soils which is found in Jimma Town have high plastic index and low CBR value. These soils are a consequence for expansive and unstable subgrade soil. As a result, they make pavement structure failure Hence, this study pertains to the use of FEM to simulate the response of flexible pavements of Jimma Town roads in which bagasse ashes with lime as a subgrade soil stabilizer.

1.3 Research Question

This research aimed to answer the following research questions:

1 What are the properties of weak subgrade soil stabilized with SCBA and lime?

2. How the structural response of flexible pavement to be determined using 3D FM model with and without subgrade treatment?

3. What are the effects of the stabilized and un stabilized subgrade on the tensile strain at the bottom of the HMA layer and at the top of subgrade?

1.4 Objectives

1.4.1 General Objective

To Simulate a Road Pavement Response Model Using Bagasse Ashes with Lime as a Weak Subgrade Stabilizer.

1.4.2 Specific objectives

- To determine the properties of weak subgrade soil stabilized with SCBA and lime
- To determine the structural response of flexible pavement using the 3D FE model with and without subgrade treatment.
- To determine the effect of stabilized and un stabilized subgrade layer at the bottom of HMA layer and at the top of subgrade

1.5 Significance of the Study

The production of traditional stabilizers, such as cement and lime, is environmental unfriendly processes. So it is important to find another option which is environmentally friendly and cost advantage. Understanding such material behavior under loading is of great importance for effective pavement design. Recent studies undertaken on the use of waste and by-product materials as soil stabilizers have left a gap, between bagasse ashes as soil stabilizer (empirical design approach) and its computer-aided design for pavement structures. As a result, this study save time, and cost of laboratory experiments in carrying The research will serve as a reference guide for practicing civil engineers and researchers that practice in the area of study. This is useful in the sense that, it will cut down initial cost of new projects which are to commence and add our knowledge on the behavior of expansive soils and FEM.

1.6 Scope of the study

This study was supported by different types of literatures and a series of laboratory experiments. However, the findings of the research were limited to the two weak soil samples to conduct in this study. And finally the simulation is conducted with the average of the two sample due to related properties of both samples with stabilized and un stabilized materials. However, the model was conducted in this research was developed from

empirical correlated formulas due to lack of laboratory instrument. The relevant laboratory tests in this research was Proctor test, Sieve analysis test, CBR and Atterberg limit test.

CHAPTER TWO

RELATED LITERATURE REVIEW

Before any design of pavement structure, an appropriate pavement type selection is of importance as it is usually based on some critical factors such as soil composition, climate, traffic volume, life cycle, constructability and cost. In addition, there are secondary factors that need to be also considered, including: tire-pavement noise generation, surface smoothness and environmental sustainability. Flexible pavements have suitably met all the requirements, which made it to be used most frequently (Asphalt Pavement Alliance, 2010)

Flexible pavements with asphalt on the surface are used all around the world. The various layers of this pavement structure (Kim, 2007) have different strength and deformation characteristics which make the layered system difficult to analyses in pavement engineering. At the surface there is a viscous material with its behavior depending on time and temperature, and pavement foundation geomaterials; coarse-grained unbound granular materials in base/sub-base course; and fine-grained soils in the sub-grade, exhibiting stress-dependent non-linear behavior (Kim, 2007).

2.1 Pavement Composition and Behavior

Pavement structure a composite system, consisting of superimposed layers of processed materials above the natural soil sub-grade, with the primary function of distributing the applied vehicle loads to the sub-grade. This structure's ultimate aim is to ensure that the transmitted stresses due to the loading are sufficiently reduced, so that they will not exceed sub-grade bearing capacity (Ghanizadeh & Ziaie, 2015)

In other words, the tensile and compressive stresses induced on the pavement by heavy wheel loads decreases with increasing depth. In order to take maximum advantage, pavement layers are usually arranged in order of descending load bearing capacity, with the highest load-bearing capacity material on the top and the lowest load-bearing capacity material at the bottom, as seen in flexible pavement (Figure 2.1). However, in flexible pavements the unbound granular layers serve as a major structural component of the structure (Adu-Osei, 2001). Further, in developing countries like Ethiopia, the main

structural element is formed by the unbounded granular layer as thick base and sub-base layers placed over the sub-grade; and for economic purpose, the asphalt layer is very thin, with a limited structural function, which mainly provides protection against water ingress (Araya, 2011). These are: inter-particle friction, particle distribution, cohesion, elasticity, particle hardness, durability and porosity. In addition to fundamental properties, there are the situational properties that influence the behavior, such as density of material, moisture content and temperature. (Adu-Osei, 2001). The majority of these properties are considered in the design of pavement, but the most essential of these are the engineering properties which are actually the basic results in the design. Some of the engineering properties are: ultimate strength, elastic modulus, resistance to deformation and crack propagation and fatigue, all obtained from various laboratory tests.

Furthermore, various factors that have influence on the soil behavior can be loading condition, strain state, soil composition, compaction and soil properties (Kim, 2007). As a result of these factors the material characteristics of the entire pavement change continuously over time with environmental changes which later result in pavement failure. To avert pavement failure and reduce the cost of hauling natural materials, researchers introduced the use of secondary materials.

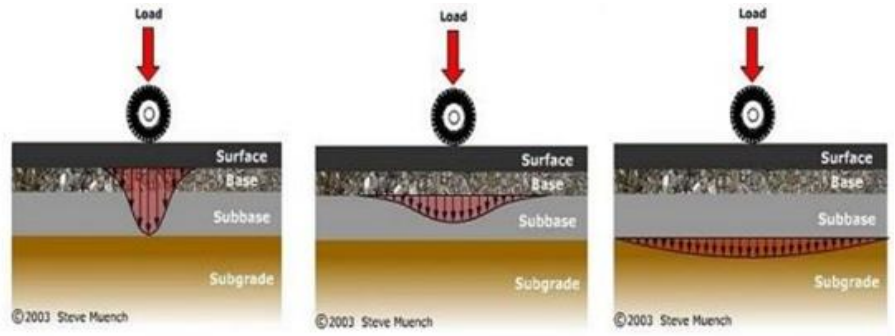

Fig 2. 1 Typical Flexible Pavement and Load Distribution (Steve, Muench,2003)

2.2 Secondary Materials

Using by-products, recycled and waste materials as alternatives to naturally occurring aggregates in the construction of roads helps to conserve the supplies of good-quality aggregates, leads to less energy and environmental cost associated with the extraction and

transportation of conventional aggregates, and assists in problems arising from the disposal of unwanted materials (Sherwood, 1974). Such materials are referred to as secondary materials or aggregates. Some of the secondary materials considered for road works are blast furnace and steel slag, spent oil shale, china clay waste, slate waste, rice husk ash, millet husk. (Heyns & Mostafa , 2013). All in all, secondary materials are inferior to the natural materials used in construction, but the lower cost of these inferior materials makes it an alternative if adequate performance can be achieved (Heyns & Mostafa , 2013).

2.3.1. Soil Stabilization Concept

In South Africa, the bearing capacity of the pavement is provided by the unbound base and sub-base or by the unbound base and stabilized sub-base (Araya, 2011). The asphalt layer provides a smooth riding surface and provides skid resistance. These structures have been successfully used in South Africa for moderately and heavily loaded roads. However, the minimum California Bearing Ratio (CBR) required for the sub-grade is 15 percent; when this is not reached, improvement of the sub-grade should take place. (Molenaar, 2009).

The asphalt layer provides a smooth riding surface and provides skid resistance. These structures have been successfully used in South Africa for moderately and heavily loaded roads. However, the minimum California Bearing Ratio (CBR) required for the sub-grade is 15 percent; when this is not reached, improvement of the sub-grade should take place (Molenaar, 2009).

Soil stabilization mainly aims at improving soil strength and increasing resistance to softening by water through bonding the soil particles together, water proofing the particles or a combination of the two (Sherwood, 1993). It is used to treat a wide range of materials including expansive clays to granular materials (Openshaw, 1992). The stabilization process can be accomplished by several methods. All these methods fall into two broad categories namely:

2.3.1.1 Mechanical stabilization

Stabilization is achieved via a physical process by altering the physical nature of natural soil particles by either induced vibration or compaction and also by introducing coarse or

fine materials and geosynthetic materials. Recently, mechanical stabilization has been used for pavement structure through geotextiles materials (Hejazi, et al., 2019). Which yielded a great increase in the property strength of the structures. Further, using a geogrid, (Al-Azzawi, 2012). Noted that placing this reinforcement at the base asphalt interface leads to the highest reduction of the fatigue strain.

2.3.1.2 Chemical stabilization

Stabilization by chemical additives are the oldest and most common method of ground improvement. Chemical stabilization refers to mixing of soil with one or a combination of admixtures of powder, slurry or liquid to improve or control its stability, strength, swelling, permeability and durability. Soil improvement by means of chemical stabilization can be grouped into three chemical reactions; Cation exchange, flocculation-agglomeration pozzolanic reactions(Mitchell & Soga, 2005)

i. Cation Exchange

The extra ions of opposite charge that of the surface of clay, over those of like charge present with in the diffuse double layer are known as exchangeable ions. These ions can be substituted by a group of different ions with having the same total charge, by changing the chemical composition of the equilibrium electrolyte solution. Negatively charged clay atoms adsorb cations of specific type and amount. The replacement of cations depends on numerous factors, mainly the valence of the Cation. Higher valance cations such as the calcium ion (Ca++) easily replace cations of lower valance such as sodium ions (Na+). For ions of the same valance, size of the hydrated ion becomes important; the larger the ion, the greater the replacement power. If the other conditions are equal, trivalent cations areheld more tightly than divalent and divalent cations are held more tightly than monovalent cations(Mitchell & Soga, 2005).

A typical replace ability series is:

$$Na^{+}<Li^{+}<K^{+}<Rb^{+}<Cs^{+}<Mg^{2+}<Ca^{2+}<Ba^{2+}<Cu^{2+}<Al^{3+}<Fe^{3+}<Th^{4+}$$

The exchangeable cations may be present in the surrounding water or be gain stabilizers. An example of the Cation exchange;

Ca^{2+} + Na^{+}-Clay ⟶ Ca^{2+}-Clay + Na^{+}

The thickness of the diffused double layer decreases as replacing the divalent ions (Ca^{2+}). From stabilizers with monovalent ions (Na^{+}) of clay. Thus, swelling potential decreases(Başer, 2009).

ii Flocculation and Agglomeration

The cation exchange reactions are result in the flocculation and agglomeration of soil particles with consequent decrease in the amount of clay-size materials and hence the soil surface area, which inevitably accounts for the reduction in plasticity. Due to change in texture, a significant reduction in the swelling of the soil occurs(Yazıcı, 2004).

iii Pozzolanic Reactions

The time dependent pozzolanic reactions play a key role in the stabilization of the soil, then they are responsible for the improvement in the several soil properties. Pozzolanic ingredients produces calcium silicate hydrate (CSH) and calcium aluminate hydrate (CAH).

Ca^{2+} + $2(OH)^{-}$ + SiO2 (Clay Silica) ⟶ CSH

Ca^{2+} + $2(OH)^{-}$ + Al2O3 (Clay Alumina) ⟶ CAH

Calcium silicate gel initially form coats and binds lumps of clay together. then the gel crystallizes to form an interlocking structure which increases the soil strength(Meron, 2013).

2.4 Bagasse Ash: Is a pozzolanic material which is very rich in the oxides of silica and aluminum and sometimes calcium (Guilherme , et al., 2004). Pozzolans usually require the presence of water in order for silica to combine with calcium hydroxide to form stable calcium silicate, which has cementations properties. (Alavéz-Ramírez, et al., 2012). Noted that Bagasse ash exhibits satisfactory behavior in blended cementations materials in concrete and has greater potential for use in other applications.

2.5. Abundance of Bagasse Ash in Ethiopia

In concern of the abundance of bagasse ash, contemporarily, giant sugar factories are under construction and some already started production with their partial or full production capacity in addition to the existing factories. Among these are: Kessem project found in Fentallie and Dulecha Woredas of Afar Regional State (expected capacity of 11,000ton of sugar per day), Tendahu found in lower Awash River Basin of Afar regional state around Millie, Doubti, Assaeitta and Affambo Woredas at a distance of 670 km from Addis Ababa (with completion of phase two of the project production capacity will be of 619,000 ton of sugar per annum) and Omo Kuraz found in South Omo zone (Selamago and Gnanegatom Woredas), Bench - Maji Zone (Surma Maji and Mieinitshasha Woredas) and Keffa zone (Diecha Woreda) of Southern Nations, Nationalities & People Region (when full capacity attained a production of 278,000 tons of sugar per annum will be expected) (Corporation, 2015). The molasses disposed from the existing factories is mostly utilized for ethanol production. And when all the factories become fully operational, the bagasse ash from all these factories will be expected to be in thousands of tones as shown on the table 2.1. As per the information from Ethiopian Sugar Corporation, all of the factories that are operating currently are now using bagasse as a fuel for boiler. Not only the current factories but the future intended projects will also operate in the same manner as this method reduces energy consumption. Table 2.1. Annual sugar production capacity and expected bagasse ash amount of sugar factories when fully operational capacity attained (Ethiopian Sugar Corporation (Communication department), unpublished, 2016).

Table 2. 1 Annual sugar production (Source Ethiopian Sugar Corporation, 2016))

S.No.	Sugar factories	Tone of cane per day (TCD)	Annual crushing capacity (Ton)	Bagasse (Ton)	Bagasse ash (Ton)
1	Wonji Shoa	12,500	3,000,000	870,000	108,750
2	Metehara	5,000	1,200,000	348,000	43,500
3	Fincha	12,000	2,880,000	835,200	104,400
4	Tendahu	26,000	6,240,000	1,809,600	226,200
5	Beles I	12,000	2,880,000	835,200	104,400
6	Beles II	12,000	2,880,000	835,200	104,400
7	Beles III	12,000	2,880,000	835,200	104,400
8	Kuraz I	12,000	2,880,000	835,200	104,400
9	Kuraz II	12,000	2,880,000	835,200	104,400
10	Kuraz III	12,000	2,880,000	835,200	104,400
11	Kuraz IV	24,000	5,760,000	1,670,400	208,800
12	Kuraz V	24,000	5,760,000	1,670,400	208,800
13	Kesem	11,000	2,640,000	765,600	95,700
14	Arjo dedesa	8,000	1,920,000	556,800	69,600
15	Wolkayte	24,000	5,760,000	1,670,400	208,800
		218,500	**52,440,000**	**15,207,600**	**1,900,950**

2.6 Lime Stabilization

Lime stabilization is the most widely used means of chemically transforming unstable soils into structurally sound construction foundations. The use of lime in stabilization creates a number of important engineering properties in soils, including improved strength; improved resistance to fracture, fatigue, and permanent deformation; improved resilient properties; reduced swelling; and resistance to the damaging effects of moisture. Interactions of lime with soil particles can be described by a sequence of complex physical and chemical processes that affect the mechanical behavior of soils. Additional, lime

addition rises the optimum moisture content but reductions in maximum dry density and finally direct increase in strength and results in a stable platform that facilitates the mobility of equipment. (Meron, 2013).There are two effects through lime treatment(Muntohar, A.S. and Hantoro, G., 2000). At first, there is a short-term or immediate effect, which occurs in the following hours of interaction between the lime and the soil and leads to flocculation / agglomeration of the soil particles. The results are change in the texture of the soil. In the second step, the effect said to be long-term, in which pozzolanic reactions occur. These reactions, which take place in the presence of water, between the lime and compounds composed of silicon and aluminum, lead to the formation of pozzolanic compounds that develop through time

2.7 Subgrade Stabilization

Deep stabilization for subgrade has been primarily used to control swelling soils, expedite construction, and construct unsurfaced haul roads (Thompson, 1972). For this study, layers stabilized at depths beyond 100mm, 150 and 200mm are considered to be deep stabilized layers for lime and sugar cane bagasse ashes stabilized soils, respectively. These typical depths for ERA standard subgrade stabilization are used as basis for this research.

2.8. Flexible Pavement Design

Flexible road pavements are intended to limit the stress created at the subgrade level by the traffic traveling on the pavement surface, so that the subgrade is not subject to significant deformations. In effect, the concentrated loads of the vehicle wheels are spread over a sufficiently larger area at subgrade level. At the same time, the pavement materials themselves should not deteriorate to such an extent as to affect the riding quality and functionality of the pavement. These goals must be achieved throughout a specific design period (ERA, 2013).

The deterioration of paved roads caused by traffic results from both the magnitude of the individual wheel loads and the number of times these loads are applied. It is necessary to consider not only the total number of vehicles that will use the road but also the wheel loads (or, for convenience, the axle loads) of these vehicles. Equivalency factors are used to convert traffic volumes into cumulative standard axle loads. Traffic classes are defined

for paved roads, for pavement design purposes, by ranges of cumulative number of equivalent standard axles (ERA, 2013).In order to limit the stress created at the subgrade level by the traffic traveling on the pavement surface, material layers are usually arranged in order of descending load bearing capacity with the highest load bearing capacity material (and most expensive) on the top and the lowest load bearing capacity material (and least expensive) on the bottom.

2.9. Flexible Pavement Layers and Materials

Obviously, surface course is the layer in contact with traffic loads and normally contains the highest quality of materials. Surface course play an important role in characteristics of friction, smoothness, noise control, rut and shoving resistance and drainage. Furthermore, surface course serves to prevent the entrance of excessive quantities of surface water into the underlying base, sub base and subgrade. This top structural layer of material is sometimes subdivided into two layers (Lanham, 1996).

1. Wearing Course**.** This is the top layer in pavement structure and direct contact with traffic loads. A properly designed preservation program should be able to identify pavement surface distress while it is still confined to the wearing course.

2. The purpose of this layer is to distribute load from wearing course. This layer provides the bulk of the HMA structure.

Base course

The base course is a course of specified material and design thickness, which supports the structural course and distributes the traffic loads to the sub base or subgrade. It provides additional load distribution and contributes to drainage and frost resistance. A wide range of materials can be used as unbound road bases including crushed quarried rock, crushed and screened, mechanically stabilized, modified or naturally occurring `as dug' gravels. Their suitability for use depends primarily on the design traffic level of the pavement and climate (ERA, 2013).

Sub base

The sub base course is between the base course and the subgrade. The sub base generally consists of lower quality materials than the base course but better than the subgrade soils. The sub base consists of granular material - gravel, crushed stone, reclaimed material or a combination of these materials. It enables traffic stresses to be reduced to acceptable levels in the subgrade, it acts as a working platform for the construction of the upper pavement layers and it acts as a separation layer between subgrade and base course. Under special circumstances, it may also act as a filter or as a drainage layer. For a pavement constructed over a high quality stiff subgrade may not need the additional features offered by a sub base course (ERA, 2013).

2.10. Overview of AASHTO Guide for Design of Pavement Structures

In 1972, the AASHTO pavement design guide was first published as an interim guide. Updates to the guide were subsequently published in 1986 and 1993; a new mechanistic based design guide is currently planned for completion in 2002. The AASHTO design procedure is based on the results of the AASHTO Road Test that was conducted in 1958 - 1961 in Ottawa, Illinois a proximately 1.2 million axle load repetitions were applied to specially designed test tracks, it is the largest road test ever conducted (Officials, 1993).

2.10.1 Flexible Pavement Thickness Design

The American Association of State Highway Officials (AASHO) has carries out a Road Test at Ottawa; Illinois provided the basis for calculating the required pavement thickness. Models (Road Test) were developed to related pavement performance, vehicle loadings, strength of roadbed soils, and the pavement structure (AASHTO, 1993).

Roadbed Soil Resilient Modulus (MR)

Subgrade support is characterized by the subgrade resilient modulus (MR).The Resilient Modulus (MR) is a measurement of the stiffness of the roadbed soil (AASHTO, 1993). A material's resilient modulus is actually an estimate of its modulus of elasticity (E). While the modulus of elasticity is stress divided by strain for a slowly applied load, resilient

modulus is stress divided by strain for rapidly applied loads – like those experienced by pavements (Muench, et al., 2003).

It is recognized that many agencies do not have equipment for performing the resilient modulus test. Therefore, suitable factors are reported which can be used to estimate MR from standard CBR, R-value, and soil index test results or values. A widely used empirical relationship developed by Heukelom and Klomp (1962) and used in the 1993 AASHTO Guide is equation (Muench, et al., 2003).

$$M_R(psi) = 1500 * CBR$$ ----------**Equation 2.1**

The resilient modulus of the hot mix asphalt is the most common method of measuring stiffness modulus. The test procedures for conducting this test are described in ASTM D4123 (Association, 2006) . In which MR is the resilient modulus in psi. The coefficient, 1500, could vary from 750 to 3000, with a factor of 2. Available data indicate that Eq. 1 provides better results at values of CBR less than about 20.

Overview of Ethiopian Roads Authority (ERA) Manual

This manual gives recommendation for the structural design of flexible pavement and gravel roads in Ethiopia. The manual is intended for engineers responsible for the design of new road pavements and is appropriate for roads which are required to carry up to 30 million cumulative equivalent standard axles in one direction. This upper limit is suitable at present for the most trafficked roads in Ethiopia (ERA, 2013).

ERA manual which also known as overseas road notes was developed by Transport Research Laboratory (TRL) to design flexible pavement thickness besides understanding the behaviors of road building material, also interaction in pavement structural layers' design. I advance, overseas road notes is confident to be applying in tropical and sub-tropical regions associated with climate and various types of material and reliable road maintenance levels (Laboratory, 1993).To give satisfactory service, a flexible pavement must satisfy a number of structural criteria or considerations; some of these are illustrated in Figure 2-2. Some of the important considerations are:

1. The subgrade should be able to sustain traffic loading without excessive deformation; this is controlled by the vertical compressive stress or strain at this level,
2. Bituminous materials and cement-bound materials used in road base design should not crack under the influence of traffic; this is controlled by the horizontal tensile stress or strain at the bottom of the road base,
3. The road base is often considered the main structural layer of the pavement, required to distribute the applied traffic loading so that the underlying materials are not overstressed. It must be able to sustain the stress and strain generated within itself without excessive or rapid deterioration of any kind.
4. In pavements containing a considerable thickness of bituminous materials, the internal deformation of these materials must be limited; their deformation is a function of their creep characteristics,
5. The load spreading ability of granular sub base and capping layers must be adequate to provide a satisfactory construction platform

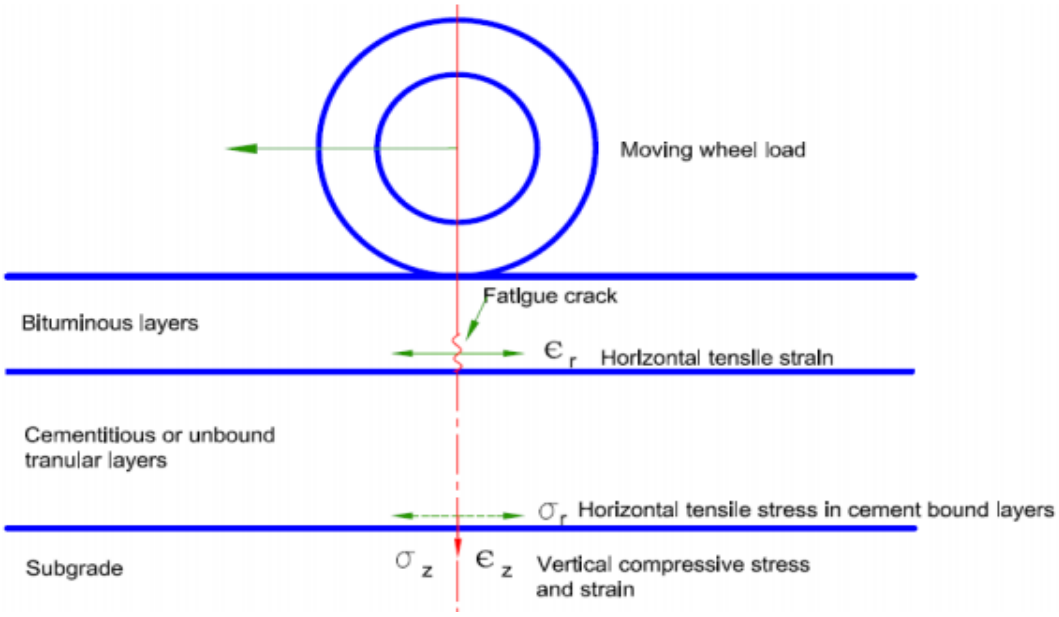

Fig 2. 2 Critical Stresses and Strains in a Flexible Pavement (ERA,2013)

In practice, other factors have to be considered such as the effects of drainage. When some of the above criteria are not satisfied, distress or failure will occur. For instance, rutting

may be the result of excessive internal deformation within bituminous materials, or excessive deformation at the subgrade level (or within granular layers above) (ERA, 2013).

Main Characteristics of Major Material Types: Granular Materials

Granular materials include selected fill layer; gravel sub base, road base or wearing course; and crushed stone sub base or road base. These materials exhibit stress dependent behavior, and under repeated stresses, deformation can occur through shear and/or densification. The selected fill, compacted at 95% MDD (AASHTO T180) exhibits a minimum soaked CBR of 10%. Its minimum characteristics are specified by a minimum grading modulus (0.75) and maximum plasticity index (20%). The gravel sub base and road base materials have minimum soaked CBRs of 30% and 80% respectively, when compacted to 95% and 98% MDD respectively (ERA, 2013).

Thus, ERA manual structural catalogue had been produce in order to design the flexible pavement thickness design based on the traffic and subgrade strength classes' requirement

2.11 Mechanistic or Analytic methods of Flexible Pavement Design

In contrast to the empirical pavement design methods, analytical or mechanistic methods consider the mechanical behavior of the pavement materials in an iterative method to determine the thicknesses fulfilling the requirements of the design (Huang, 2004; O'Flaherty, 2002). In an analytical pavement design the influence of stresses, strains and deflections due to the accumulated traffic loads and environmental conditions on the deterioration of the pavement structure is also considered. Most of the analytical pavement design methods use linear elastic theory to determine stresses, strains and deflections (Tutumluer, 1995) such as Chevron (Warrenand Dieckman, 1963) and BISAR (De Jong et al., 1973). The theory assumes materials of the pavement structure behave linear elastically; are homogeneous and isotropic; and require only the modulus of elasticity and Poisson's ratio for characterization.

Table 2. 2 material properties of pavement structure (ERA ,2013

Material	Parameter	Value	Comment
Asphaltic concrete wearing course and binder course	Elastic modulus (MPa)	3000	A balance between a value appropriate for high ambient temperatures and the effect of ageing and embrittlement
	Volume of bitumen	10.5%	
Asphaltic concrete road base	Elastic modulus (MPa)	3000	
	Volume of bitumen	9.5%	
Granular road base	Elastic modulus (MPa) Poisson's ratio	300 0.30	For all qualities with CBR > 80%
Granular sub-base	Elastic modulus (MPa) Poisson's ratio	175 0.30	For CBR ≥30%
Capping layer	Elastic modulus (MPa) Poisson's ratio	100 0.30	For CBR ≥15%

2.12 Pavement Response Models

The purpose of the pavement response models is to determine the stresses, strains and deflections from traffic loads and environmental conditions. The critical values of these responses are used as input in the distress models or transfer functions to predict the life of the pavement; this facilitates design, management and setting maintenance strategies for the road pavements.

2.12.1 Multi-Layer Elastic System

Boussinesq's theory was the only solution for determining stresses, strains and deflections before the development of the layered theory by Burmister (Huang, 2004) Boussinesq assumed a concentrated load, applied on one homogeneous, half-space, isotropic and linearly elastic layer with modulus elasticity of (E) and Poisson's ratio (v). By integrating the responses from a concentrated load, stresses, strains and deflections of a circular loaded

area can be determined at any point within the half-space (Huang, 2004) see Figure 2.3. Flexible pavements with thin surface asphalt and base layers, and a modulus ratio between the pavement and subgrade close to unity, can be analyzed with this theory (Huang, 2004)

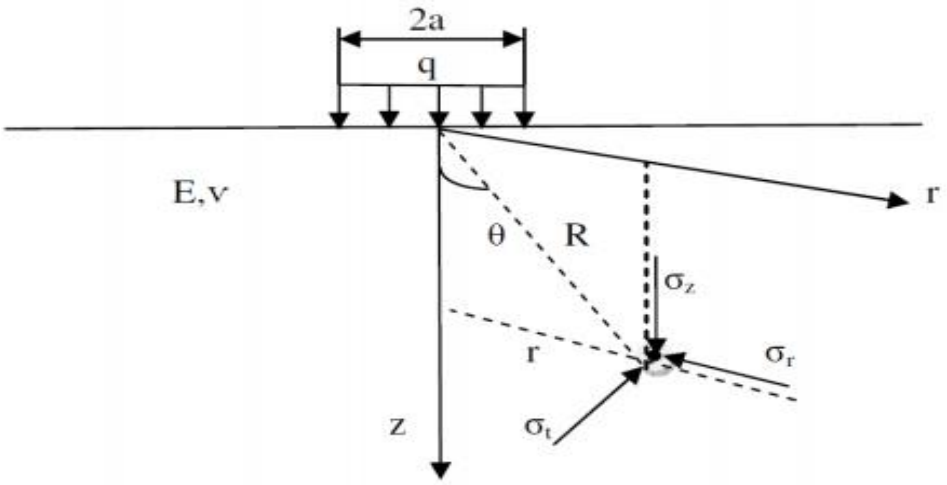

Fig 2. 3 Multi-Layer Elastic System

Vertical stress (σz), radial stress (σr), tangential stress (σt), shear stress (τrz) and vertical deflection (w) can be determined from charts presented by Foster and Ahlvin (1954). Strains then can be obtained using the following equations:

$$\epsilon z = 1/E\ [\sigma z - v\ (\sigma r + \sigma t]$$

$$\epsilon r = 1/E\ [\sigma r - v\ (\sigma t + \sigma z]$$

$$\epsilon t = 1/E\ [\sigma t - v\ (\sigma z + \sigma r]$$

Where ϵz, ϵr and ϵt are vertical, radial and tangential strains, E is modulus of elasticity and v is Poisson's ratio

2.12.2 Two Layer System

Burmister (1943) developed the theory of a two-layer system. He assumed the pavement system to be homogeneous, linearly elastic, isotropic layers with infinite horizontal dimensions and weightless layers resting on a semi-infinite subgrade layer.

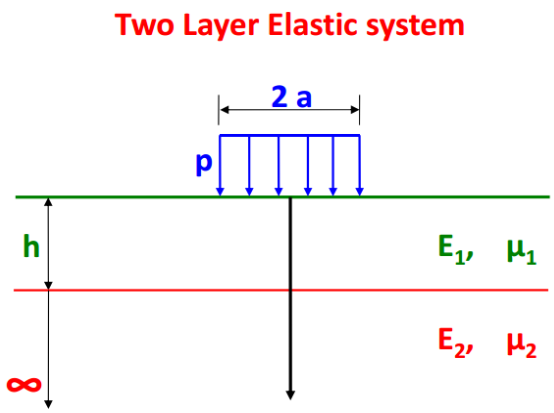

Fig 2. 4 An n layer system subjected to a circular load. (Huang, 2004)

2.12. 3 Three Layer System

Burmister (1945) broadened his theory of layered systems to a three-layer system and solved the problems of determining the responses at different positions in the three-layer system

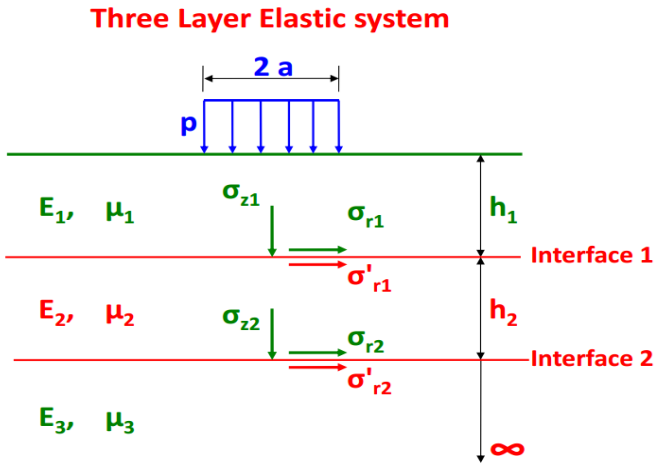

Fig 2. 5 Stresses at interfaces of a three layered system (Huang, 2004)

2.13. Finite Element Modelling (FEM)

In FEM, the whole problem is divided into small and simpler parts through mesh generation which are called finite elements and solved by calculus of variation in order to minimize associated error function (Yagawa, 209).Over the years, FEM has been applied extensively in road engineering (Peng & He, 2009) and so far, it is the most versatile of all analysis techniques, with capabilities for 2D and 3D geometric modelling, able to analyses stable

(static), time-dependent problems, non-linear material characterization, large strains/deformations, dynamics analysis and other sophisticated features (NCHRP, 2003). Furthermore, FEM can deal with complicated loading (static, dynamic and spatially distributed form) conditions and more accurate than the multilayer elastic method. The application of FEM to solve any problem consists of three separate stages

Pre-processing (Modelling)

This is the first stage in any FEM analysis, and here can be referred to as the input files stage, which is the most critical for the accurate prediction of the result in terms of stress, strain and deflection. At this stage the following selection/input are made:

- The geometry of pavement (in terms of dimensions),
- Material characterization, relationship between parts (assembling and interactions),
- Loading and boundary conditions, and analysis type.

Processing (evaluation and simulation)

In this stage, the job step is the main step and the input files are processed to produce the results (output file). Basically, at this stage the analysis process is only monitored in case an error is detected

Post processing

This stage is a graphic rendering phase of the output file from the processing stage. Results are well represented in the realistic format and the maximum and critical area of interest can easily be accessed. The post-processor describes the results of variables computed at the various nodes of the structure and involves the following

- Nodal displacement values
- Elemental stress values
- Reactions at constrained nodes
- Graphical display of displacements
- Graphical display of stress contours

2.14. Development of Flexible Pavement Model

Finite element modeling of flexible pavement has been used by many researchers during the past years to simulate pavement responses and investigate materials' behavior to different forms of traffic loading. (Duncan, 1968) was the first researcher who applied finite element modeling to flexible pavement, which was essentially based on the elastic theory. His approach was later adopted to develop computer programs such as ILLIPAVE (Raad et.al 1980), MICHI-PAVE (Harichandran et.al 1989), and FLEXPASS (Lytton. et.al 1990). All these FE-based programs were developed based on the elastic theory to simulate elastic response of the flexible pavement. One of the disadvantages of these FE programs is the inability to change or update material properties, load configurations and boundary conditions, which are sometimes necessary to accurately analyze and understand pavement responses (Wu.et al 2011). On the other hand, commercial software such as ANSYS and ABAQUS provide users optimum flexibility to manipulate a variety of FE models with sophisticated geometry and boundary conditions (Wu et al 2011). This commercial software was used by many researchers to model flexible pavement to investigate not only the elastic response for pavement materials, but also plastic responses in different environmental conditions (Al-Qadi, 2005).

2.14.1 Material Properties

Material properties of all layers were considered homogenous linear elastic in this model, and all layers were characterized by their elastic moduli and Poisson's ratios (Helwany, S., Dyer, J., & Leidy, J, 1998). Assuming the pavement materials behave elastically is appropriate for short-timed studies since non elastic material behavior requires many input parameters that are not readily available and might be assumed. Assumed parameters will not accurately produce reliable results (William, 1999). Therefore, elastic properties of pavement materials were appropriate for this model and this investigation.

2.14.2 Loading and Boundary Conditions

In fact, the pavement is subjected to a moving load; however, several researchers have used static traffic load in their analysis rather than dynamic load because of the theoretical and practical difficulties involved in the analysis when using a dynamic traffic load (Kim, D, 2002) stated that the maximum stress at a specific point in the pavement occurs when the wheel load is directly above it, while the stress can be assumed zero when the load is quite far from that point. Therefore, it is reasonable to consider a static loading in this model since loaded trucks sometimes need to be stopped for a while during the construction of the road to provide the site with the required construction materials and tools. A standard equivalent single axel load (18000 lb.) with dual tires has been considered in this model. However, only one set of the dual tires of 9,000 lb. was modeled due to the symmetry of the model geometry. The load was assumed to be transferred to the pavement over a rectangular contact area having a length of (0.8712L) and width of (0.6L). These dimensions were derived by assuming that the rectangular area is an equivalent of two semicircles of 0.6L diameter at the end and a central rectangle (Yoder and Witczak, 1075). The contact area shape and derivations are shown in Figure.2.7. Contact pressure was assumed to be equal to the tire pressure which is typically taken as 80 psi. The boundary condition used in this 3D model were the conventional ones which are basically rollers along the sides of the model where no horizontal movement is allowed and fixed at the bottom of the subgrade layer where no deflection existed beyond a specific depth (Saad et al,2006)

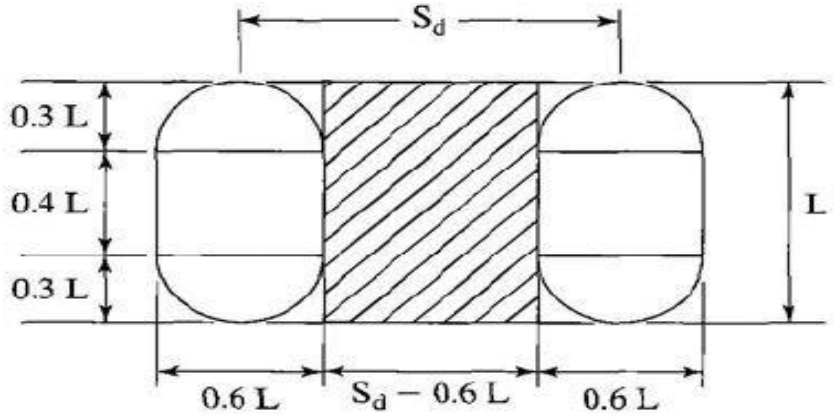

Fig 2. 6 Contact area of the dual tires on the flexible pavement Huang (2004)

The acceptable approximation shape of contact area for each tire is composed of a rectangle and two semicircles, having length L and width 0.6L. This shape of two semicircles and rectangle is converted to a single rectangle as suggested by Huang (2004) having a contact area of 0.5227L2 and a width of 0.6L

The area of contact $Ac = \pi(0.3L)\ 2 + (0.4L)\ (0.6L) = 0.5227L^{\ 2}$

$$L = \sqrt{\frac{A_c}{0.5227}}$$

The contact area, A_c is obtained by dividing the Load on each tire by tire inflation pressure as:

$$L = \frac{P}{P_i}$$

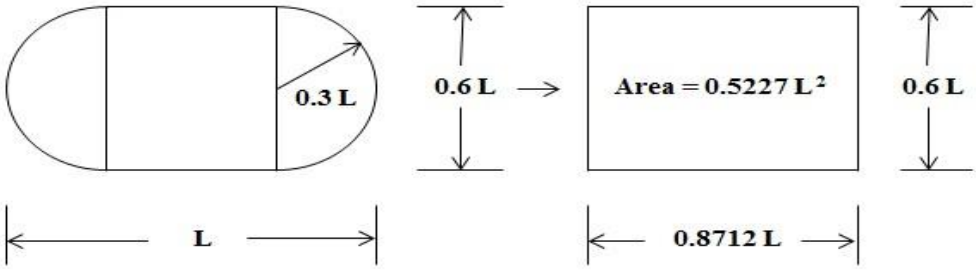

Fig 2. 7 Dimension of tire contact area between tire and pavement surface

2.14.3 Model Mesh and Element Type

In order to keep the size of the problem manageable in terms of time and storage capacity (Saad, 2006), a fine mesh was used only at the center of the model over which the axel load is distributed. On the other hand, larger mesh was used gradually as moving away from the center of the model. The 20-node quadratic brick with reduced integration was employed for this model since quadratic elements produce more accurate results than linear elements (Kuo et al 1995).

2.14.4 Pavement Performance Prediction

The mechanistic empirical pavement design Guide (NCHRP 1-37A), based on the model of the Asphalt Institute, provides a fatigue transfer function to determine the fatigue life of the pavement. Once the response is obtained under a given load condition, computation of pavement life is based upon fatigue and rutting (permanent deformation). For this, Asphalt Institute, AI (1982) models were used for the prediction of design repetitions for the standard 80kN (18 Kips) Single Axle load. The two models used are given below:

$$N_f = 0.0796(\varepsilon_t)^{-3.291}(E_1)^{-0.854} \quad \text{..... 2.1}$$

N_f : number of repetitions to failure

ε_t : tensile strain at bottom of asphalt layer

E_1 : elastic modulus of asphalt layer

For rutting criteria, the relationship between rutting failure and compressive strain (ε_c) at top of the subgrade is represented by number of load repetitions and is given as

$$N_f = 1.365\,x\,10^{-9}\,(\varepsilon_c)^{4.477} \quad \text{.....2.2}$$

.

CHAPTER THREE

RESEARCH METHODOLOGY

In order to complete this study, it was necessary to undertake a laboratory investigation on both unstabilized and stabilized subgrade soils to determine their properties; which then could be input into pavement analysis/design. The chapter includes detailed information about the experimental testing and finite element simulation program.

3.1 Study Area

Jimma is located at about 354 Kms in Southwest of Addis Ababa. The Geographical condition of the town approximately 7°41'N Latitude and 36°50'E Longitude. The town has a temperature of 19-29°C with an average annual rainfall 800-2400mm.The town is found in an area of the altitude of 1730-1900m above sea level.

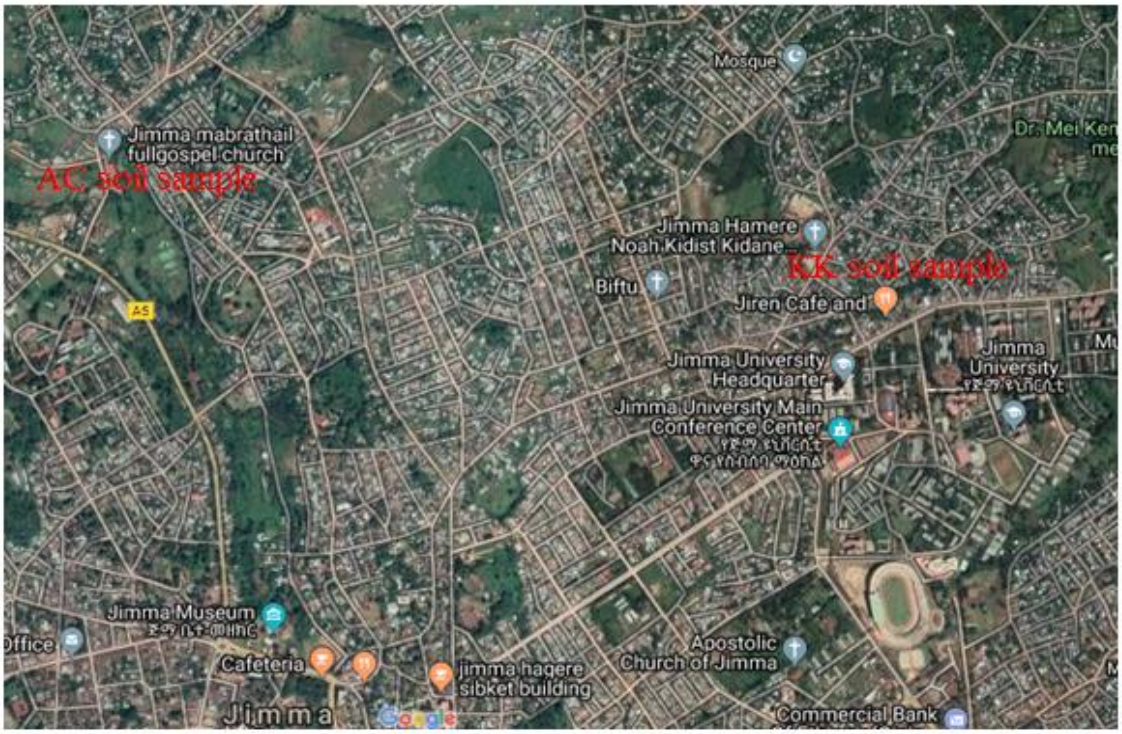

Fig 3. 1.Location map of study area (Google information, 2019)

It lies in the climatic zone locally known as Woynā Dagā which is considered ideal for agriculture as well as human settlement (Mengesha, 1886). According to the Central Statistical Agency (CSA), the total projected population of the town from 1907 is 129,244.

3.2 Materials

3.2.1 Bagasse Ash

Bagasse is the fibrous residue obtained from sugarcane after the extraction of juice at sugar mill factories and previously was burnt as a means of solid waste disposal. However, as the cost of fuel oil, natural gas and electricity has increased, bagasse has become to be regarded as a fuel rather than refuse in the sugar mills. The fibrous residue used for this purpose leaves behind about 8-10% of bagasse ash, Hailu, (2011). In this research the geochemical (oxide) tests are carried out to know quantitatively main oxides of the bagasse ash. The result of the oxide composition was adapted from Azeb L., 2018, who brought the bagasse ash from the same place, ARJO DIDESA Sugar Factory.

3.1.3 Lime

The lime used in this study was purchased from in Jimma Town on the counter. It was found to contain calcium oxide (CaO) commonly known as burnt lime. As a commercial product, lime often also contains magnesium oxide, silicon oxide and smaller amounts of aluminum oxide and iron oxide. Muntohar, and Hantoro, (2000).

Table 3. 1 Chemical composition of lime and (Hantoro, 2000)

Description	**Abbreviation**	**lime (%)**
Silica	SiO_2	0.00
Iron	Fe_2O_3	0.08
Calcium	CaO	95.03
Magnesium	MgO	0.04
Sodium	Na_2O	0.05
Potassium	K_2O	0.03
Loss of Ignition	-	4.33
Alumina	Al2O3	0.13
Sulphur trioxide	SO3	0.02

Manganese	MnO	0.60
Phosphorus	P2O5	0.00
Water	H_2O	0.04

3.2 Methodology

This research methodology consists of three tasks

1 Experimental work

- Grain Size Analysis
- Atterberg Limits
- Soil Classification
- Standard Proctor Compaction
- California Bearing Ratio

2 Finite element simulation of the pavement's responses to the applied load

3 Determination of the effect of stabilized and unstablized subgrade at the top of subgrade and at the bottom of HMA layer

3.3 Study design

The research was follow the experimental type and theoretical works of study. The stages involved in experimental study include: -

- ✓ Taking sample (disturbed sample)
- ✓ Preparation of sample for each laboratory tests
- ✓ Laboratory tests on properties of bagasse ash stabilized with lime
- ✓ Find out maximum replacement amount that satisfies requirement of the standard specification.

Finite element modeling and simulation -

- Determination of pavement geometry (in terms of dimensions),
- Material characterization, relationship between parts (assembling and interactions),
- Loading and boundary conditions
- Meshing size geometry
- 3D finite element modelling
- Simulation of layered system of the pavement structure.

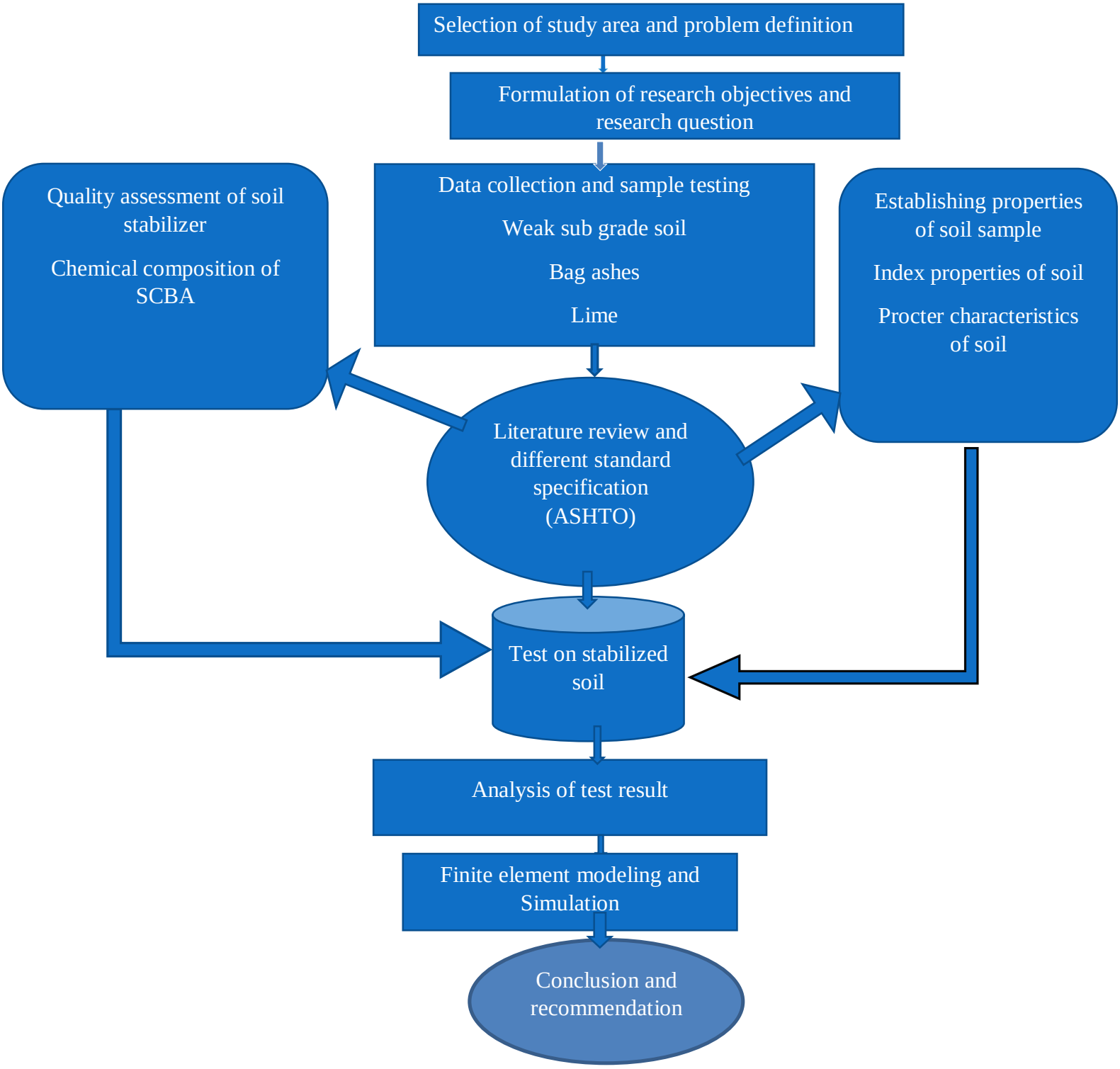

Fig 3. 2 Flow Charts of Research Design

3.4 Sampling Techniques and Sample Size

3.4.1 Sampling Techniques

The sampling technique used for this research was a purposive sampling which is non – probability method. This sampling technique was proposed based on goal of the researcher to be achieved and based on the information that to determine the strength of the expansive soil.

3.4.2 Sampling Size

For this study, sub grade soils were taken from different road corridors in Jimma Town. From those two most weak soils will be selected by observations and because of time constraint. The collected samples for this study taken at a depth of below 1.5 m to remove organic matter.

3.5 Study Variable

There are two types of variables that were taken into consideration both independent and dependent variables.

A) **Independent variables**

- Grain Size Analysis
- Soil Classification
- Atterberg limits
- Compaction
- CBR
- Material behavior under loading condition

B) Dependent variables

Finite element simulation, and 3Dmodelling

3.6 Data Collection Methods

The primary research data was collected through experiments, site visit whereas the secondary data also collected through the existing relevant documents and literature review and analyze the issues related to the concerned objectives of the study.

3.7 Data Processing and Analysis

The research was conducted first by identification of the effects of bagasse ashes on weak sub grade soils through laboratory. The results of laboratory tests are going to be analyzed using excel to draw different kind of graphs. And also the flexible pavement was modelled and simulated with and without treatment subgrade using ABAQUS software (version 12.14-1)

3.8 Laboratory Tests

Tests for soil classification which included grain size distribution, and Atterberg limits. These are indicative tests that are usually used for identifying whether the soil is expansive or not. The conducted tests however included hydrometer analysis, Atterberg limits, sieve analysis, moisture density relation, and CBR

3.9 Subgrade Soil

3.9.1 Sample Collection

After gathering information and Field investigations, 4 sub grade soils were taken from different locations in Jimma town. From those two, most weak soils were selected by observations and free swell index tests, because of time constrain and the intension of the study is to determine the suitability of SCBA ash as subgrade stabilizers, therefore the weakest sample is believing representing other populations. Those are around agricultural campus along the road to Jimma Agaro and Kochi kebele (around michael church). The collected samples for this study were disturbed samples at a depth of below 1.5 m to remove organic matter.

Fig 3. 3 Photos of sample taken for both station

3.9.2 Sample preparation

The soil samples were first air dried, properly pulverized and additives were mixed in such a way that the additive is first added to the prepared sample and dry mixed with the soil. The weak subgrade soil was mixed with SCBA-Lime by percentage of the weight of soil taken for each test starting from 0% to 4% within 1% difference for both SCBA and Lime, this percentage mix-ratio was fix by with some basis of observation from different scholars, some of them (Amruta P. Kulkarni, 2016) . As the respective of each test procedures preparing uniform samples for Atterberg Limits, Compaction and Californian bearing ratio test was conducted. Soil sample was first dry mixed with the respective lime and sugar cane bagasse ash was added there after followed by a thorough mixing.

Fig 3. 4 Photos of mix proportion of SCBA with L

3.9.3 Expansive soil

3.9.3.1 Grain Size Analysis

This test was performed to determine the percentage of different grain sizes contained within a soil. The mechanical or sieve analysis was performed to determine the distribution of the coarser, larger-sized particles according to AASHTO T 088-93. Wet sieve analysis and hydrometer analysis, using sodium hex metaphosphate and hydrogen per oxide used as dispersing agent and burning the organic content of the soil respectively.

Fig 3. 5 Photos of hydrometer analysis

3.9.3.2 Atterberg Limit Test

The test procedure adapted for the determination of Liquid limit, Plastic Limit and plasticity index for both untreated and treated soil sample was in accordance with AASHTO T89-94 and T90-94 respectively. A sample weighting about 200 gm was taken from the mixture prepared for liquid limit and plastic limit test for each samples. Soil samples were first air dried and pulverized and then sieved with number 40 sieve. Soil passing number 40 sieve was mixed with different proportion of lime-bagasse ashes at

optimum water content and sealed with plastic for 24 hours in order to give sufficient time for chemical reaction before test. Hand mixing in a porcelain pan was the method of mixing. The liquid limit of each soil had been determined by using casagrande apparatus. The plastic limit of each soil was determined by using soil passing through a 475 μm sieve and rolling 3-mm diameter threads of soil until they began to crack.

Fig 3. 6 Photos of liquid and plastic limit

3.9.4 Soil Classification

The most widely used soil classification systems are AASHTO and USCS systems. The AASHTO Classification system is useful for classifying soils for high way. On this research each Soil was classified using the AASHTO Soil Classification System using particle size distribution and Atterberg limits.

3.9.5 Compaction Test

This laboratory test was conducted to determine optimum water content at maximum dry density of soil. Compaction is when mechanical loads applied to soil result in expulsion of air, increase in bulk density and resistance to penetration. The laboratory standard proctor test was performed as per AASHTO T 99-95. The test was performed on disturbed samples of soil passing sieve sizes 4.75mm or 19mm mixed with water to form samples at various moisture contents ranging from the dry state to wet state. These samples were compacted in five layers at 56 blows per layer in accordance with the specified nominal compaction

energy of modified proctor test. Dry density was determined based on the moisture content The corresponding water content at which the maximum dry density occurs is termed as the optimum moisture content.

Fig 3. 7 Photos Compaction test and procedures and the unit weight of compacted soil.

3.9.6 California Bearing Ratio Test (AASHTO T-193)

The CBR is expressed by force exerted by the plunger and the depth of its penetration into the specimen; it is aimed at determining the relationship between force and penetration. A three point CBR test at 10, 30 and 65 blows were conducted according to AASHTO T193 and the CBR values at 95% MDD was determined. The CBR test indirectly measures the shearing resistance of a soil under controlled moisture and density conditions. The CBR is obtained as the ratio of load required to affect a certain depth of penetration of a standard penetration piston into a compacted specimen of the soil at some water content and density to the standard load required to obtain the same depth of penetration on a standard sample of crushed stone. The equation to be computing the CBR value is as follows.

$$CBR(\%) = \frac{\text{Applied load on sample}}{\text{standard load on the crushed stone}} \times 100 \quad \text{.....3.1}$$

For 2.54 mm Penetration = 6.9 MPa and for 5.08mm penetration = 10.3 MPa. The required quantity of soil, kaolin, cement and water for one specimen were calculated using bulk density and moisture content determined from Proctor Test and the total quantity of each needed to prepare the required number of test specimens at each prescribed stabilizers percentage of maximum dry unit weight and water content was known.

Fig 3. 8 Photos of CBR test and procedures

3.10 Bagasse Ashe

Investigations were made on Bagasse ashes obtained from ARJO DIDESA Sugar Factory. It was tested for physical properties per AASHTO. The chemical and physical properties of the bagasse ashes used in this research were listed in Table 3.2

Fig 3. 9 Processed of SCBA preparation

3.11 Finite element Modelling

The Finite Element Method (FEM) allows structural modeling of a multi-layer pavement section having material properties that can vary both vertically and horizontally throughout the profile. The general idea of finite element technique is the partitioning of the problem into small discrete elements (mesh), formulating an approximation to the stress and strain variations across each individual element. In this study the following modeling and simulation was considered: -

- This model was essentially 3D FE model developed to simulate a layered system of the pavement structure with and without subgrade treatment.
- The effect of the subgrade stabilization on the tensile strain at the bottom of the HMA layer with four-layer and five system
- Determination of rutting and fatigue criteria using asphalt institute method

3.11.1 Materials Properties

The material was assumed in this model is to be homogenous isotropic linear elastic materials because of nonlinear behavior requires a lot of input parameters and computational time. Therefore, the stabilized subgrade and natural subgrade materials were modeled in terms of the elastic modulus and Poisson's ratios.

Poisson's ratio is the ratio of the strains perpendicular to the direction of the applied load divided by the strains in the direction parallel to the load. It is a property of linear-elastic, homogeneous and isotropic materials relating lateral to longitudinal strain relative to the direction of load application. but due to lack of resilient modulus test it is customary to assume a reasonable value for use in design, rather than to determine it from actual tests. For Poisson's ratio the common practice is to use typical value based on the type of material.

Table 3. 2 Poisson ratio for different material after (Hung 2004)

Material	Range	Typical
Hot mix asphalt	030-0.40	0.35
Portland cement concrete	0.15-0.20	0.15
Untreated granular materials	0.30-0.40	0.35
Cement-treated granular materials	0.10-0.20	0.15
Cement-treated fine-grained soils	0.15-0.35	0.25
Lime-stabilized materials	0.10-0.25	0.20
Lime—fly ash mixtures	0.10-0-15	0.15
Loose sand or Silty sand	0.20-0.40	0.30
Dense sand	0.30-0-45	0.35
Fine-grained soils	0.30--0.50	040
Saturated soft clays	0.40-0.50	0.45

Resilient Modulus Models

Models used for determining the "Mr. **Resilient Modulus** " value can be classified into two main categories;

1. The model which is not the stress dependent characteristics of materials, generated from some empirical correlations based on the California Bearing Ratio (CBR) test or stabilometer test (R).
2. Models, developed from the repeated load triaxial test results, describing the stress-dependent non-linear behavior of the materials.

Due to lack of resilient modulus test, in this study the resilient modules of the material determined from empirical correlations based on the California Bearing Ratio (CBR) test

Mr = 1500 (CBR) ……1 where the CBR is less than **20 (**Heukelom and Klomp (1962)

Elastic material properties of the stabilized and natural subgrades were obtained from laboratory tests conducted for both kochi Keble and around agricultural campus station to examine the engineering properties of stabilized subgrade soils (4 days curing) in Jimma town. These soils were classified as A-7-5 for Kochi Keble and A-7-5 for around agricultural campus station respectively. Each soil sample was treated (Bagasse ashes mixed with lime) as show in table 3.4

Table 3. 3 Material properties of treated and untreated subgrade

Soil Type and location	Stabilization		CBR(Psi)	Resilient Modulus (Mpa)	
	Lime %	Bagasse ashes %			Poisson's Ratio
KK A-7-5	0	0	1.58	16.3	0.4
	0	4	2.78	28.73	0.4
	1	4	3.82	39.48	0.4
	2	3	6.21	64.18	0.4
	3	2	8.8	90.95	0.4
	4	1	10.4	107.48	0.4
AC A-7-5	0	0	1.72	17.78	0.4
	0	4	2.80	28.94	0.4
	1	4	3.96	40.92	0.4
	2	3	7.79	80.50	0.4
	3	2	9.35	98.9	0.4
	4	1	11.04	114.09	0.4
Average of the two soil samples (CBR and Mr)	0	0	1.65	17.06	0.4
	0	4	2.79	28.83	0.4
	1	4	3.89	40.20	0.4
	2	3	7	72.35	0.4
	3	2	9.07	93.80	0.4
	4	1	10.72	110.86	0.4

3.11.2 Loading and Boundary Conditions

Using 3-D FE modeling of the flexible pavement is the ability to simulate a rectangular footprint of the contact area over which the tire loading is distributed rather than a circle contact area which is usually assumed for the 2-D and axisymmetric models (Saad et al,2006). The load was assumed to be transferred to the pavement over a rectangular contact area having a length of (0.8712L) and width of (0.6L). These dimensions were derived by assuming that the rectangular area is an equivalent of two semicircles of 0.6L diameter at the end and a central rectangle (Huang 2004). The 40 kN wheel load to represent a set of dual tires is assumed to be uniformly distributed over the contact area between tire and flexible pavement surface and with 80 (psi) inflation pressure investigated. The loading configuration allow developing a symmetric FE model edge of the mesh in order to represent the middle of pavement of others opposite side of vertical edge is also fixed in horizontal direction over the whole pavement section while the bottom of the FE mesh is fixed on both horizontal and vertical direction.

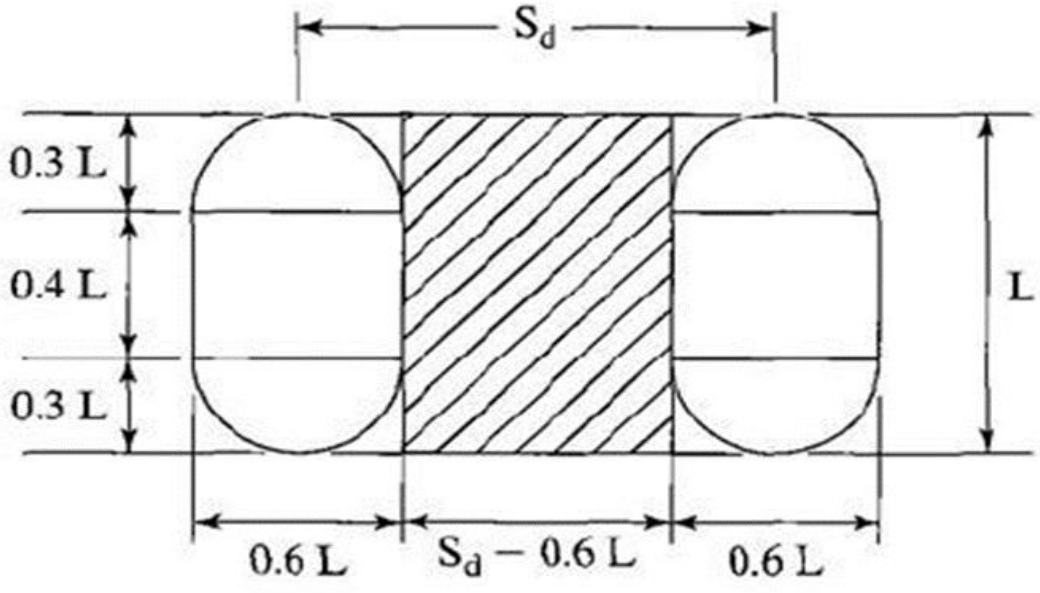

Fig 3. 10 Equivalent contact area for a dual tire (Huang 2004)

Let P is the load on one tire and Pi is the contact pressure then the area of the tire

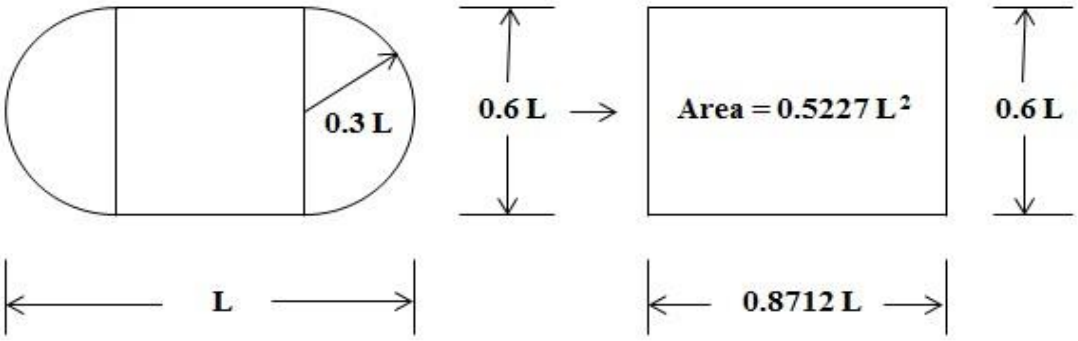

Fig 3. 11 Dimension of tire contact area between tire and pavement surface(Huang 2004)

$$Ac=\pi(0.3l)^2+(0.4l*0.6l) =0.5227l^2$$

$$L = \sqrt{\frac{A_c}{0.5227}} \quad \text{.....1}$$

The contact area, A_c is obtained by dividing the Load on each tire by tire inflation pressure

$$L = \frac{P}{P_i} \quad \text{.....2}$$

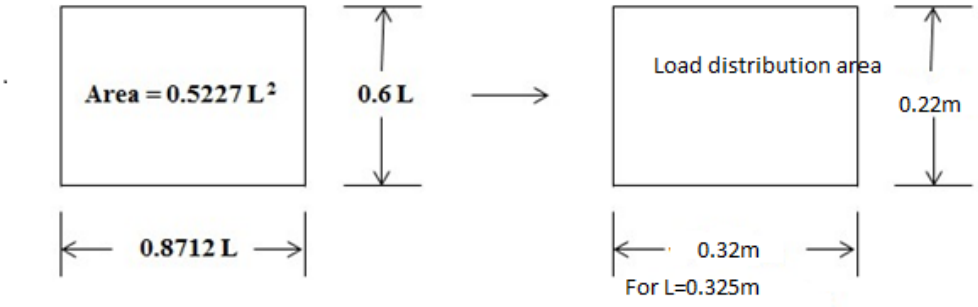

Fig 3. 12 Equivalent contact area for a dual tire (Huang 1993)

The dimensions of the tire footprint were approximately rectangular, 320 mm long and 220 mm wide. The weight transmitted by the tire was 40 kN. Therefore, the average contact pressure is given by

P=F/A……3

Where P=pressure(kPa) 40/0.32*0.22

F=force (KN) 568.18 Kpa =0.57Mpa

A=Area(m^2)

For finite element analyses, it was necessary to move the fixed bottom boundary to a depth of 140-times the radius (140R) of the loading area and move the vertical roller boundary at a horizontal distance of 20-times the radius (20R) of the loading area from the corner of loading. Only one-quarter of the pavement cross-sections are modeled to reduce the computational time required to run the analysis as well as memory storage needed for the analysis. Therefore, in this study the model was done with the dimension (3.2× 3.2) in transversal and longitudinal direction respectively with depth 21m

3.11.3 Model Mesh and Element Type

The three-dimensional FE mesh contains an 8-node, first-order quadratic element with reduce-integration (C3D8R) (linear) and a 20-node quadratic reduced-integration (C3D20R) (nonlinear) was used for this model in ABAQUS. Therefore, these element types are generally the best choice for most general stress and/ or displacement simulations.

3.11.4 Geometry of Flexible Pavement Structure

The thickness of each layers are the same throughout Jimma road except at some places where there is capping layers where California bearing ratio is less than fifteen. The components are surface course, base course, sub base course, and subgrade course. The flexible pavement structure contains a finite-element discretization of a four -layer system having a 50 mm-thick HMA layer, a 175 mm-thick unbound base layer,175 mm subbase (Source: Jimma Road upgrade document). Stabilized subgrade layer (200,150 and 100mm Typical cross-section of conventional flexible pavement setup: load of dual tires, material properties, pavement thickness and center space between the dual tires

Table 3. 4 Properties of pavement materials ERA (2013)

Material	Parameter	Value	Comment
Asphaltic concrete wearing course and binder course	Elastic modulus (MPa)	3000	A balance between a value appropriate for high ambient temperatures and the effect of ageing and embrittlement
	Volume of bitumen	10.5%	
Asphaltic concrete road base	Elastic modulus (MPa)	3000	
	Volume of bitumen	9.5%	
Granular road base	Elastic modulus (MPa) Poisson's ratio	300 0.30	For all qualities with CBR > 80%
Granular sub-base	Elastic modulus (MPa) Poisson's ratio	175 0.30	For CBR ≥30%
Capping layer	Elastic modulus (MPa) Poisson's ratio	100 0.30	For CBR ≥15%

In this modelling, the approach used for estimating equivalent section for pavement having deep subgrade stabilization was presented. The controlling factor is the load repetitions to failure of control pavement section containing ERA standard subgrade stabilization depth between (100 ,150 and 200 mm). The thickness of the subgrade stabilization layer was the main difference between the three sections. All three pavement sections used the same materials including the underlying untreated subgrade foundation

3.12 Finite Element Model of the Flexible pavement

This model was essentially 3D FE model developed to simulate a layered system of the pavement structure. The stabilized layer essentially consists of the same natural subgrade material in which the maximum results were achieved at 1% SCBA and 4% lime. The natural subgrade depth for the analysis purpose and boundary condition, it was assumed to be 140 times the loading area in vertical direction and 20 times horizontal direction (Kim,

et al., 2009). Due to the double symmetry of the geometry around X and Y axes, only one quarter of the geometry was modeled.

Table 3. 5 Material Properties used in the Three-dimensional Finite Element Modeling

Model	Layer	Thickness (mm)	Modulus(Mpa)	Poisson's Ratio
With treatment of subgrade	HMA	50	3000	0.35
	Base	175	300	0.30
	subbase	175	175	0.30
	Stabilized Subgrade	100/150/200/	110.79	0.4
	subgrade	2160	17.05	0.40
Without treatment of subgrade	HMA	50	3000	0.35
	Base	175	300	0.30
	subbase	175	175	0.30
	Subgrade	2140	17.05	0.4

3.13 Response of pavement Structure

The response to be analyzed in this study was tensile strain at the bottom of HMA layer and vertical compressive strain at the top of subgrade. Some values of the critical responses – such as tensile strains at the bottom of the HMA and vertical strain at the top of the subgrade layers determined by ABAQUS software version (12.14-1)

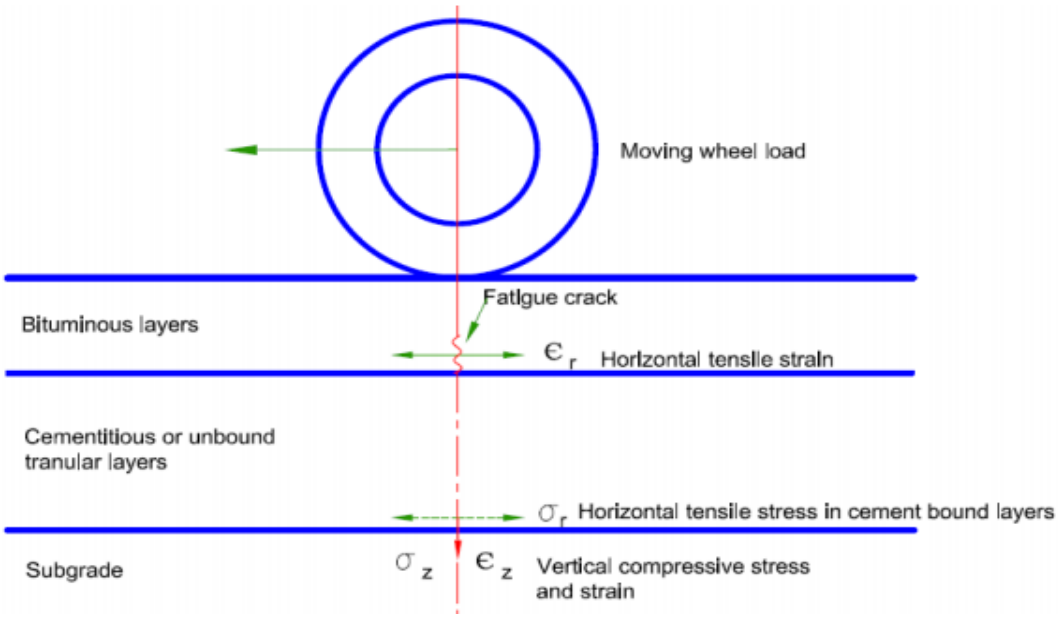

Fig 3. 13 Critical location of pavement response

3.14 Pavement Performance

Fatigue cracking and rutting are primarily caused by stresses and strains due to cumulative repetitive and/or high traffic loading. Other factors such as material mix-design, temperature, moisture, ageing, oxidation, etc. directly or indirectly contribute to pavement distress. However, these factors are not discussed in this paper.

Fatigue Cracking is the progressive cracking of the asphalt surfacing or stabilized base layers due to cumulative repeated traffic loading. This occurs as a result of tensile stresses and strains in the bottom zone and propagates upward to the top. On the pavement surface, it finally manifests as alligator cracks along the wheel tracks. Once the response is obtained under a given load condition, computation fatigue cracking based upon Asphalt Institute, AI (1982) models were used for the prediction of design repetitions for the standard 80kN (18 Kips) Single Axle load.

$$N_f = 0.0796(\varepsilon_t)^{-3.291}(E_1)^{-0.854}$$

Where N_f : number of repetitions to failure

$\boldsymbol{\varepsilon_t}$: tensile strain at bottom of asphalt layer

$\boldsymbol{E_1}$: elastic modulus of asphalt layer

Rutting is defined as the permanent deformation of a pavement due to the progressive accumulation of viscos-plastic vertical compressive strains under traffic loading. On the pavement surface, it manifests as longitudinal depressions in the wheel tracks. Once the response is obtained under a given load condition, computation fatigue cracking based upon Asphalt Institute, AI (1982) models were used for the prediction of design repetitions for the standard 80kN

$$N_f = 1.365\,x\,10^{-9}\,(\varepsilon_c)^{-4.477}$$

Where N_f : number of repetitions to failure

$\boldsymbol{\varepsilon_c}$: tensile strain at bottom of asphalt layer

E_1 : elastic modulus of asphalt layer

CHAPTER FOUR

RESULT AND DISCUSSION

4.1 Introduction

This chapter presents test results, discussion and analysis of all experimental work that were performed on untreated and treated soil samples with bagasse ashes and lime combination mixtures. Primarily, properties of materials (untreated soil, and bagasse ashes) were examined, then the effect of stabilizers on Atterberg limits, moisture-density relation, CBR, values were investigated by varying percentage of stabilizers from 1% ,2%. 3%, and 4% increment and compared with native soil/untreated soil engineering properties. Then effect of stabilizers on the properties of treated soil was compared and contrasted with standard specification and manuals.

4.2 Chemical Analysis of SCBA

The chemical analysis indicated that the ash contained mainly silica, calcium, magnesium and aluminum with other minor elements Table 4.1. The combined percent composition of SiO2, Al2CO3 and Fe2O3 of the ash is more than 70% hence exhibits pozzolanicity property according to ASTM C618 – 12 (ASTM 2012) standards for pozzolanic reaction

Table 4. 1 Chemical analysis of Bagasse Ash (ARJO DIDESA Sugar Factory,2019)

Description	**Abbreviation**	**Ash (%)**
Silica	SiO_2	82.66
Iron	Fe_2O_3	3.18
Calcium	CaO	0.64
Magnesium	MgO	0.58
Sodium	Na_2O	0.24
Potassium	K_2O	3.70
Water	H_20	0.27
Alumina	Al_2O_3	6.84
Titanium	TiO_2	0.43
Manganese	MnO	0.14
Phosphate oxide	P_20_5	0.50
Loss of ignition	LOI	1.01
Silicate	So_3	0.22
Chlorine	CL	<0.01

4.3 Expansive Clay Soil

Results of the study on physical properties on neat sample of clay is given in Table 4.2 and indicated that the sample belonged to expansive clay

Table 4. 2 Properties of expansive clay soil

Parameters	Test Results in, %	
	Kochi Keble(KK)	Agricultural campus(AC)
Natural Moisture Content, %	39.9	40.70
Percentage of passing No.200sieve, %	94.5	92.08
Liquid limit, %	88.5	96.55
Plastic limit, %	40.1	37.8
Plasticity index, %	48.5	58.75
AASHTO soil classification	A-7-5	A-7-5
Maximum dry density g/cm^3,	1.320	1.280
Optimum moisture content, %	32	28
Soaked CBR value, %	1.58	1.72

Generally Liquid limit less than 35% is low plasticity, between 35% and 50% intermediate plasticity, between 50% and 70% high plasticity and between 70% and 90% very high plasticity (Whitlow, 1995). As a result, these values indicate both the soil sample are very high plastic clay. Therefore, the subgrade shrink and swell easily and does not resist internal and external load. Finally, the structure make crack and easily demolished.to protect this failures stabilization using different additives should be required.

4.3.1 Particle size distribution

A basic element of a soil classification system is the determination of the amount and distribution of the particle sizes in the soil. Distribution of particle sizes greater than 0.075 mm is determined by sieving, while a sedimentation process (hydrometer test) is used to determine the distribution of particle sizes smaller than 0.075 mm. To determine the distribution of coarser particles, 1000g of the natural subgrade soil is taken and washed on sieve size of 75µm.A hydrometer test is conducted on 50gm of soil sample passing sieve No.200.The soil sample was soaked in chemical solution (Sodium hexa-meta phosphate and hydrogen per oxide) for dispersing and burning of the organic content for 24 hours. The tabular experimental results are presented in appendix A and B, and the particle size distribution curves are shown in Fig 4.1and Fig 4.2 The soil for both sample KK and AC is dark gray, and almost 92.09% and 94.5 respectively of the soil are passing through No.200 sieve as shown in Figure 4.1.and fig 4.2

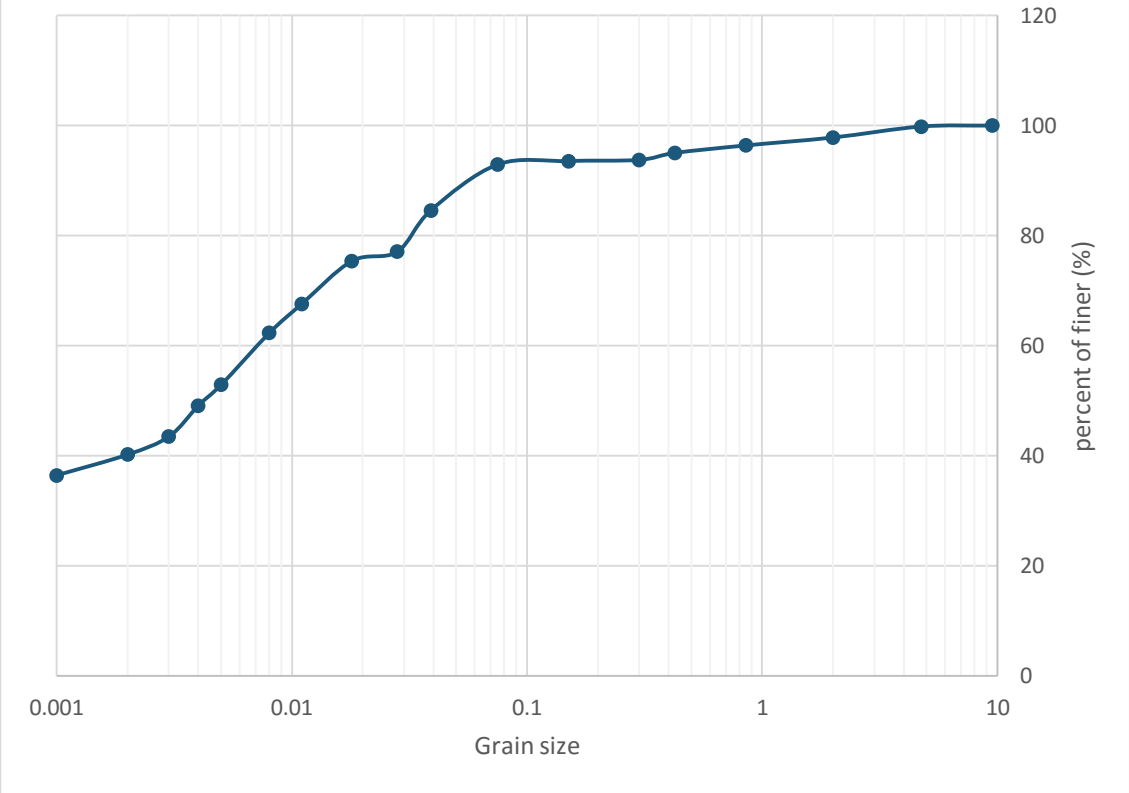

Fig 4. 1 Grain size distribution curve of AC soil sample

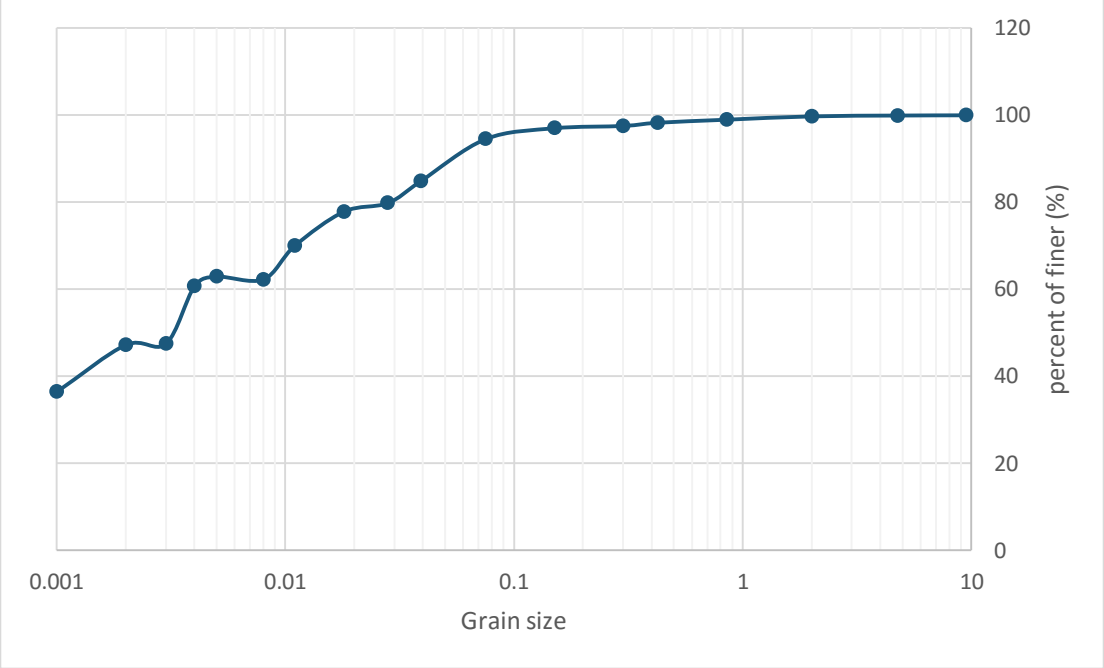

Fig 4. 2 Grain size distribution curve of KK soil sample

According to Atterberg limit test result as shown by Table 4. 2 The KK and AC soil sample changed from liquid state to plastic state and got an average liquid limit of 96.55 and 88.5 respectively. The given soil sample translate from plastic state to semisolid state and got an average plastic limit of 40.1 and 37.8 AC and KK soil sample respectively. At this state the soil rolled into threads. The difference between the liquid limit and plastic limit is called Plastic Index. The soil sample also has Plastic Index of 48.4 and 59.75% for both soil sample respectively. As result of Plastic Index indicates both the native subgrade soil samples have poor for sub grade material unless it treated.

4.3.2 Soil Classification

4.3.3.1 AASHTO Classification system

The AASHTO system uses similar techniques as that of USCS but the dividing line has an equation of the form PI= LL-30. It generally classifies a soil broadly into granular material and silt-clay material. The granular material is further divided into three groups which are called A-1, A-2 and A-3. The silt-clay material is in turn divided into four groups namely, A-4, A-5, A-6 and A-7. The results indicate that generally the soils of the study area were very poor for subgrade material

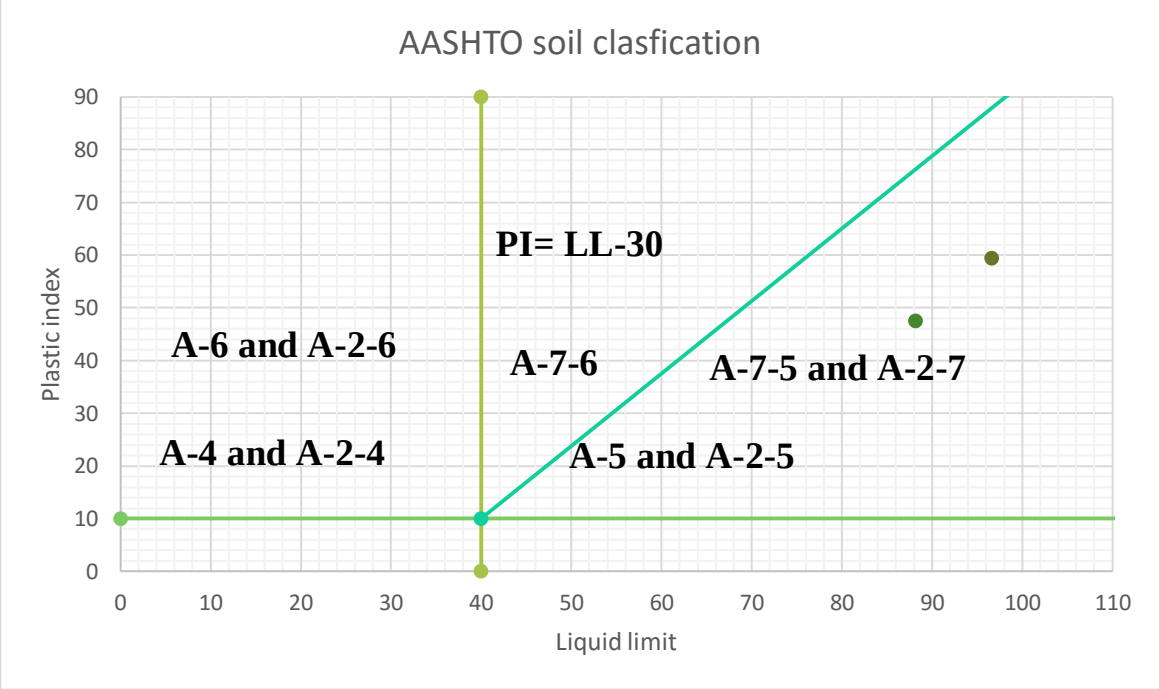

Fig 4. 3: Soil classification according to AASHTO system

- As results of Atterberg limit test KK and AC subgrade soils has different Liquid limit and plastic Index, however according to AASHTO soil classification system both soil samples have classified under group A-7-5 with rating Fair-to- Poor. Thus, material is unsuitable to be used as subgrade material without employing some improvement methods.

4.3.3.2 Unified soil classification (USCS) system

This system describes a system for classifying minerals and organic-mineral soils for engineering purposes based on laboratory determination of particle-size characteristics, liquid limit and plasticity index and shall be used when precise classification is required (ASTM).

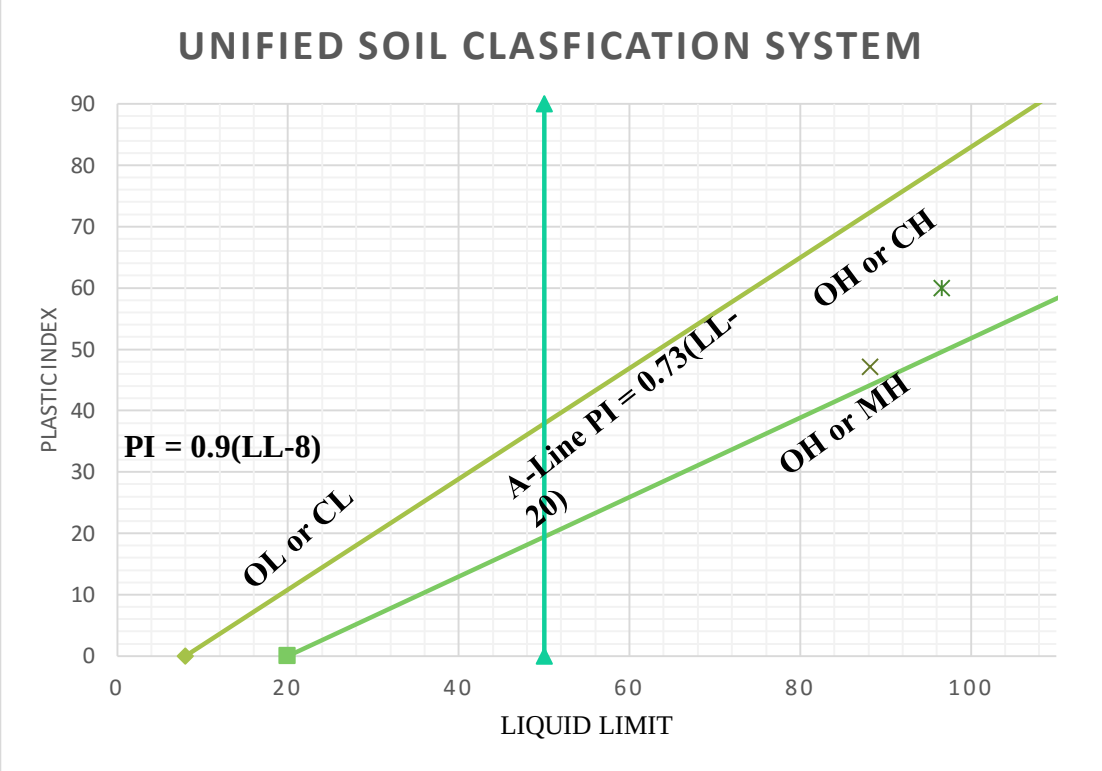

Fig 4. 4: Soil Classification according to Unified soil classification System.

According to USCS, if the Liquid limit are greater or equal to 50% the soil can be clay, silt, or organic depends on whether the soil coordinates plot above or below the A line. Since both soil sample has Liquid limit more than 50% and above A-Line, so they are classified under high to very high CH.

4.3.3.3 Compaction test results of natural subgrade soil

Standard Proctor compaction tests were conducted on the soil to determine the relationship between the moisture content and dry density for specific compaction effort according to AASHTO T99-94. The AK soil sample has optimum moisture content 33% and the

maximum dry density is 1.40gm/cm3.Also, the AC soil sample has optimum moisture content 28.5 % and the maximum dry density is 1.38gm/cm3 as shown below in Fig 4.5and 4.6

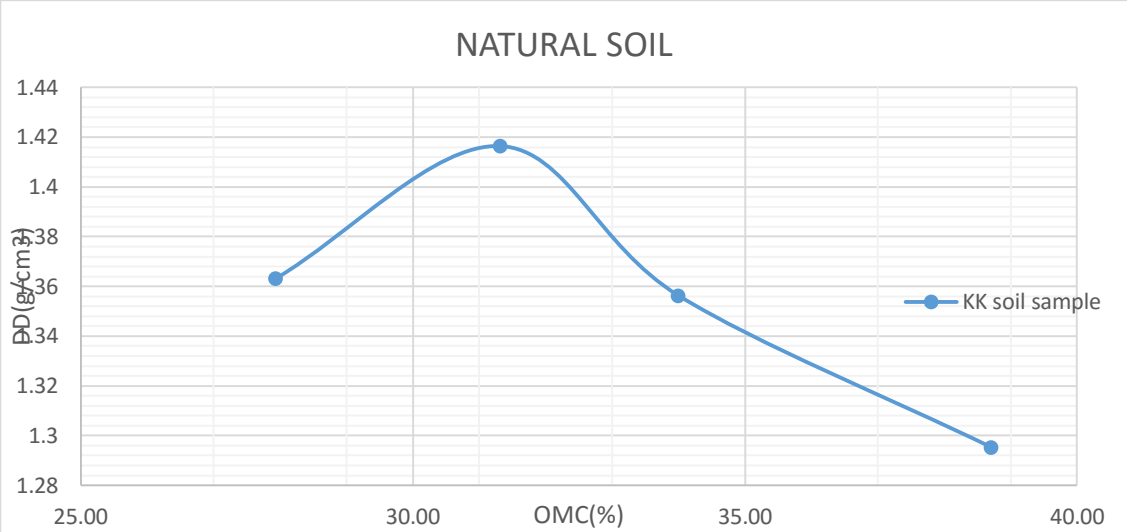

Fig 4. 5 Compaction test results of natural subgrade KK soil sample

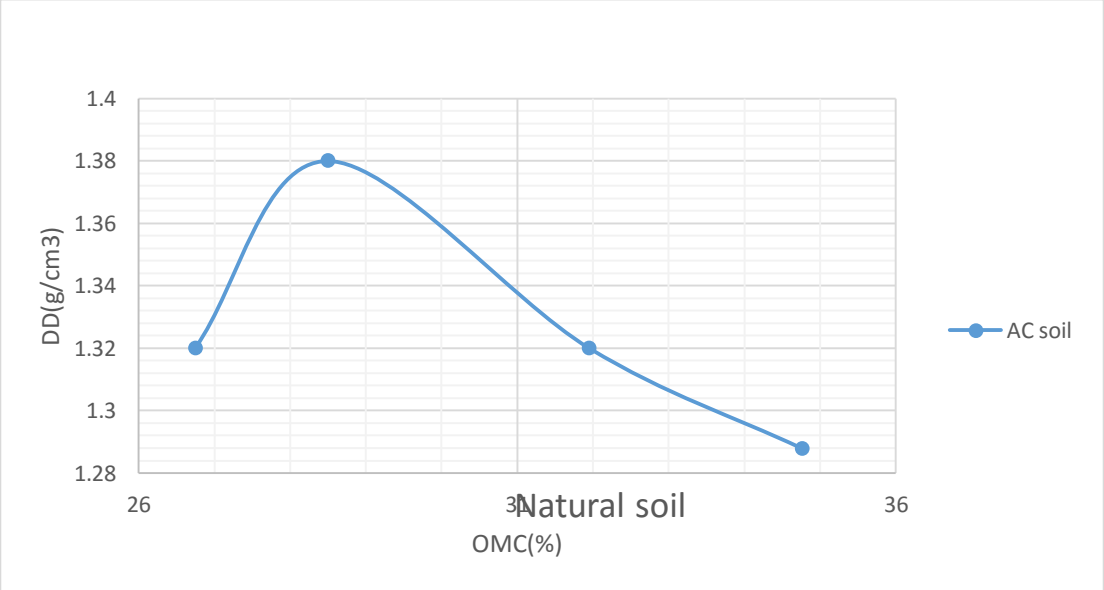

Fig 4. 6 Compaction test results of natural subgrade AC soil

4.3.3.4 CBR test result of natural subgrade soil and treated soil

Strength of the soil has also been determined. A three point (65,30 and 10 blows) soaked CBR test was conducted according to AASHTO T193, summary of results as presented

Table 4. 3: Summary of CBR Test results for KK and AC treated soil sample

Mix-ratio of additives(%)		**CBR Value (%)**						**CBR @ 95% MDD**	**ERA Requirement**	**Subgrade Class**
		10 blows		**30 blows**		**65 blows**				
Bagasse ashes	**lime**	**2.54 mm**	**5.08 mm**	**2.54 mm**	**5.08 mm**	**2.54 mm**	**5.08 mm**			
0	0	1.5	1.06	1.55	1.72	2.62	2.15	1.72	CBR >3%	S1
4	0	1.41	1.4	2.77	2.7	3.67	3.4	2.80	CBR > 3%	S1
4	1	2.34	2.09	2.65	2.33	2.92	2.62	3.96	CBR > 3%	S2
3	2	7.38	5.05	7.8	6.1	8.13	6.24	7.79	CBR > 3%	S3
2	3	8.25	6.6	8.4	7.2	8.97	7.95	9.35	CBR > 3%	S3
1	4	10.15	8.92	11.08	9.06	13.37	10.05	11.04	CBR > 3%	S4

Table 4. 4 Summary of CBR Test results for KK treated soil sample

Mix-ratio of additives(%)		CBR Value (%)						CBR @ 95% MDD	Era requirement	Subgrde Class
		10 blows		30 blows		65 blows				
Bagasse ashes	lime	2.54 mm	5.08 mm	2.54 mm	5.08 mm	2.54 mm	5.08 mm			
0	0	1.44	1.1	1.57	1.4	1.87	1.74	1.58	CBR > 3%	Control
4	0	2.7	1.96	2.77	2.32	2.98	2.43	2.78	CBR > 3%	S1
4	1	3.16	3.09	3.9	3.32	4.12	3.97	3.82	CBR > 3%	S2

3	2	8.1	7.05	9.15	8.2	10.08	9.05	6.21	CBR > 3%	S3
2	3	8.25	6.6	8.4	7.2	8.97	7.95	8.8	CBR > 3%	S3
1	4	9.72	8.94	10.1	9.22	11.59	10	10.4	CBR > 3%	S4

In table 4.3 and 4.4 it can be seen that, there was an initial increase from the control value of 1.57% to 9.8% for KK and 1.72% to 11.04% for AC levels of percentage of SCBA and lime mix-ratio. However, all mix ratios proportions satisfied the minimum requirements as per ERA specification used as a road subgrade material.

4.3.3.5 Laboratory test results of stabilized expansive soil

One of the important and principal aims of the present study was to evaluate the changes of liquid limits, plastic limits and plasticity index with addition of Sugar cane ash mixed with lime to the selected soil samples. To achieve this objective, liquid limit and plastic limit tests were conducted on sugarcane bagasse ash-limes-soil mixtures according to consistency test of AASHTO T89 and T90, respectively. Soil samples were first air dried and pulverized and then sieved with no 40 sieve. Soil passing no 40 sieve was mixed with different proportion of SCBA-lime at optimum water content and sealed with plastic for 24 hours in order to give sufficient time for chemical reaction before test. From Table 4.5 SCBA-lime-soil mixtures, the following observations have been made and/are illustrated in figure 4.4 and figure 4.5 below for AC and KK samples respectively.

Table 4. 5 Laboratory test results of stabilized expansive soil

Sample Location	**Mix-Proportion of additives (%)**		**Atterberg's Limit (%)**		
	Bagasse ashes	**Lime**	**Liquid Limit**	**Plastic Limit**	**Plasticity Index**
AC	0	0	88.15	40.6	47.55
	4	0	87.02	41.2	45.82

	4	1	79.62	44.1	34.6
	3	2	78.4	54.4	24
	2	3	76.79	63.2	13.59
	1	4	75.21	64.3	10 .91
KK	0	0	96.59	37.2	59.39
	4	0	94.93	44	50.93
	4	1	92.23	52.3	39
	3	2	89.6	66	25.6
	2	3	84.05	67.05	17
	1	4	80.04	68.2	11.84

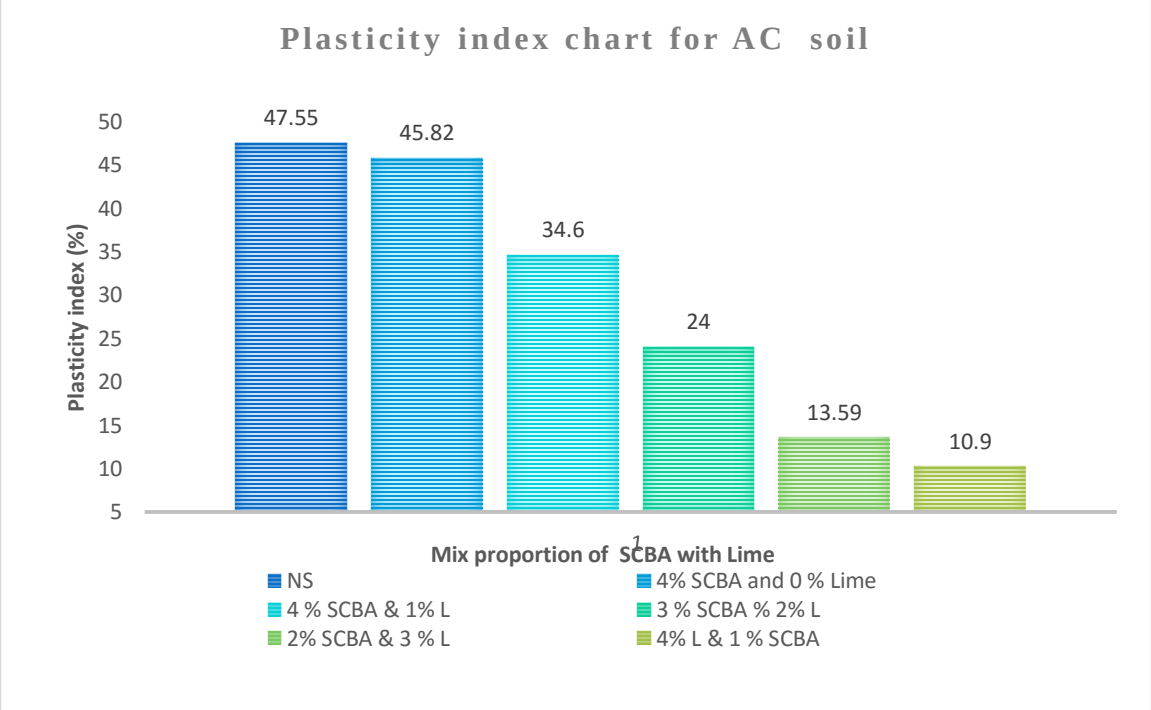

Fig 4. 7 Plasticity index chart for Stabilize AC soil Sample

- The Liquid limit decreases with slight changes for both soil samples from control value 88.15%-75.21.5% and 96.59%-80.04% for AC and KK soil sample respectively.

However, the additives not shown significant change on liquid limit of the soil because the dispersing effect of the additive doesn't affect the liquidity natures of the soil but its plastic limit only. It has been recognized that the type of mineral present in a soil type determines Cation exchange capacity and hence, the effect the addition of soil stabilizers will have on the Atterberg limits (Dainti, etal..., 2005). According to the results observed from the laboratory test, one can judge that the behavior of soil sample was changed from high plasticity soil to low plasticity soil. As a result, when the percentage of lime increased plasticity index of the treated soil samples are significantly decreased whereas it becomes increase when the percentage of SCBA increased, soil with SCBA mixed with Lime have brought very appreciable result in decreasing the plasticity index of both soil samples. According to ERA 2002 specification the maximum value of PI and LL were 30% and 60% respectively to use the soil as a subgrade material. Therefor both soil samples are satisfied ERA specification requirements are attained simultaneously at (1%SCBA + 4%L) regard to plasticity index

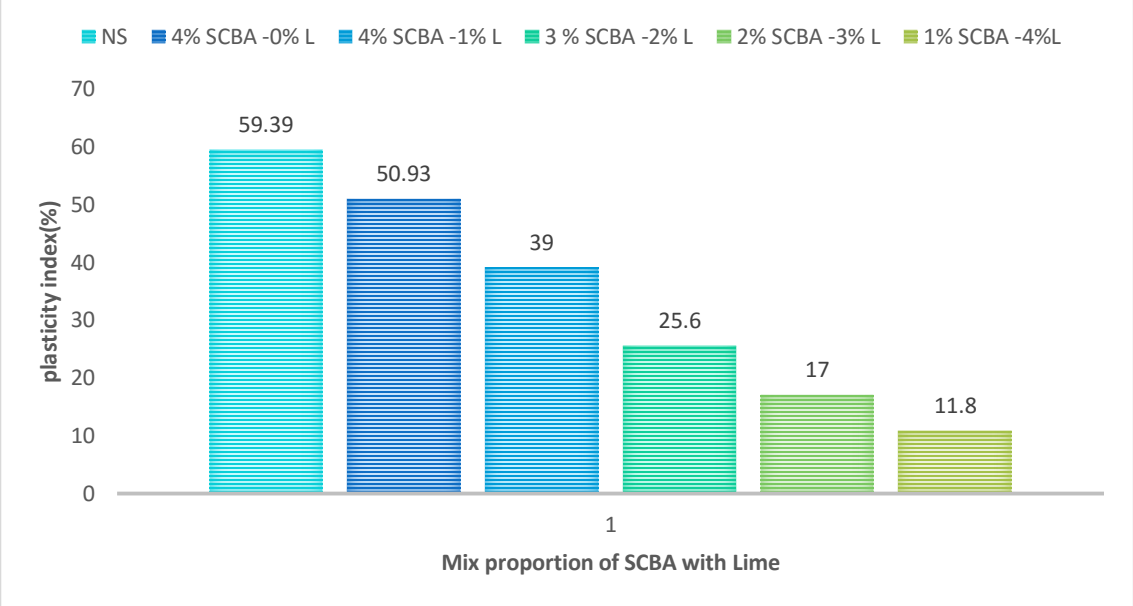

Fig 4. 8 Plasticity index chart for Stabilize KK soil Sample

Fig 4. 9 Plasticity index chart for Stabilize KK soil Sample

4.3.3.6 The effect of addition of Bagasse Ashe-Lime on Moisture density relationship

The detail process of standard Procter compaction test of both soil samples was presented in table below moreover, further laboratory test analysis data were illustrated in Appendix-A and B

Table 4. 6 The effect of addition of Bagasse Ashe-Lime on Moisture density relationship

AC				**KK**			
Mix-Proportion of additives (%)		**OMC (%)**	**MDD (gm/cm^3)**	**Mix-Proportion of additives (%)**		**OMC (%)**	**MDD (g/cm^3)**
Bagasse ashes	**Lime**			**Bagasse Ashe**	**Lime**		
0	0	33	1.30	0	0	31.3	1.41
4	0	34	1.29	4	0	32.12	1.30
4	1	28.3	1.26	4	1	29.17	1.34
3	2	27.6	1.32	3	2	27.68	1.35
2	3	27.3	1.36	2	3	26.88	1.37
1	4	26	1.37	1	4	26.5	1.40

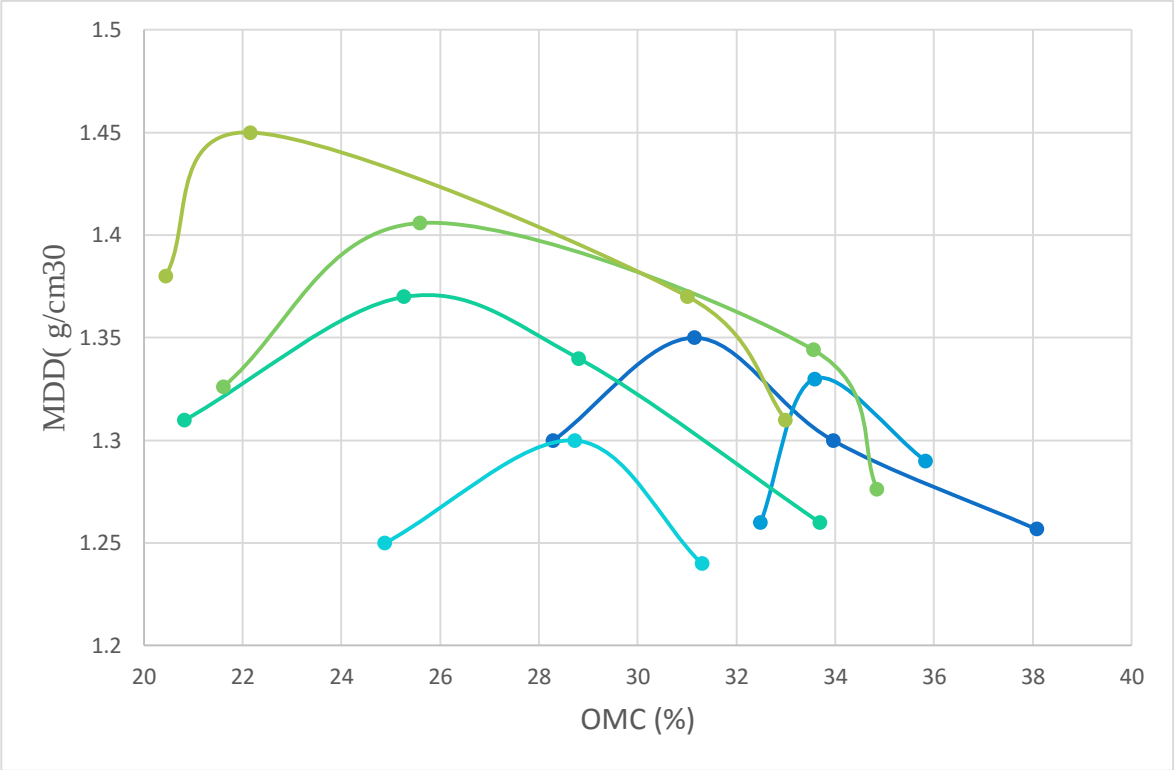

Fig 4. 10 : Summary of OMC and MDD of treated soil sample of AC

The MDD shows a slight increase and OMC shows a decrease in the treatment of weak subgrade soil with additive agent. The MDD increases from 1.26 g/cm^3 to 1.37 g/cm^3 and OMC decreases from 33% to 26%.

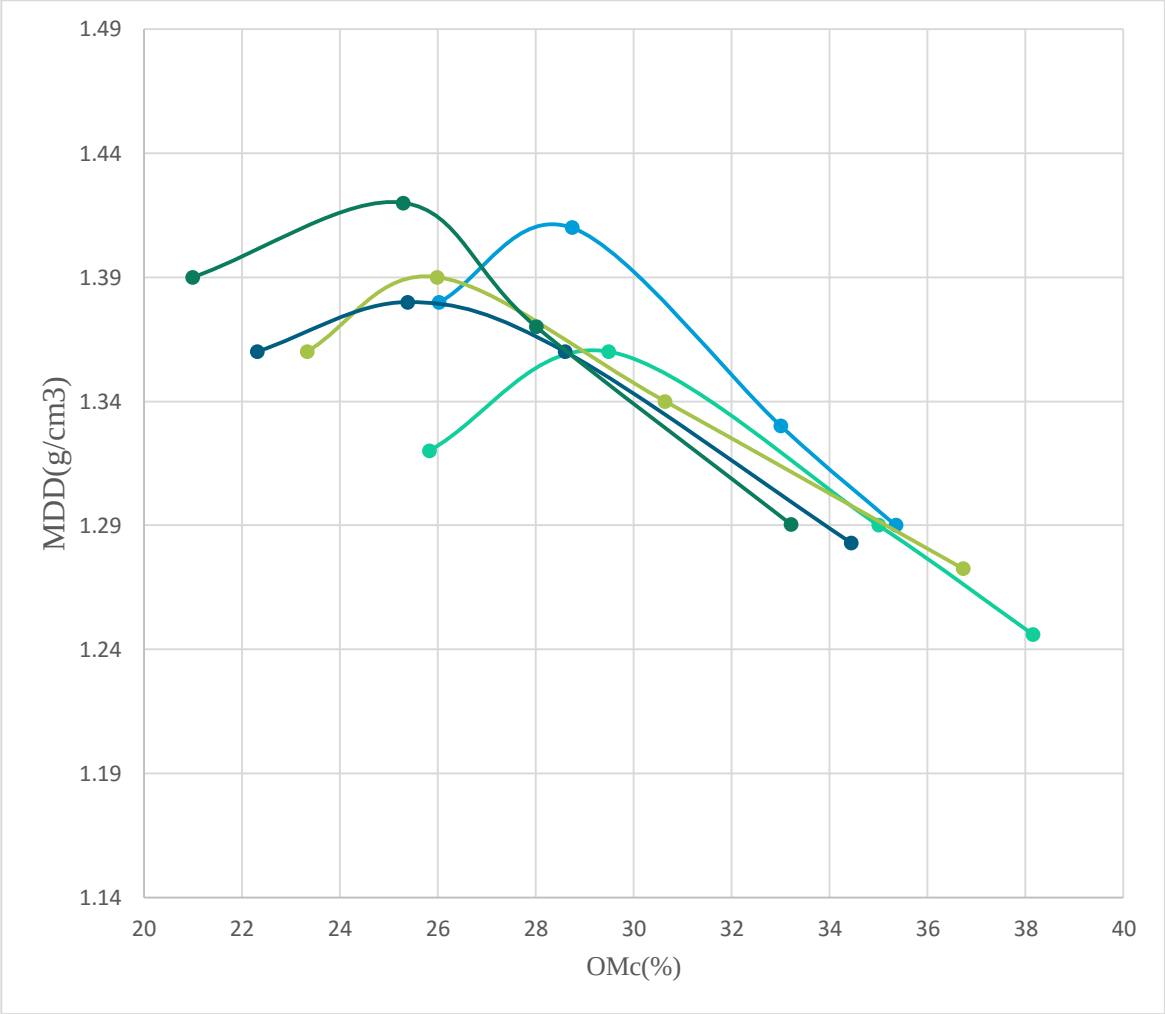

Fig 4. 11 : Summary of OMC and MDD of treated soil sample of KK

As it can be seen that from the above figure, the MDD shows a slight increase and OMC shows a decrease in the treatment of weak subgrade soil with SCBA-lime additive agents. The MDD increases from 1.34 g/cm^3 to 1.40 g/cm^3 and OMC decreases from 31% to 26.5%. Generally, in fig4.9 and 4.10 it can be seen that increasing the percentage of lime ratio in SCBA-lime mix-ratio leds increase in the maximum dry density and decrease optimum moisture content. But when increasing the percentage of sugar cane ash in SCBA-lime mix-ratio the maximum dry density becomes decreased and also the optimum moisture content increased.

4.4 Simulation Result

Finite element methods are one of the techniques available for determining road pavement responses to the applied traffic loads. Flexible pavement analysis is performed using finite element method; a 3-D dimensional finite element model using ABAQUS (ver. 6.14-1) computer program are developed. The pavement response such as, stress, strain and number of load repetition are investigated with stabilization of subgrade materials

4.4.1 Material Properties and Pavement Geometry

Table 4. 7 Material Properties and pavement geometry

Section	Element	Thickness (mm)	E (MPa)	ν	Material Properties
HMA	20-noded solid	50	3000	0.35	Isotropic and Linear Elastic
Base	20-noded solid	175	300	0.30	Isotropic and Linear Elastic
Subbase	20-noded solid	175	175	0.30	Isotropic and Linear Elastic
Stabilized subgrade	20-noded solid	Trial and errors (100,150 and 200)	110.79	0.40	Isotropic and Linear Elastic
Natural subgrade	20-noded solid	21	17.05	0.40	Isotropic and Linear Elastic

Material properties of all layers were considered homogenous linear elastic in this model, and all layers were characterized by their elastic moduli and Poisson's ratios. Assuming the pavement materials behave elastically is appropriate for short-timed studies since non elastic material behavior requires many input parameters that are not readily available and might be assumed. Assumed parameters will not accurately produce reliable results

Therefore, elastic properties of pavement materials were appropriate for this model and this investigation.

4.4.2 Loading and Boundary Condition

The boundary condition used in this 3D model were the conventional ones which are basically rollers along the sides of the model where no horizontal movement is allowed and fixed at the bottom of the subgrade layer where no deflection existed beyond a specific depth The 3-D finite element model developed using ABAQUS/CAE 6.14-1 has dimensions 3.2 by 3.2. The side boundary of the model is approximately 20 times the tire radius in order to minimize edge effects. The subgrade layer, which implicitly is assumed to be 140 times the radius.

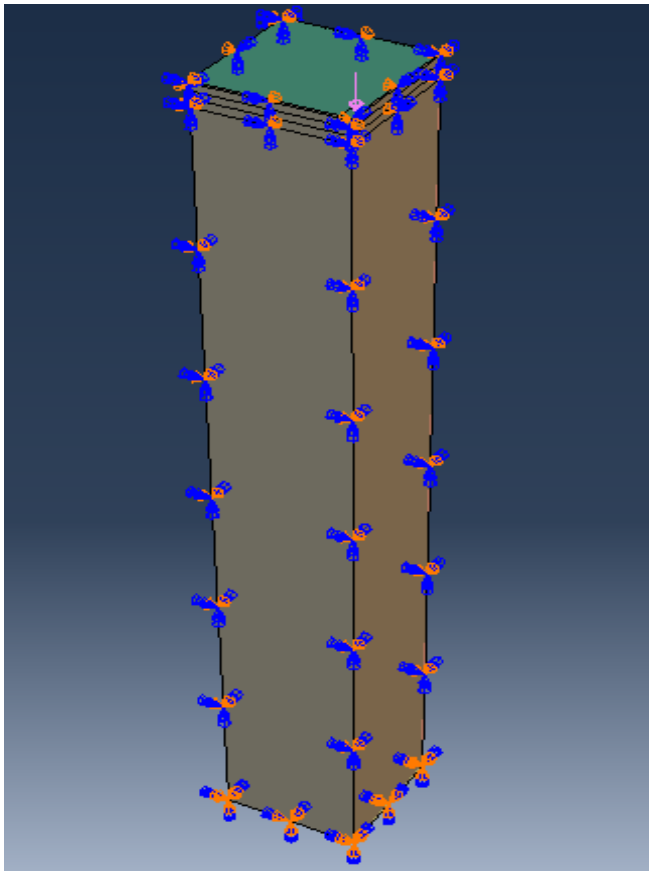

Fig 4. 12 Boundary condition and loading of flexible pavement (3D-FE) model analysis for stresses and strains characteristic behavior applying dual tires.

4.4.3 Model Mesh and Element Type

Partitioning of the problem into small discrete elements (mesh), is very important for formulating an approximation to the stress and strain variations across each individual element**.** Therefore, the pavement layer was seeded at 0.025 m at the loading area because displacement gradients are higher in this region, while other areas were seeded at 0.1 m; as a result, meshes are fine in/near loading area and coarse at distances away from applied load for efficient modelling, the 20-node quadratic brick with reduced integration (C3D20R) was employed for this model since quadratic elements produce more accurate results than linear elements (C3D8R)

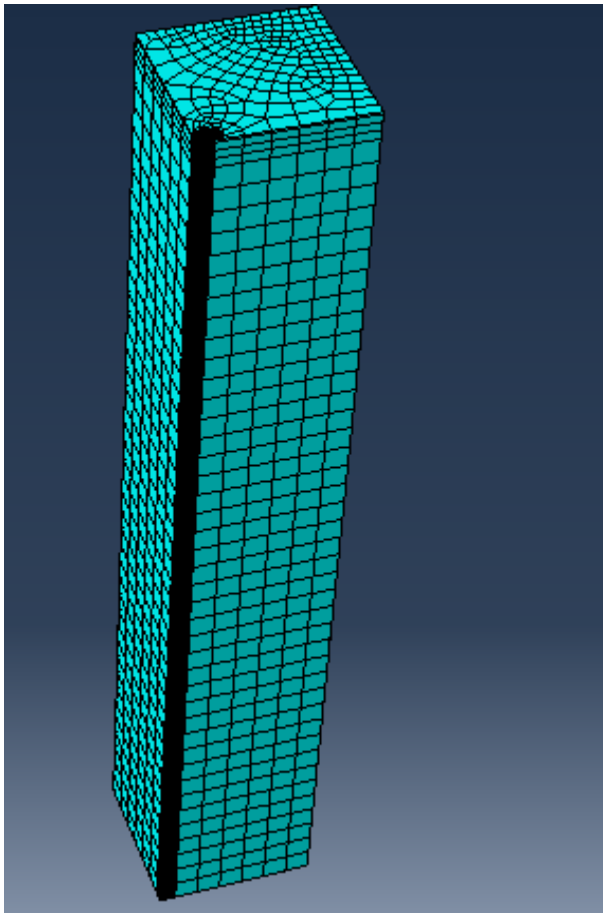

Fig 4. 13 Model meshing of flexible pavement (3D-FE)

4.4.4 Effect of treated and untreated subgrade at the Bottom of HMA Layer and at the Top of Subgrade

The main output for pavement analysis are the critical response points which represent the vertical and horizontal Tensile Strain at the bottom of HMA and Vertical Compressive Strains at the Top of Subgrade due to applied traffic axle load. In this section the distribution of strains over the whole pavement structure are enumerated since the finite element technique is to obtained approximate solution in continuum structure of pavement (each divided small point in the mesh). Figure 4.13) and (4.14) the horizontal tensile strain distribution at the bottom of HMA for both stabilized and un stabilized material respectively for pavement under the static wheel load. As it can be seen from the analysis, the contours' range of the linear elastic model has maximum horizontal tensile strain ($1.490\times10^{-4)}$ μm) without stabilization and then decreased gradually with the maximum horizontal strain to reach about (1.351×10^{-4} μm) with stabilization corresponding to approximately (9.32%) strain reduction with the reinforcement of subgrade and also in Fig 4.15 and 4.16 it can be seen that the vertical compressive strains at the top of subgrade which the contours' range of the linear elastic model shows that the maximum vertical compressive strain (2.555×10^{-4} μm) without stabilization then decreased to (1.446×10^{-4} μm) with stabilization which is almost 43% strain reduction at the top of subgrade. The increasing and decreasing of vertical compressive strain and horizontal tensile strain indicate that natural subgrade layer in this simulation are about less in stiffness without stabilization than that of the vertical strain with stabilization at the bottom of HMA layer and at the top of subgrade respectively.

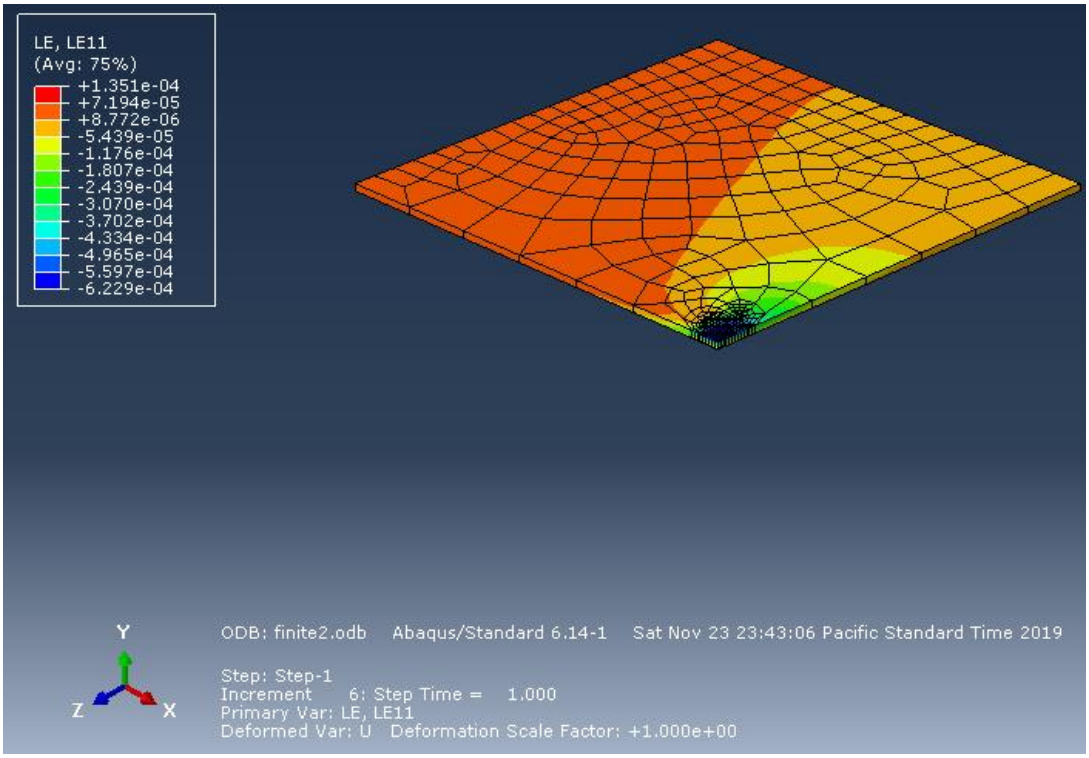

Fig 4. 14 Horizontal tensile strain at the bottom of HMA of flexible pavement with stabilization

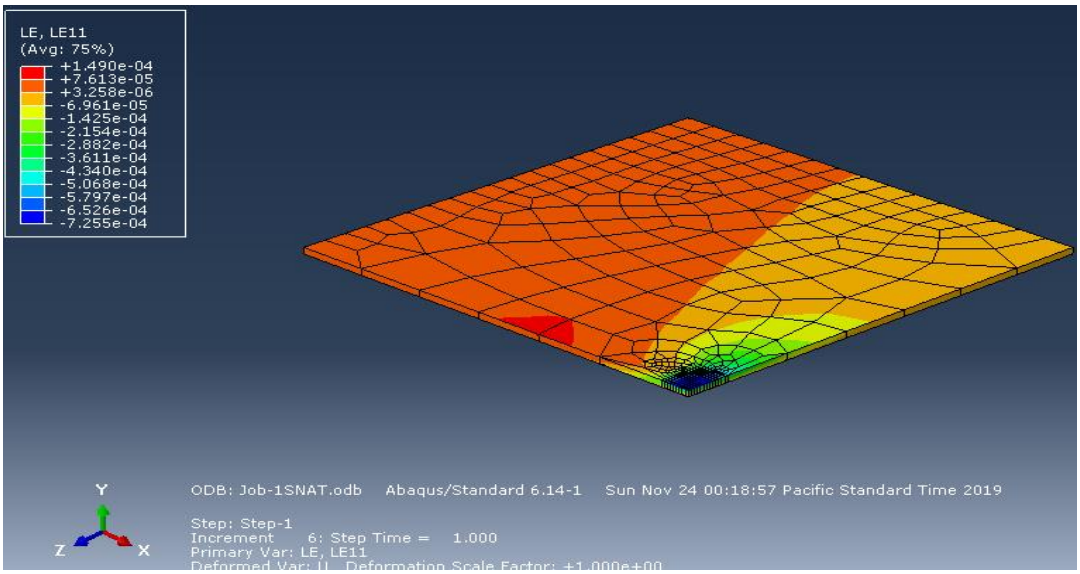

Fig 4. 15 Horizontal tensile strain at the bottom of HMA without stabilization

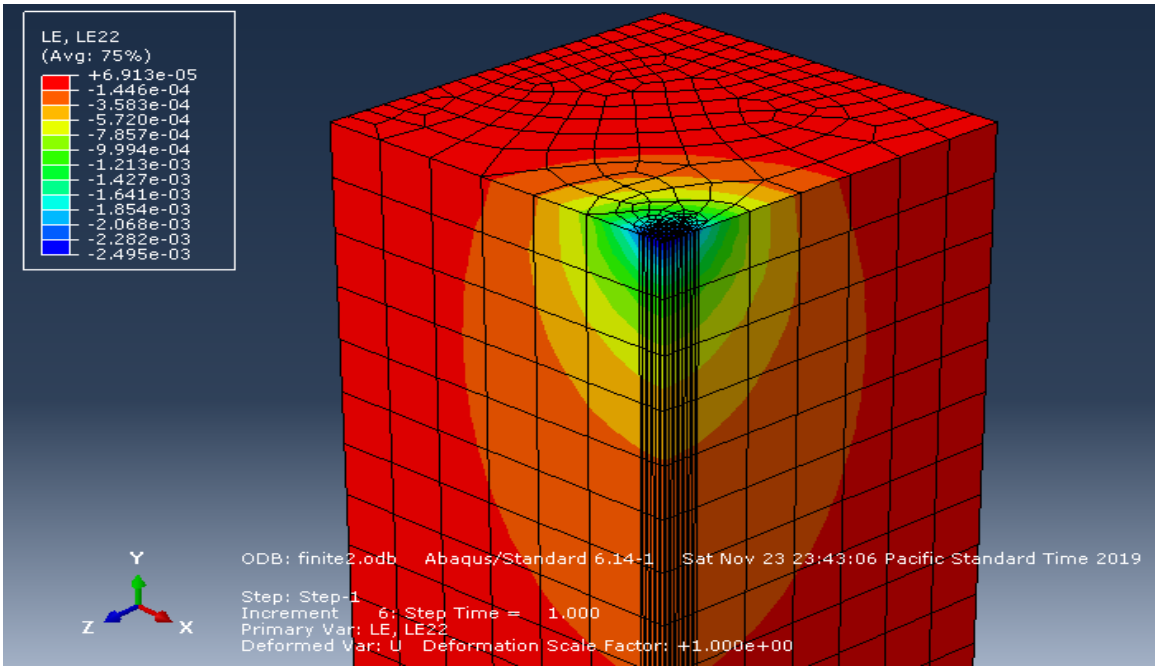

Fig 4. 16 Vertical compressive strain (εv) at the top of subgrade (με) with stabilization

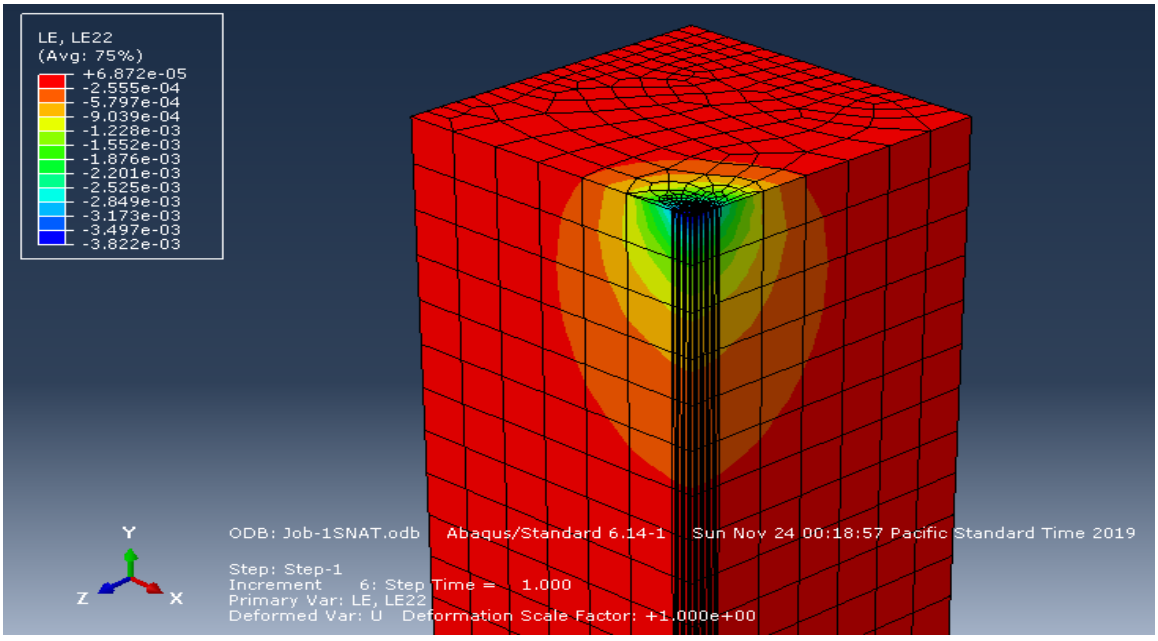

Fig 4. 17 Vertical compressive strain (εv) at the top natural subgrade (με) without stabilization

3D FEM Response of Pavement structure

There are four critical responses which play a vital role in flexible pavement design. These responses are surface deflection at the center of loading, tensile strain at the bottom of the asphalt layer, vertical strain, and stress at the top of the subgrade layer the result are as shown in table 4.8 below

Table 4. 8 Pavement Responses from Three Dimensional Linear Elastic Analyses with and without treatment of subgrade

Pavement Response	ABAQUS Linear Elastic Analysis Three-Dimensional Model (20R X 140R)			
	Unit	Stabilized	Un stabilized	Difference (%)
Surface Deflection	mm	0.00593	0.00719	0.126
Tensile Strain at the bottom of HMA layer	με	0.000118	0.000245	0.0127
Tensile Stress at the bottom of HMA layer	MPa	-0.192513	0.69055	49.803
Vertical Strain at the top of Subgrade	με	-0.0145575	-0.00686548	0.769
Vertical Stress at the top of Subgrade	MPa	–0.0595	–0.0653	0.58

However, for the analysis purpose depending on specific objectives only table 4.9 and 4.10 respectively can be used. The critical responses are, tensile strain at the bottom of the asphalt layer and, vertical strain at the top of the subgrade layer with and without subgrade treatment

Table 4. 9 Pavement Responses from Three Dimensional Linear Elastic Analyses with treatment of subgrade at the top of natural subgrade and bottom of HMA.

	ABAQUS Linear Elastic Analysis		
Pavement response	Three-dimensional model (20R X 140R)		
	100 mm	**150mm**	**200mm**
ε_t at the bottom of AC(με) with subgrade treatment	0.0001511333	0.00013091	0.000118439
ε_v at the top of stabilized subgrade (με)	0.00432955	0.00406845	0.00157021
ε_v at the top of Natural subgrade (με)	-0.0215759	-0.0178682	-0.0145575

Table 4. 10 Pavement Responses from Three Dimensional Linear Elastic Analyses without treatment of subgrade at the top of natural subgrade and bottom of HMA.

	ABAQUS Linear Elastic Analysis	
Pavement response	Three-dimensional model (20R X 140R)	
ε_t at the bottom of AC(με)	50mm	0.000245172
ε_v at the top of natural subgrade (με)	At debth 0.4	-0.00686548

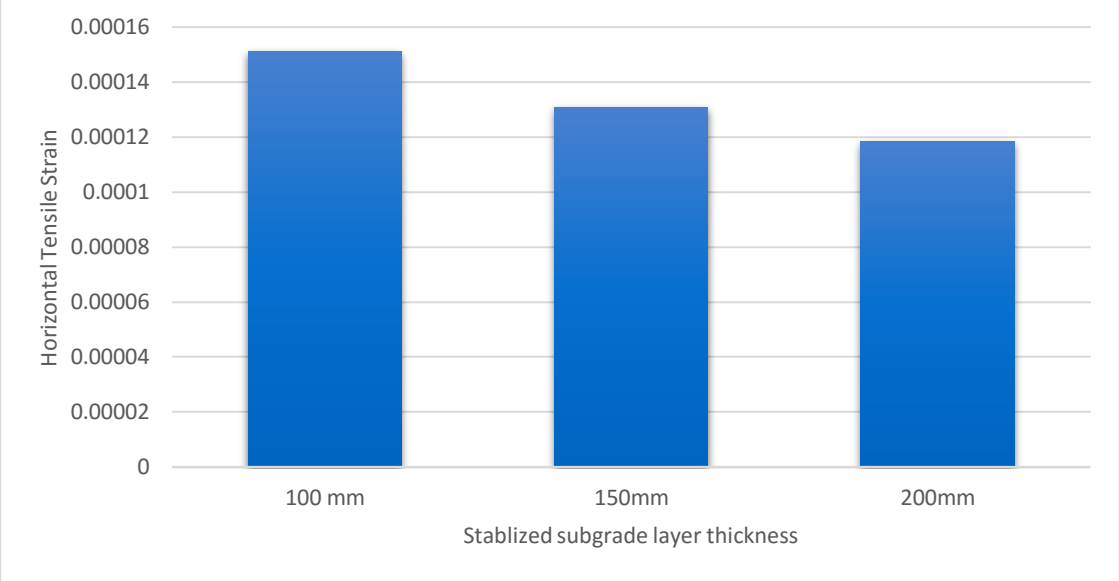

Fig 4. 18 Effect of horizontal tensile strain at the bottom of HMA layer when the subgrade stabilized with (200 ,150 ,100) thickness

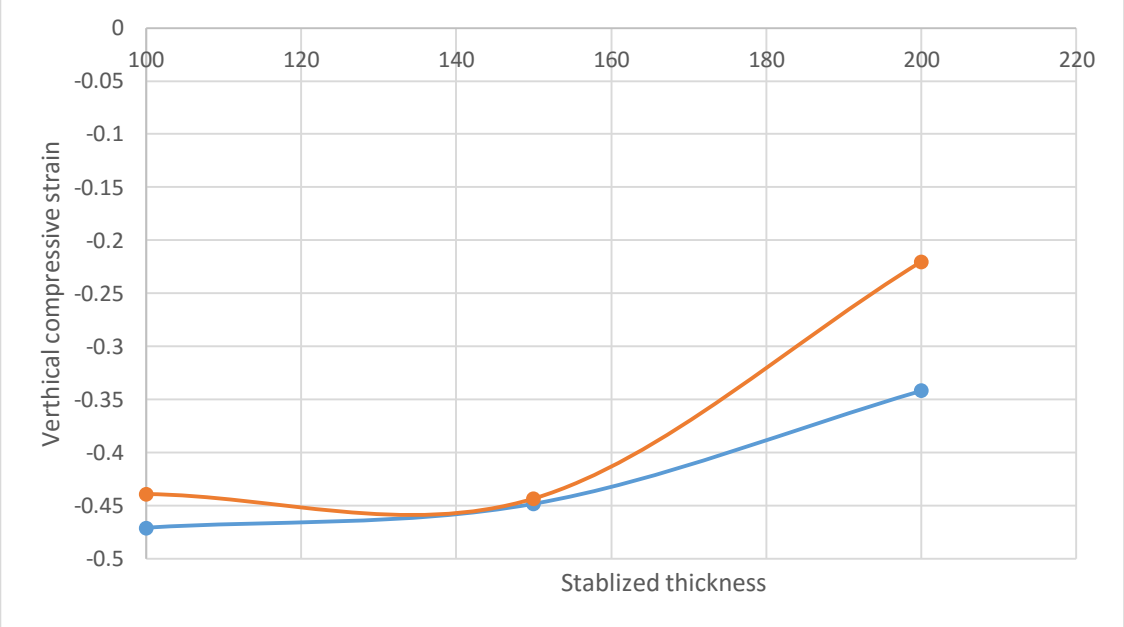

Fig 4. 19 Vertical compressive strains at the top of natural subgrade versus stabilized subgrade thicknesses

It can be seen from the table 4.10 that the vertical strain at the top of subgrade layer decreases with increasing the thickness of stabilized subgrade. It appeared that the decreasing in percentage of the vertical strain with increasing the stabilized subgrade

thickness. The three-dimensional finite element model was conducted to study the effect of stabilized subgrade presence on the tensile strain at the bottom of asphalt layer. The model was run several times on a stabilized section by changing the Stabilized subgrade layer thickness. The results showed that flexible pavement with a stabilized subgrade layer produces lower tensile strain than the flexible pavement without a stabilized layer as shown in table 4.11and 4.12 respectively. Similarly, the vertical compressive strain and stress at the top of sub-grade layer decrease with the stabilized layer thickness increase.

4.4.5 Predicting Pavement Distress/Failure

Pavement distress/failure will provide the relationship between the critical pavement response and the allowable number of load applications before failure. Two types of failure modes that occur in a pavement system are rutting and fatigue cracking. Pavement damage models used in predicting failure in pavement systems are empirical-mechanistic models that calculate the deformation and fatigue cracking in the pavement systems (AASHTO, 2008). The results obtained from this analysis was used to determine the performance of the pavement under heavy loading conditions The predicted analysis based on Asphalt Institute Response model as shown below table 4.11

Table 4. 11 Fatigue and rutting failure analysis based on Asphalt Institute Response

Stabilized subgrade Layer Thickness (mm)	Fatigue Criterion		Rutting Criterion	
	Tensile Strain Ɛt at the bottom of HMA layer	No. of Load Repetitions to Failure N_f	Vertical Strain (Ɛc) in stabilized Sub-grade	No. of Load Repetitions to Failure N_r
100	0.0001511333	3.2E+08	0.0215759	0.039065
150	0.00432955	5.13E+08	0.0178682	0.090596
200	0.0215759	7.14E+08	0.0145575	0.225593
Un stabilized	0.000245172	6.5E+07	0.00686548	0.0064655

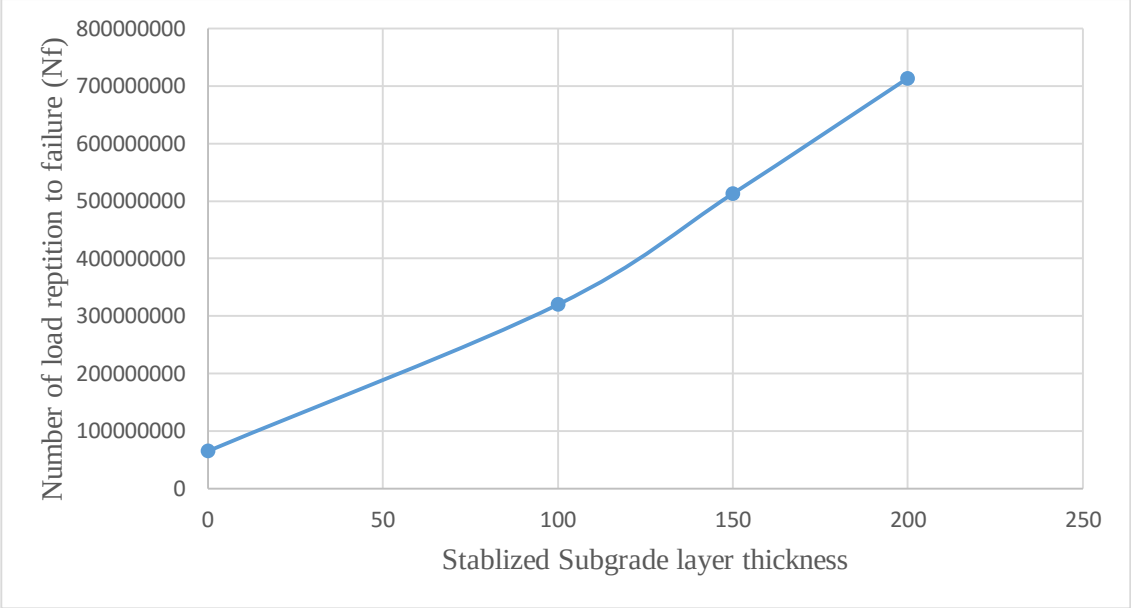

Fig 4. 20 Load Repetition for Bottom-HMA layer for Different Subgrade Stabilization Layers (ABAQUS predicted strain responses)

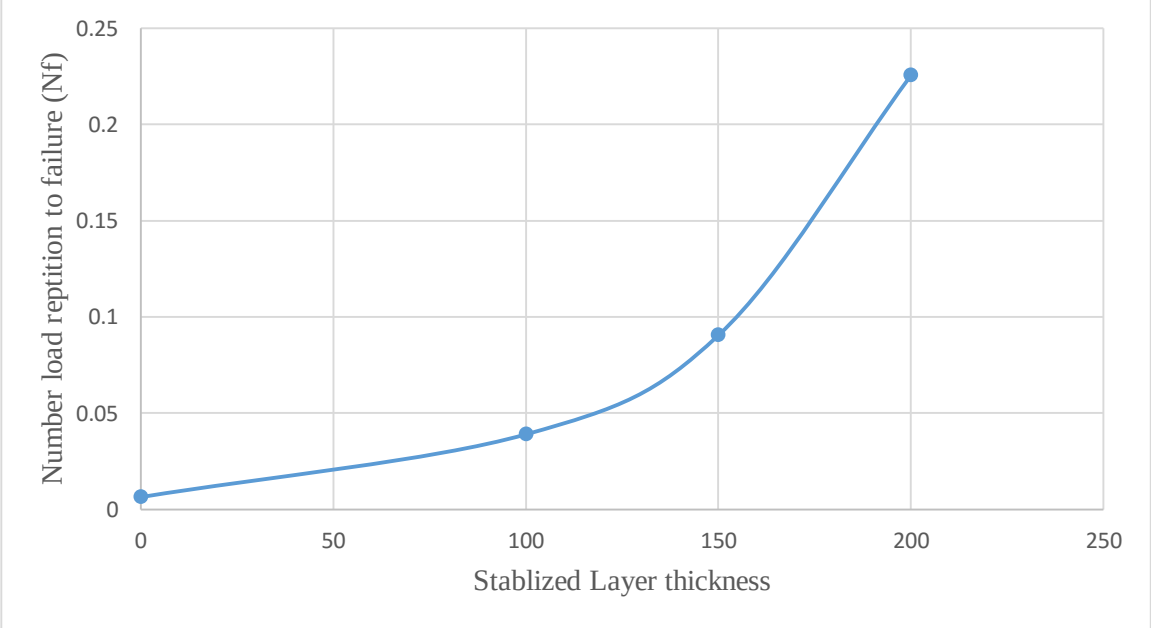

Fig 4. 21 Load Repetition at the top of stabilized subgrade for different Subgrade Stabilization Layers (ABAQUS predicted strain responses)

From above figure 4.19 it can be seen that number of load repetition increases from with treatment of subgrade thickness (100,150 and 200) respectively at the bottom of asphalt layer and from the fig 4.20 it can be seen that number the of load repletion increases with treatment of subgrade thickness (100mm,150mm and 200mm) at the top of subgrade respectively, therefore, it can be concluded that the minimum required stabilized thickness was found to be significantly influenced by the number of the expected load repetitions. As the number of load repetitions increases, the desired minimum thickness increase.

CHAPTER FIVE

CONCLUSION AND RECOMMENDATION

As a result of the experimental, modelling and simulation which were performed in this study the following conclusions were obtained;

5.1 Conclusion on Experimental Result

1. As observed from the test was performed under this study, the maximum results were achieved at 1 % SCBA with 4% lime by weight. Since most parameters achieve the ERA requirement and have got maximum strength or CBR value.

2. CBR test, there was an initial increase from the control value of 1.57% to 9.8% for KK and 1.72% to 11.04% for AC levels of percentage of SCBA and lime mix-ratio. However, all mix ratios proportions satisfied the minimum requirements as per ERA specification used as a road subgrade material.
3. SCBA standalone is not improving some of the engineering properties of highly plastic clay soils. However, SCBA mixed with lime can effectively stabilize this poor soil. Therefor mixing of the two stabilizers can effectively treat the poor geotechnical properties of the weak.
4. The MDD shows a slight increase and OMC shows a decrease in the treatment of weak subgrade soil with SCBA-lime additive agents. For AC, MDD increases from 1.320 g/cm^3 to 1.346 g/cm^3 and OMC decreases from 33% to 26.5%. For KK, MDD increases from 1.34 g/cm^3 to 1.40 g/cm^3 and OMC decreases from 33% to 26% at optimum mix-ratio of at (1%SCBA + 4%L). Generally, when increasing the percentage of lime in SCBA-lime mix-ratio led increase in the maximum dry density and decrease optimum moisture content rather than SCBA.

5.2 Conclusion on Simulation Result

1 Increase in the thickness (100,150 and 200 mm) of stabilized subgrade layer increases the resistance of pavement to failure in terms of strains at the top sub-grade layer and at the bottom of HMA layer.

2 Subgrade stabilization does not only reduce the level of vertical compressive strain in subgrade but also reduces the tensile strain at bottom of asphalt layer

3 It was found from the finite element analysis that including the stabilized subgrade into pavement structure significantly reduces the tensile strain at the bottom of the asphalt layer which is a major cause of pavement cracking.

4 The minimum required thickness was found to be significantly influenced by the number of the expected load repetitions. As the number of load repetitions increases, the desired minimum thickness increase with stabilized subgrade.

5 The contours' range of the linear elastic model has maximum horizontal tensile strain ($1.490\times10^{-4)}$ μm) without stabilization and then decreased gradually with the maximum horizontal strain to reach about (1.351×10^{-4} μm) with stabilization corresponding to approximately (9.32%) strain reduction with the reinforcement of subgrade at the bottom of HMA layer and also the vertical compressive strains at the top of subgrade which the contours' range of the linear elastic model shows that the maximum vertical compressive strain (2.555×10^{-4} μm) without stabilization then decreased to (1.446×10^{-4} μm) with stabilization which is almost 43% strain reduction at the top of subgrade with the stabilization of subgrade. The increasing and decreasing of vertical compressive strain and horizontal tensile strain indicate that natural subgrade layer in this simulation are about less in stiffness without stabilization than that of the vertical strain with stabilization at the bottom of HMA layer and at the top of subgrade respectively.

5.3 RECOMMONDATION

The study was done for specific area and specific stabilizers; it is recommended as more investigation shall be performed on different parts of the country by mixing with other stabilizers such as Cement. The present study was conducted by taking limited parameter. The numerical analyses here were conducted to study the performance of stabilized and unestablished pavement cross-section under static loadings. It is recommended to extend the study to dynamic loading. It is also recommended to use the concept of interface interlocking and shear strength towards the purpose.

REFERENCE

1) ASHTO, 1993. ASHTO guide for design of pavement structures, s.l. Washington, D.C.

2) Abaqus, 2003. *Analysis of geotechnical problems with ABAQUS,* s.l. ABAQUS .

3) Adu-Osei, A., 2001. *Characterization of Unbound Granular Layers in Flexible Pavements,* Texas: Technical Reported, Texas A&M University Texas Transportation Institute College Station.

4) Alavéz-Ramírez, R. et al., 2012. The use of sugarcane bagasse ash and lime to improve the durability and mechanical properties of compacted soil blocks. *Construction and Building Materials,* Volume 34, pp. 296-305.

5) Al-Azzawi, A. A., 2012. Finite element analysis of flexible pavements strengthened with geogrid. *ARPN Journal of Engineering and Applied Sciences,* Volume 7(10), pp. 1295-1299.

6) Amruta P. Kulkarni, M. K. S P., 2016. Black cotton soil stabilization using bagasse ash and lime. p. 460–471.

7) Association, P. A. P., 2006. *Providing Quality Service to Pennsylvania's Hot-Mix Asphalt Industry,* s.l.: Pennsylvania.

8) Bindu , J. & Vysakh, . P., 2012. Stabilisation of Lateritic soil using coconut shell, leaf and husk ash. *Institution of Electrical and Electronics Engineers,* Volume 12, pp. 247-279.

9) Blight, G., 1897. *Mechanics of Residual soils,* netherlands: in A.A Balkema, the Netherlands.

10) Chusilp, N., Likhitsripaiboon, N. & Jaturapitakkul, C., 2009. Development of bagasse ash as a pozzolanic material in concrete. *Asian Journal on Energy and Environment,* Volume 10(3), pp. 50-62.

11) Dainti, etal..., 2005. *Family of compaction curve for chemicaly modified soils.* s.l.:Joint Transportation Research Program, INDOT and Purdue University, West Lafayette, Indiana, US..

12) ERA, 2013. *ERA pavement design manual.* Addis ababa, Addis Ababa Ethiopia..

13) Ghanizadeh, A. R. & Ziaie, A., 2015. NonPAS: A Program for Nonlinear Analysis of Flexible Pavements. *International Journal of Integrated Engineering,* 7(1), pp. 21-28.

14) Guilherme , C. et al., 2004. Influence of mechanical grinding on the pozzolanic activity of residual sugar cane bagasse ash. *Engng. Agric,* Volume 24(3), p. 484 – 492.

15) Hejazi, S. M., Sheikhzadeh, M., Abtahi, S. & Zadhoush, A., 2019. A simple review of soil reinforcement by using natural and synthetic fibres. *Construction and Building Materials,* Volume 30, pp. 100-116.

16) Helwany, S., Dyer, J., & Leidy, J, 1998. Finite-element analyses of flexible pavement. Volume 124(5), 491-499..

17) Heyns, . M. W. & Mostafa , H. M., 2013. South Africa Class F Fly Ash for roads physical and chemical analysis. *Interim: Interdisciplinary Journal,* Volume 12(3), pp. 28-41.

18) Inc, A., 2003. *Analysis of geotechnical problems with ABAQUS,* s.l.: Abaqus Inc.

19) Jimoh, Y A; Apampa, O A, 2014. An Evaluation of the Influence of Corn Cob Ash on the Strength of subgrade. *Civil and Environmental Research, University of Ilorin, Nigeria,* 6(5).

20) Kim, M., 2007. *Three-Dimensional Finite Element Analysis of Flexible Pavements Considering Nonlinear Pavement Foundation Behaviour,* s.l.: Department of Civil Engineering, Graduate College of the University of Illinois at Urbana Champaign.

21) Kordi, N., Endut, I. R. & Baharom, B., 2010. *Types of Damages on Flexible Pavement for Malaysian Federal Road.* s.l., Proceeding of Malaysian Universities Transportation Research Forum and Conferences.

22) Laboratory, T. O. R., 1993. *A Guide To The Structural Design Of Bitumen Surfaced Road in Tropical and Sub-Tropical Countries,* s.l.: Transportation Of Research Laboratory (TRL).

23) Lanham, M., 1996. *National Asphalt Pavement Association Research and Education Foundation,* s.l.: s.n.

24) Mallela, J., Harold Von Quintus, P. E., Smith, K. L. & Consultants, E. R. E. S., 2004. *Consideration of lime-stabilized layers in mechanistic-empirical pavement design,* s.l.: The National Lime Association.

25) Mengesha, 1886. *Geological Map of Ethiopia,* addis ababa: Addis Ababa, Ethiopia.

26) Mgangira, M. B., 2006. Laboratory assessment of the influence of the proportion of waste foundry sand on the geotechnical engineering properties of clayey soil. *Journal of the South African Institution of Civil Engineering ,* Volume 48(1), pp. 2-7.

27) Molenaar, A. A. A., 2009. *Part III: Design of flexible pavements.* [Online] Available at: http://www.citg.tudelft.nl.[Accessed 28 4 March 2014].

28) Muench, S., Mahoney, J. & Pierce, L., 2003. *The WSDOT Pavement Guide Interactive,* s.l.: Olympia, WA.

29) NCHRP, 2003. *Guide for Mechanistic-Empirical Design of New and Rehabilitated Pavement Structures,* Washington D.C: Transportation Research Board.

20) Nunes, N., Bridges, M. & Dawson, A., 1996. Assessment of secondary materials for pavement construction. *Technical and Environment aspects Waste management,* Volume 16(1-3), pp. 87-96.

21) Officials, A. A. o. S. H. a. T., 1993. *AASHTO Guide for Design of Pavement Structures,* Washington: Washington, D.C.

22) Openshaw, S. C., 1992. *Utilization of Coal Fly Ash,* s.l.: Master's thesis, Department of Environmental and Civil Engineering University of Florida.

23) Peng, Y. & He, Y., 2009. Structural characteristic of cement-stabilized soil bases with 3D finite element method. *Front Architect Civil Engineering China,* Volume 3(4), pp. 428-434.

24) Rodrigue , J., Slack , B. & Comtois , C., 2013. *Transportation modes,* New York: An overview In Rodrigue J The geography of transportation systems.

25) Shafabakhsh, G., Motamedi, M. & Family, A., 2013. Influence of Asphalt Concrete Thickness on Settlement of Flexible Pavements. *Electronic Journal of Geotechnical Engineering,* Volume 18, pp. 473-483.

26) Sherwood, P., 1974. *The use of waste and low-grade materials in road construction: guide to materials available,* s.l.: TRB publication.

27) Somal, G. S., Singh, G. & Walia, B., 2017. Effect of cement and corn cob ash on UCS and direct shear test of clayey soil. *International Journal of Advanced Research and Development,* 2(5), pp. 559-566.

28) Whitlow, R., 1995. *Basic Soil Mechanics.*s.l.:Addison Wesley longman limited:Edinburgh Gate.

29) Yadu, L. & Tripathi, R., 2013. Stabilization of Soft Soil with Granulated Blast Furnace Slag and Fly Ash. *International Journal of Research in Engineering and Technology,* Volume 2(2), pp. 115-119.

30) Yagawa, G., 209. Free Mesh Method fundamental conception algorithms and accuracy study. *Proceedings of the Japan Academy,* Volume 87(4), p. 115.

Appendix A

Laboratory Test Result of AC Soil sample

1 Wet Sieve Analysis KK soil sample

sieve number	sieve size(mm)	mass of retained(g)	percentage of retained%	percentage of cumulative retained%	percentage of finer particle
4	4.750	0.56	0.056	0.056	99.944
10	2.000	1.90	0.19	0.246	99.754
20	0.850	7.66	0.766	1.012	98.988
40	0.425	6.98	0.698	1.71	98.29
60	0.300	7.35	0.735	2.445	97.555
140	0.150	5.34	0.534	2.979	97.021
200	0.075	24.97	2.497	5.476	94.524
Pan		945.24	94.52	100.000	0.000
	Total	1000.000			

2 Wet Sieve Analysis AC soil sample

sieve number	sieve size(mm)	mass of retained(g)	percentage of retained%	percentage of cumulative retained%	percentage of finer particle
4	4.750	1.71	0.171	0.171	99.829
10	2.000	20.2	2	2.171	97.829
20	0.850	14.43	1.443	3.614	96.386
40	0.425	13.60	1.36	4.974	95.026
60	0.300	12.65	1.265	6.239	93.761
140	0.150	2.02	0.202	6.441	93.559
200	0.075	6.26	0.626	7.067	92.933
Pan		929.13	92.913	100.000	0.000
	Total	1000.000			

3 Hydrometer Analysis

Elapsed time (min)	Temperature	actual hyd. Reading	L(HR+1) Corrected Reading (Rc)	K	D	Ct	a	Percentage of finer %
1	20	40	41	0.013644	0.0874	0	0.98669	62.29
2	20	35	36	0.013644	0.0579	0	0.98669	52.90
5	20	33	34	0.013644	0.0371	0	0.98669	49.14
15	20	30	31	0.013644	0.0196	0	0.98669	43.50
30	21	28	29	0.013474	0.0134	0	0.98669	40.21
60	20	26	27	0.013644	0.0092	0	0.98669	36.45
120	20	24	25	0.013644	0.0062	0	0.98669	32.70
240	21	22	23.2	0.013474	0.0042	0.2	0.98669	28.47
480	21	20	21.2	0.013474	0.0028	0.2	0.98669	25.18
1440	21	20	21.2	0.013474	0.0016	0.2	0.98669	25.18

4 Atterberg Test Result

Determination	Liquid Limit			
Number of blows		38	29	19
Test	No	1	2	3
Container	No	D3	A12	3
Wt. of container + wet soil,	(g)	48.89	55.00	46.74
Wt. of container + dry soil,	(g)	34.47	37.05	33.45
Wt. of container,	(g)	17.93	16.02	18.99
Wt. of water,	(g)	14.42	17.95	13.29
Wt. of dry soil,	(g)	16.54	21.03	14.46
Moisture container,	(%)	87.2	85.4	91.9
Average	(%)	88.15		
PI	47.55			

Test	*Plastic Limit*	
code	e	4
Container	S	N
Wt. of container + wet soil,	32.00	27.00
Wt. of container + dry soil,	28.87	24.22
Wt. of container,	21.00	17.50
Wt. of water,	3.13	2.78
Wt. of dry soil,	7.87	6.72
Moisture container,	*39.8*	*41.4*
Average	**40.6**	

Liquid limit and plastic limit for 4% Bagasse Ashes and 0% Lime

Determination	***Liquid Limit***			
Number of blows		*31*	*25*	*19*
Test	No	1	2	3
Container	No	A	E	D
Wt. of container + wet soil,	(g)	28.00	34.32	55.43
Wt. of container + dry soil,	(g)	24.26	28.68	38.22
Wt. of container,	(g)	19.95	21.92	19.28
Wt. of water,	(g)	3.74	5.64	17.21
Wt. of dry soil,	(g)	4.31	6.76	18.94
Moisture container,	(%)	*86.8*	*83.4*	*90.9*
Average	(%)	87.02		
PI	45.32			

Test	**Plastic limit**	
	1	2
Container	A2	2
Wt. of container + wet soil,	36.33	35.87
Wt. of container + dry soil,	31.20	30.84
Wt. of container,	18.70	18.95
Wt. of water,	5.13	5.03
Wt. of dry soil,	12.50	11.89
Moisture container,	*41.0*	*42.3*
Average	**41.7**	

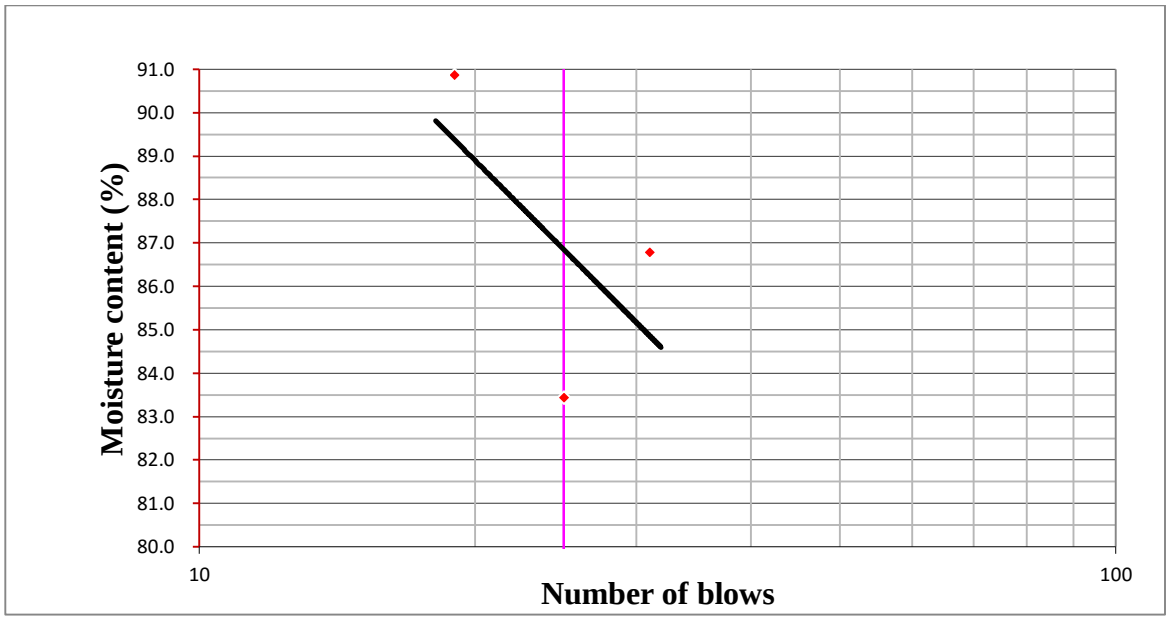

Liquid limit and plastic limit for 4% Bagasse Ashes and 1% Lime

Test	***Liquid Limit***			
No blow		*35*	*25*	*18*
code	No	1	2	3
Container	No	C12	A6	13
Wt. of container + wet soil,	(g)	25.69	29.57	31.44
Wt. of container + dry soil,	(g)	21.70	25.36	26.09
Wt. of container,	(g)	16.50	20.00	19.69
Wt. of water,	(g)	3.99	4.21	5.35
Wt. of dry soil,	(g)	5.20	5.36	6.40
Moisture container,	(%)	*76.7*	*78.5*	*83.6*
Average	79.62			
PI	35.82			

Test	***Plastic Limit***	
code	1	2
Container	21	C7
Wt. of container + wet soil,	19.52	21.89
Wt. of container + dry soil,	15.34	16.93
Wt. of container,	5.62	5.96
Wt. of water,	4.18	4.96
Wt. of dry soil,	9.72	10.97
Moisture container,	*43.0*	*45.2*
Average	**44.1**	

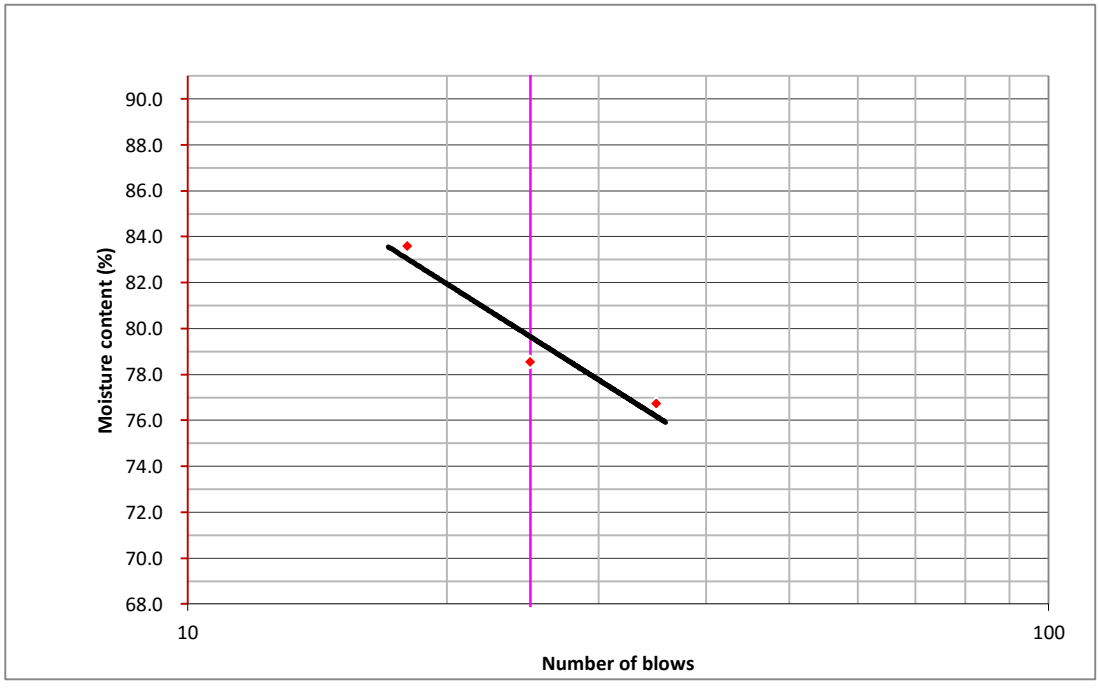

Liquid limit and plastic limit for 4% Bagasse Ashes and 1% Lime

Liquid limit and plastic limit for 3% Bagasse Ashes and 2% Lime

Determination	Liquid limit			
Number of blows		*33*	*28*	*20*
Test	No	1	2	3
Container	No	A12	B14	C4
Wt. of container + wet soil,	(g)	22.90	25.82	26.00
Wt. of container + dry soil,	(g)	20.00	22.00	22.15
Wt. of container,	(g)	16.04	17.00	17.65
Wt. of water,	(g)	2.90	3.82	3.85
Wt. of dry soil,	(g)	3.96	5.00	4.50
Moisture container,	(%)	*73.2*	*76.4*	*85.6*
Average	(%)	**78.4**		
PI	19.8			

Test	***Plastic Limit***	
No.	1	2
Container code	S	N
Wt. of container + wet soil,	10.00	22.11
Wt. of container + dry soil,	8.78	20.22
Weight of water	6.50	17.25
Weight of dry soil	1.22	1.89
Moisture content	2.28	2.97
Average	*53.5*	*63.6*
Average	**58.6**	

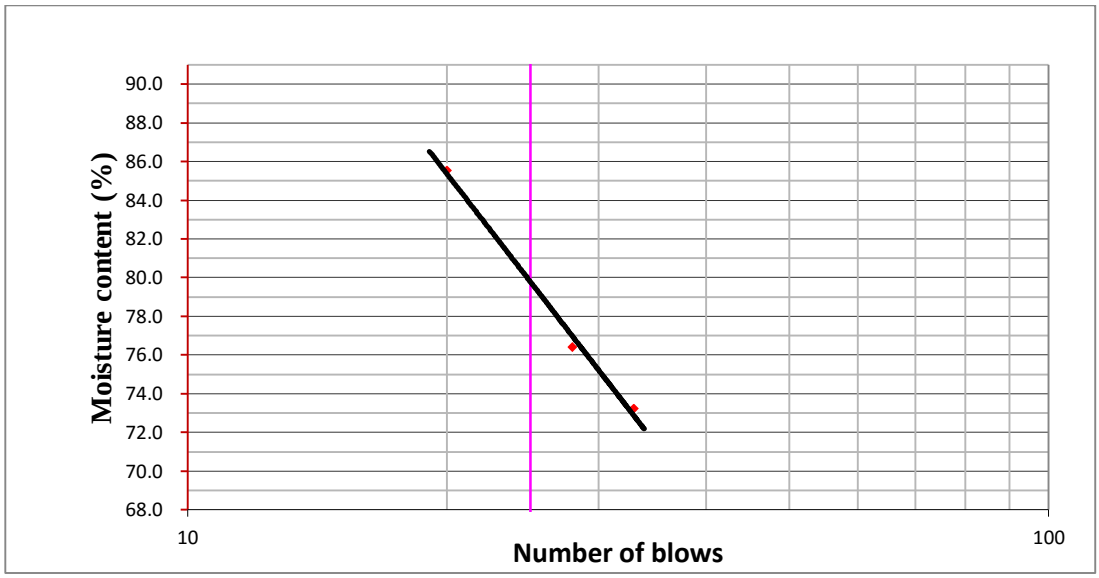

Liquid limit and plastic limit for 2% lime and3% Ashe

Determination	***Liquid Limit***				
Number of blows		*31*	*25*	*15*	
Test	No	1	2	3	
Container	No	A	E	D	
Wt. of container + wet so	(g)	21.78	23.50	23.74	
Wt. of container + dry so	(g)	15.21	15.88	15.48	
Wt. of container,	(g)	5.90	5.72	5.74	
Wt. of water,	(g)	6.57	7.62	8.26	
Wt. of dry soil,	(g)	9.31	10.16	9.74	
Moisture container,	(%)	*70.6*	*75.0*	*84.8*	
Average	(%)	76.79			

Plastic limit		
Container code	**1**	**2**
Wt. of container + wet soil,	**27.89**	**23.99**
Wt. of container + dry soil,	**25.01**	**21.1**
Weight of water	**20.89**	**15.98**
Weight of dry soil	**2.88**	**2.89**
Moisture content	**4.12**	**5.13**
Average	**69.9**	**56.4**
Average	**63.2**	

Liquid limit and plastic limit for 4% lime and 1% Ashe

	Liquid Limit		
Number of blows	*30*	*25*	*20*
Test No	1	2	3
Container No	A13	g19	C5
Wt. of container + wet soil, g	28.00	34.42	55.43
Wt. of container + dry soil, g	24.64	29.03	39.57
Wt. of container, g	19.95	21.92	19.28
Wt. of water, g	3.36	5.39	15.86
Wt. of dry soil, g	4.69	7.11	20.29
Moisture content, %	*71.6*	*75.8*	*78.2*
Average	75.21		
PI	10.21		

Plastic Limit		
Test	1	2
Container	A2	21
Wt. of container + wet soil, g	19.33	18.16
Wt. of container + dry soil, g	15.11	15.02
Wt. of container, g	8.96	9.90
Wt. of water, g	4.22	3.14
Wt. of dry soil, g	6.15	5.12
Moisture container, %	68.62	*61.3*
Average Moisture Content, %	65.0	

6 Compaction test result for Natural AC soil sample

Test No.	1	2	3	4
Mass of sample (gm)	4200	4200	4200	4200
Mass of Mold+Wet soil(gm)(A)	6270	6482.4	6422.17	6402
Mass of Mold(gm)(B)	2719.8	2725.5	2719.8	2715.8
Mass of Wet Soil(gm)A-B=C	3550.2	3756.9	3702.37	3686.2
Volume of Mold cm^3(D)	2124	2124	2124	2124
Bulk Density gm/cm^3 C/D=(E)	1.67	1.77	1.74	1.735499

Container Code .	3b	e3	t1	b12	q1	k-4	30b	a6
Mass of Wet soil+Container(gm)(F)	90.5	87.65	109.64	90.59	104.75	102.33	87.45	93.21
Mass of dry soil+container(gm)(G)	72.23	69.76	85.61	70.31	82.82	79.77	67.78	73.93
Mass of container(gm)(H)	7.35	6.8	5.34	7.65	14.03	17.18	7.61	6.82
Mass of moisture(gm)F-G=(I)	18.27	17.89	24.03	20.28	21.93	22.56	19.67	19.28
Mass of Dry soil(gm)G-H=(J)	64.88	62.96	80.27	62.66	68.79	62.59	48.11	54.65
Moisture content % (I/J)*100=K	28.16	28.41	29.94	32.37	31.88	36.04	40.89	35.28
Avg. Moisture Content % (L)	28.29		31.15		33.96		38.08	
Dry Density gm/cm^3 E/(100+L)*100	1.30		1.35		1.30		1.256859	

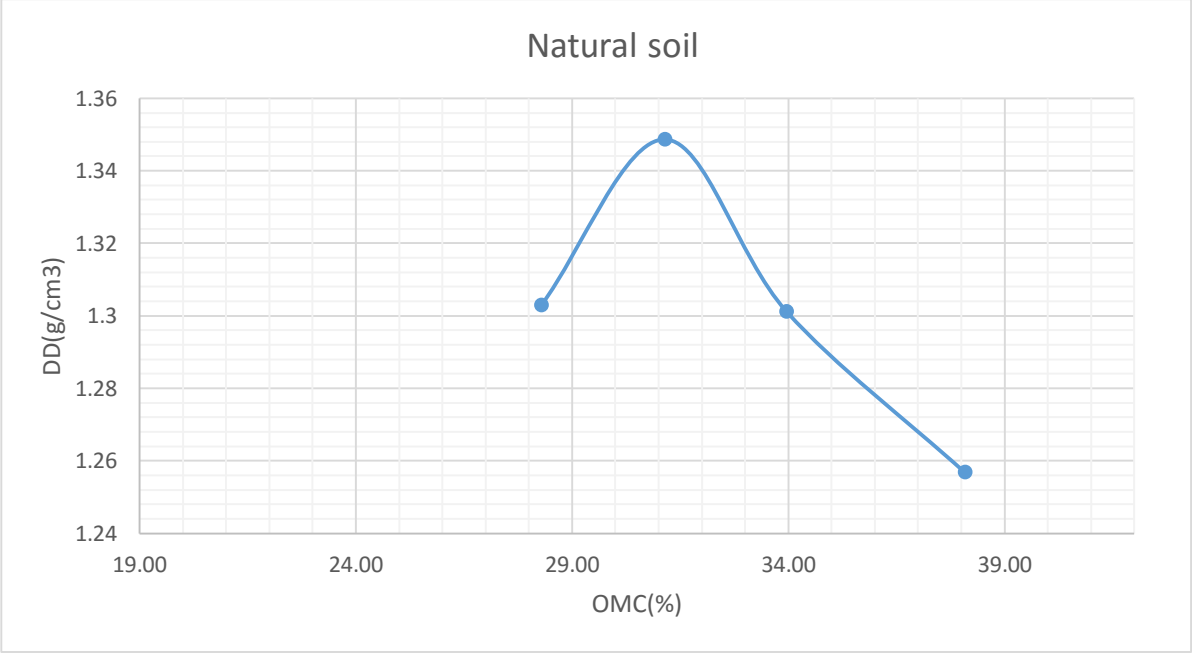

Test No.	1	2	3
Mass of sample (gm)	4200	4200	4200
Water Added(cc)	300	480	660
Mass of Mold+Wet soil(gm)(A)	6276.7	6487.7	6432.7
Mass of Mold(gm)(B)	2719.8	2725.5	2719.8
Mass of Wet Soil(gm)A-B=C	3556.9	3762.2	3712.9
Volume of Mold cm^3(D)	2124	2124	2124
Bulk Density gm/cm^3 C/D=(E)	1.67	1.77	1.75

Container Code .	3b	e3	t1	b12	q1	k-4
Mass of Wet soil+Container(gm)(F)	118.34	122.45	113.76	97.82	107.75	114.75
Mass of dry soil+container(gm)(G)	99.51	100.57	90.54	82	78.82	94
Mass of container(gm)(H)	37.35	37.5	37.33	14.75	14.03	17.18
Mass of moisture(gm)F-G=(I)	18.83	21.88	23.22	15.82	28.93	20.75
Mass of Dry soil(gm)G-H=(J)	62.16	63.07	53.21	67.25	64.79	76.82
Moisture content % (I/J)*100=K	30.29	34.69	43.64	23.52	44.65	27.01
Avg. Moisture Content % (L)	32.49		33.58		35.83	
Dry Density gm/cm^3 E/(100+L)*100	1.26		1.33		1.29	

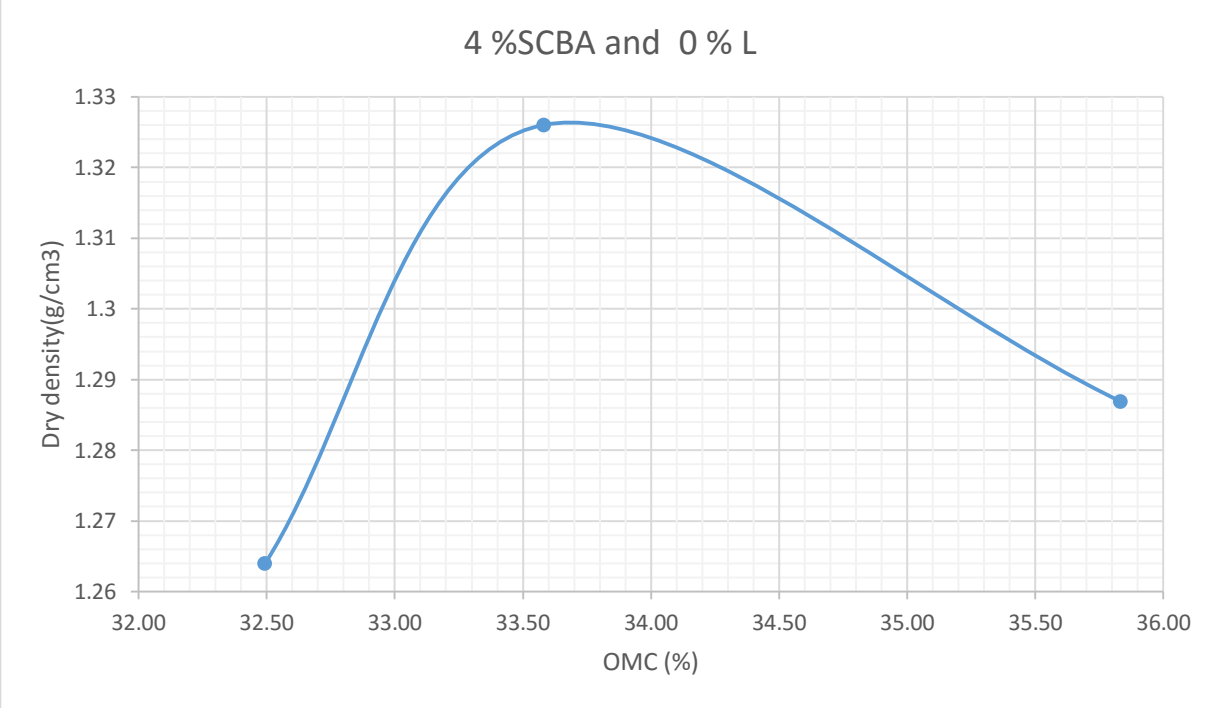

Test No.	1	2	3
Mass of sample (gm)	4200	4200	4200
Water Added(cc)	300	480	660
Mass of Mold+Wet soil(gm)(A)	6042	6266.16	6174.8
Mass of Mold(gm)(B)	2715.9	2723	2719.8
Mass of Wet Soil(gm)A-B=C	3326.1	3543.16	3455
Volume of Mold cm^3(D)	2124	2124	2124
Bulk Density gm/cm^3 C/D=(E)	1.57	1.67	1.63

Container Code .	p66	p62	c81	11	p67	2
Mass of Wet soil+Container(gm)(F)	110.39	92.43	88.41	91.05	132.76	127.47
Mass of dry soil+container(gm)(G)	93.35	76.43	70.43	71.84	109.76	105.47
Mass of container(gm)(H)	18.45	17.2	6.05	6.75	37.25	34.23
Mass of moisture(gm)F-G=(I)	17.04	16	17.98	19.21	23	22
Mass of Dry soil(gm)G-H=(J)	74.9	59.23	64.38	65.09	72.51	71.24
Moisture content % (I/J)*100=K	22.75	27.01	27.93	29.51	31.72	30.88
Avg. Moisture Content % (L)	24.88		28.72		31.30	
Dry Density gm/cm^3 E/(100+L)*100	1.25		1.30		1.24	

Test No.	1	2	3	4
Mass of sample (gm)	4200	4200	4200	4200
Mass of Mold+Wet soil(gm)(A)	6076.1	6356	6374	6317
Mass of Mold(gm)(B)	2715.9	2723	2719.8	2715.8
Mass of Wet Soil(gm)A-B=C	3360.2	3633	3654.2	3601.2
Volume of Mold cm^3(D)	2124	2124	2124	2124
Bulk Density gm/cm^3 C/D=(E)	1.58	1.71	1.72	1.69

Container Code .	T	P6	K-4	P62	G16	A	10B	AX
Mass of Wet soil+Container(gm)(F)	124.32	122.97	110.89	117.38	119.65	123.53	121.67	97.34
Mass of dry soil+container(gm)(G)	106.82	103.89	92.68	96.77	96.43	100.47	98.84	76.53
Mass of container(gm)(H)	17.45	17.42	17.44	18.53	17.91	18.19	18.65	14.73
Mass of moisture(gm)F-G=(I)	17.5	19.08	18.21	20.61	23.22	23.06	22.83	20.81
Mass of Dry soil(gm)G-H=(J)	89.37	86.47	75.24	78.24	78.52	82.28	76.01	55.72
Moisture content % (I/J)*100=K	19.58	22.07	24.20	26.34	29.57	28.03	30.04	37.35
Avg. Moisture Content % (L)	20.82		25.27		28.80		33.69	
Dry Density gm/cm^3 E/(100+L)*100	1.31		1.37		1.34		1.26	

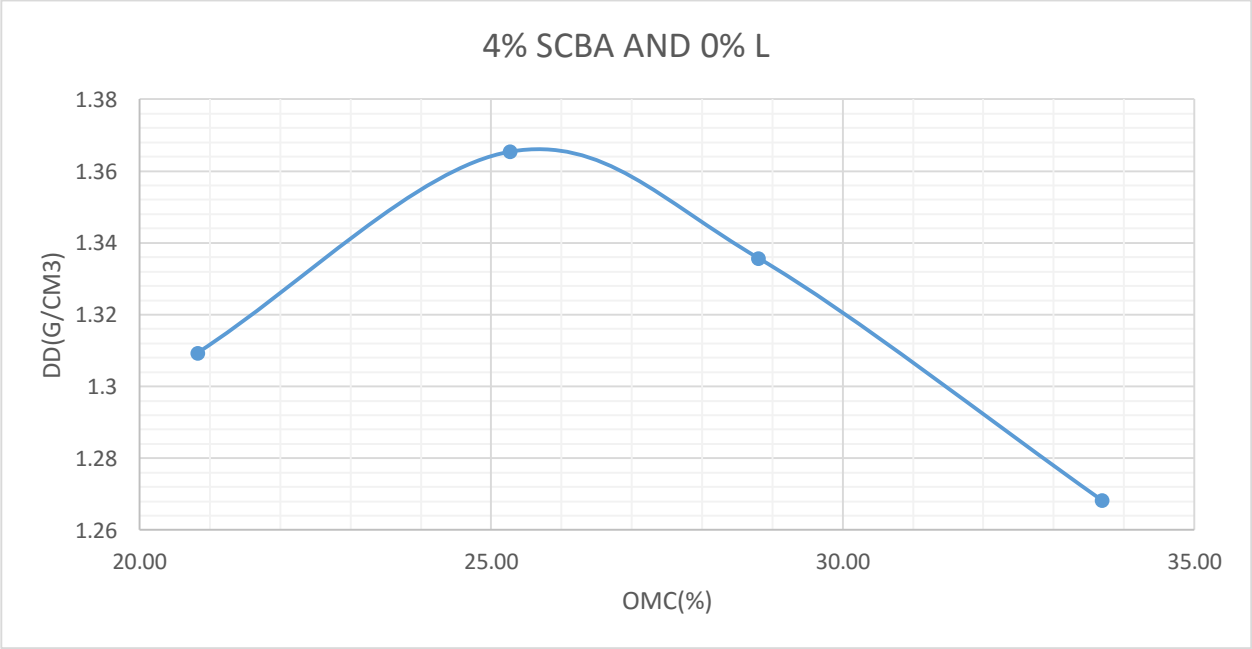

Test No.	1	2	3	4
Mass of sample (gm)	4200	4200	4200	4200
Mass of Mold+Wet soil(gm)(A)	6245.12	6476	6550.7	6420.7
Mass of Mold(gm)(B)	2719.8	2725.5	2719	2715.7
Mass of Wet Soil(gm)A-B=C	3525.32	3750.5	3831.7	3705
Volume of Mold cm^3(D)	2124	2124	2124	2124
Bulk Density gm/cm^3 C/D=(E)	1.66	1.77	1.80	1.74435

Container Code .	1	2	8	12	q1	5	30b	o
Mass of Wet soil+Container(gm)(F)	132.21	138.61	124.83	103.24	84.35	78.96	119.74	94.65
Mass of dry soil+container(gm)(G)	113.43	115.56	104.62	83.86	67.33	60.95	94.65	75.62
Mass of container(gm)(H)	17.6	18.14	17.5	14.72	7.9	14.14	18.12	6.05
Mass of moisture(gm)F-G=(I)	18.78	23.05	20.21	19.38	17.02	18.01	24.09	14.3
Mass of Dry soil(gm)G-H=(J)	95.83	97.42	87.12	69.14	59.43	46.81	71.56	61.32
Moisture content % (I/J)*100=K	19.60	23.66	23.20	28.03	28.64	38.47	33.66	23.32
Avg. Moisture Content % (L)	21.63		25.61		33.56		28.49	
Dry Density gm/cm^3 E/(100+L)*100	1.36		1.41		1.35		1.33	

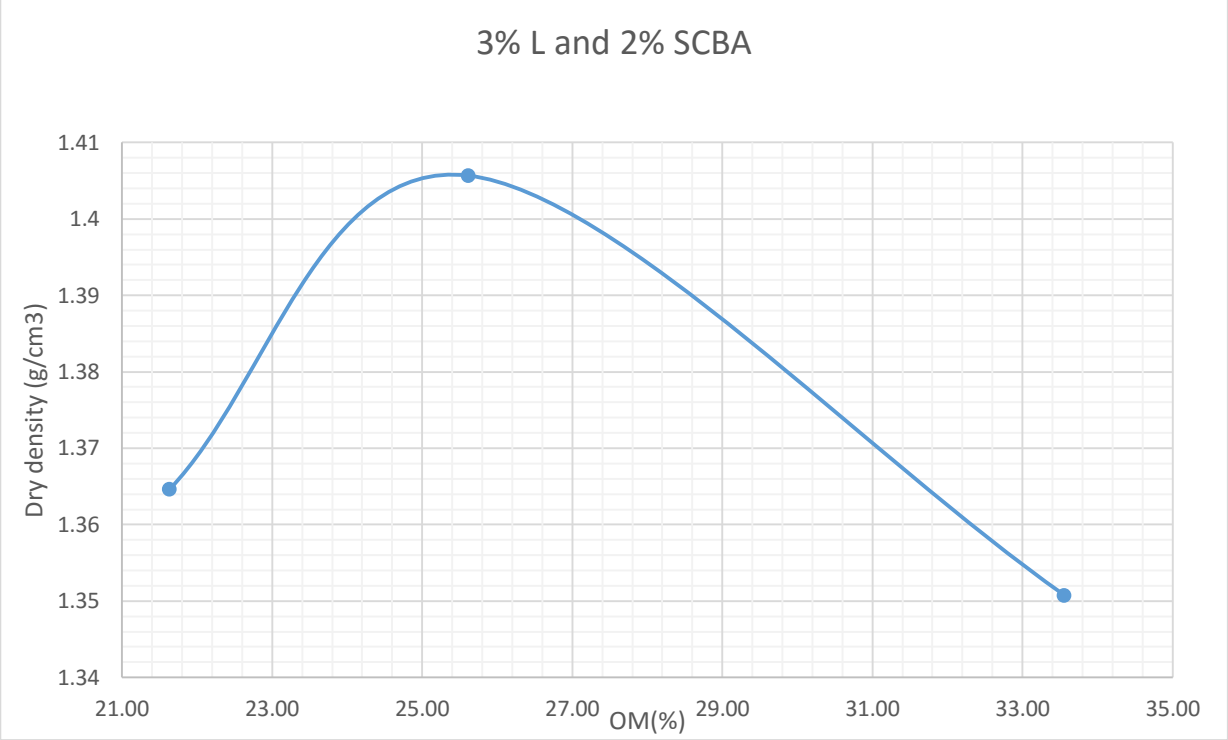

Test No.	1	2	3	4
Mass of sample (gm)	4200	4200	4200	4200
Mass of Mold+Wet soil(gm)(A)	6255.12	6486	6548	6440.7
Mass of Mold(gm)(B)	2715.8	2719.8	2723	2719.7
Mass of Wet Soil(gm)A-B=C	3539.32	3766.2	3825	3721
Volume of Mold cm^3(D)	2124	2124	2124	2124
Bulk Density gm/cm^3 C/D=(E)	1.67	1.77	1.80	1.751883

Container Code .	3b	e3	t1	b12	q1	k-4	30b	c
Mass of Wet soil+Container(gm)(F)	104.38	107.63	95.67	103.24	113.65	116.21	123.7	127.56
Mass of dry soil+container(gm)(G)	88.36	93.76	81.72	87.41	90.47	93.44	98.74	102.6
Mass of container(gm)(H)	17.4	18.02	17.25	17.62	18.4	17.18	14.43	6.05
Mass of moisture(gm)F-G=(I)	16.02	13.87	13.95	15.83	23.18	22.77	24.96	24.96

Mass of Dry soil(gm)G-H=(J)	70.96	75.74	64.47	69.79	72.07	76.26	73.78	77.64
Moisture content % (I/J)*100=K	22.58	18.31	21.64	22.68	32.16	29.86	33.83	32.15
Avg. Moisture Content % (L)	20.44		22.16		31.01		32.99	
Dry Density gm/cm^3 E/(100+L)*100	1.38		1.45		1.37		1.31	

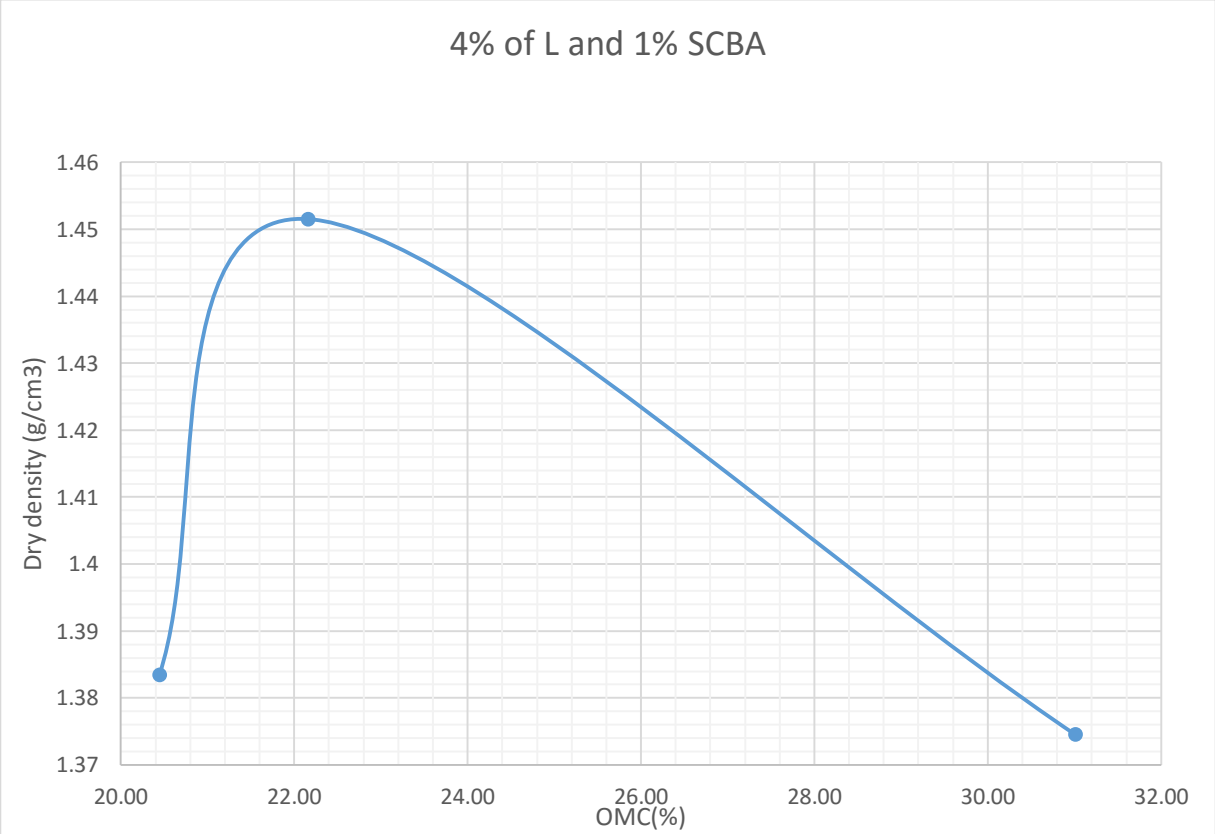

7 CBR determination for natural soil AC

BLOWS	LOAD (KN)		CBR(%)		DRY DENSITY Vs SOCKED CBR.			
	2.54mm	5.08mm	2.54mm	5.08mm				
10	0.20	0.210	1.50	1.06	No # OF BLOWS	**10**	**30**	**65**
30	0.23	0.31	1.55	1.72	DRY DENSITY	1.320	1.370	1.410
65	0.35	0.43	2.62	2.15	SOAKED C.B.R.	1.50	1.72	2.76

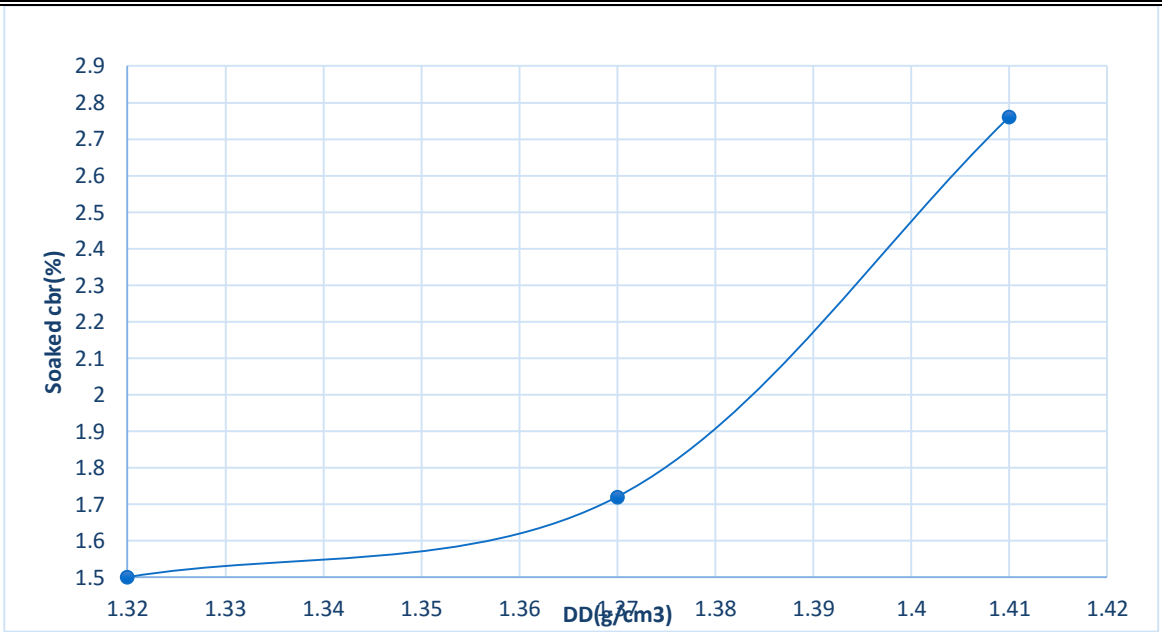

MDD (gm/cc)	1.376
95 % of MDD	1.30
C.B.R.at 95%of MDD	**1. 72**

BLOWS	LOAD (KN)		CBR(%)		DRY DENSITY Vs SOCKED CBR.			
	2.54mm	5.08mm	2.54mm	5.08mm				
10	0.190	0.280	1.41	1.40	**No # OF BLOWS**	**65**	**30**	**10**
30	0.370	0.540	2.77	2.70	**DRY DENSITY**	1.440	1.37	1.30
65	0.490	0.680	3.67	3.40	**SOAKED C.B.R.**	3.67	2.77	1.41

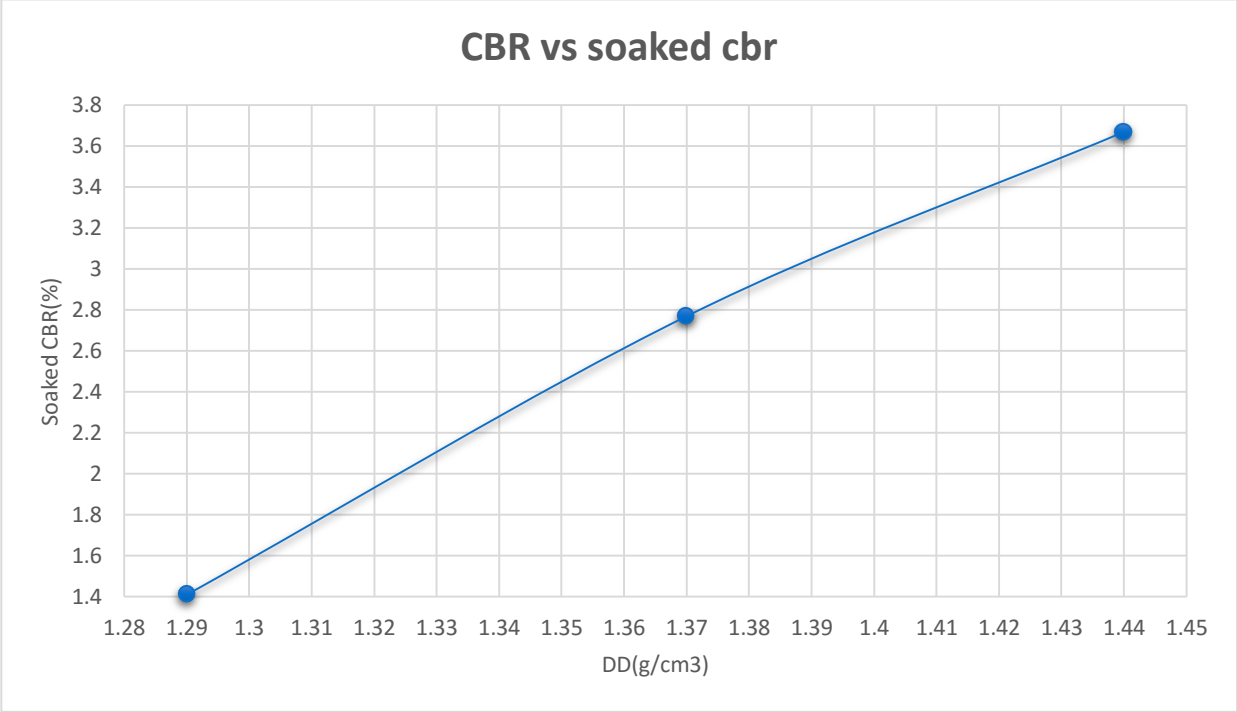

MDD (gm/cc)	1.33
95 % of MDD	1.26
C.B.R.at 95%of MDD	**2.80**

BLOWS	LOAD (KN)		CBR(%)		DRY DENSITY Vs SOCKED CBR.			
	2.54mm	5.08mm	2.54mm	5.08mm				
10	0.44	0.50	2.34	2.09	**No # OF BLOWS**	**65**	**30**	**10**
30	0.52	0.570	2.65	2.33	**DRY DENSITY**	1.36	1.32	1.28
65	0.58	0.68	2.92	2.62	**SOAKED C.B.R.**	4.38	3.96	3.31

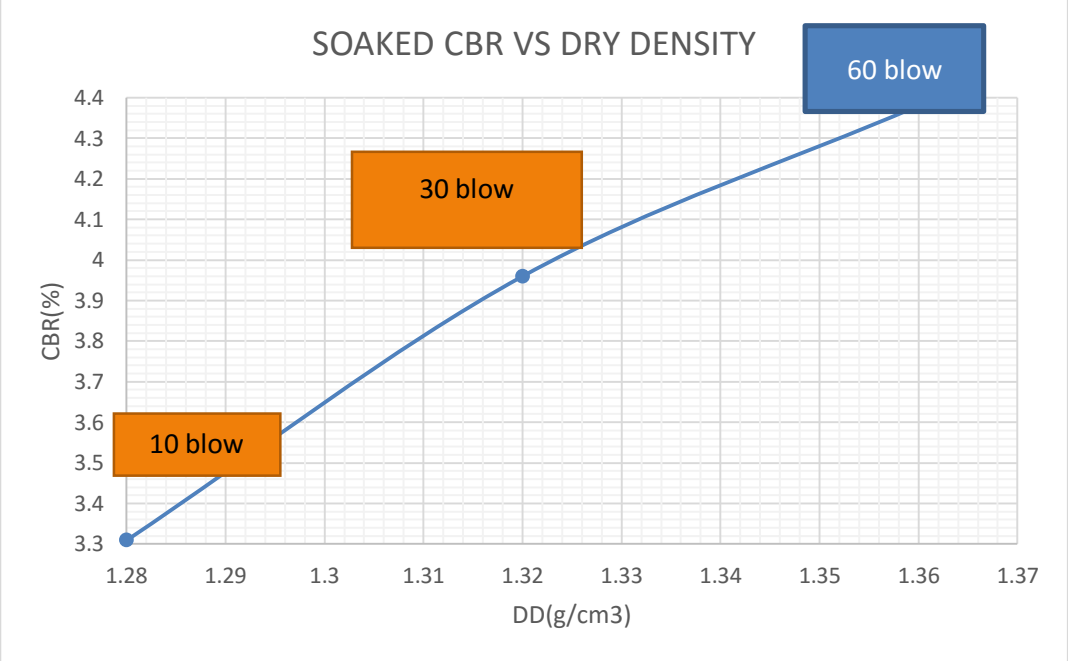

MDD (gm/cc) Proctor	1.39
95 % of MDD	1.32
C.B.R.at 95%of MDD	**3.96**

BLOWS	LOAD (KN)		CBR(%)		DRY DENSITY Vs SOCKED CBR.			
	2.54mm	5.08mm	2.54mm	5.08mm				
10	0.75	0.98	5.64	4.90	**No # OF BLOWS**	**65**	**30**	**10**
30	0.82	1.17	6.16	5.85	**DRY DENSITY**	1.29	1.22	1.19
65	0.91	1.34	6.82	6.70	**SOAKED C.B.R.**	6.82	6.16	5.64

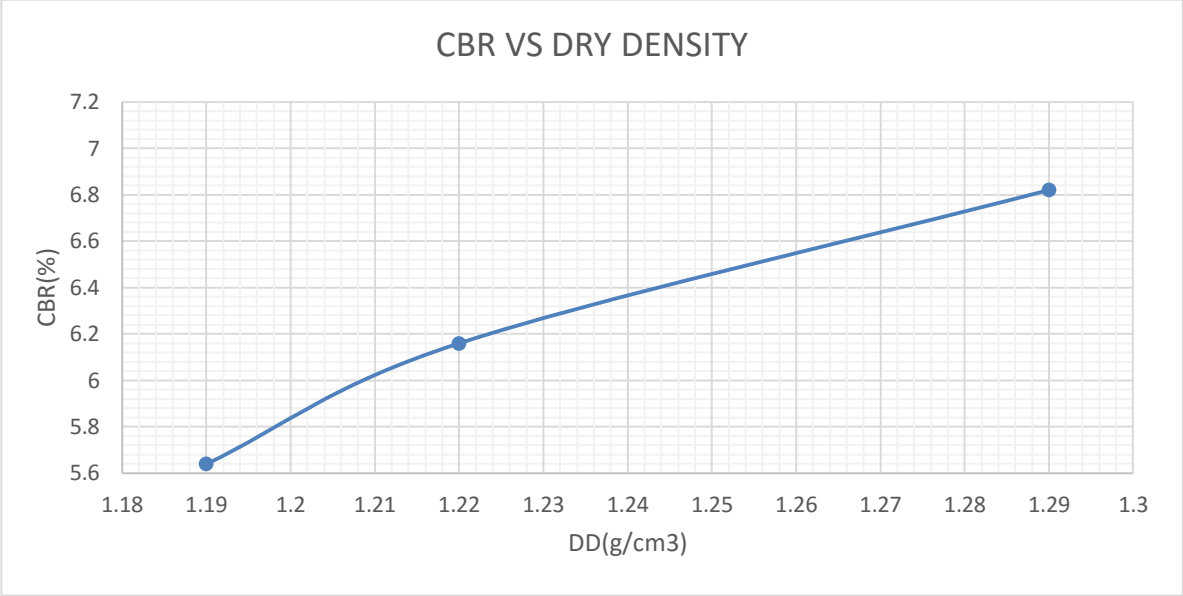

MDD (gm/cc) Proctor	1.29
95 % of MDD	1.23
C.B.R.at 95%of MDD	**6 .21**

‘

BLOWS	LOAD (KN)		CBR(%)		DRY DENSITY Vs SOCKED CBR.			
	2.54mm	5.08mm	2.54mm	5.08mm				
10	1.08	1.41	8.10	7.05	**No # OF BLOWS**	**65**	**30**	**10**
30	1.22	1.64	9.15	8.20	**DRY DENSITY**	1.21	1.16	1.10
65	1.35	1.81	10.08	9.05	**SOAKED C.B.R.**	10.08	9.15	8.10

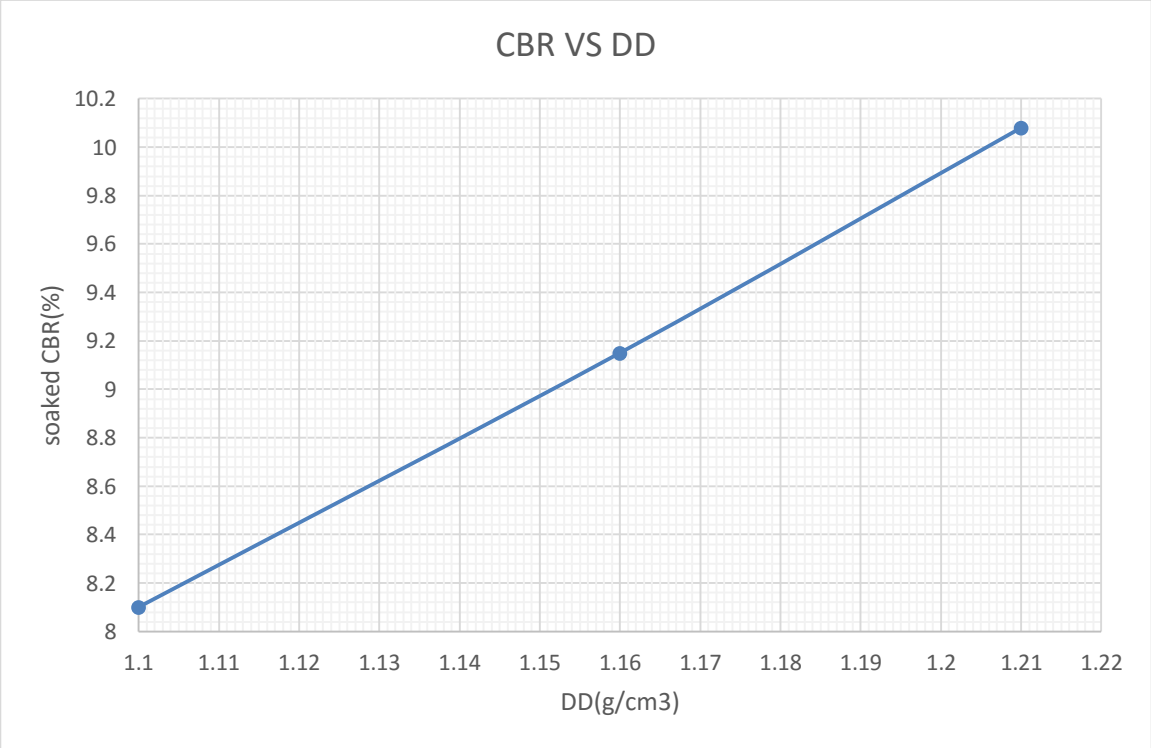

MDD (gm/cc) Proctor	1.34
95 % of MDD	1.27
C.B.R.at 95%of MDD	**8 .8**

BLOWS	LOAD (KN)		CBR(%)		DRY DENSITY Vs SOCKED CBR.			
	2.54mm	5.08mm	2.54mm	5.08mm				
10	1.46	1.78	10.15	8.92	**No # OF BLOWS**	**65**	**30**	**10**
30	1.48	1.81	11.08	9.06	**DRY DENSITY**	1.305	1.272	1.184
65	1.78	2.01	13.37	10.05	**SOAKED C.B.R.**	13.37	11.08	10.15

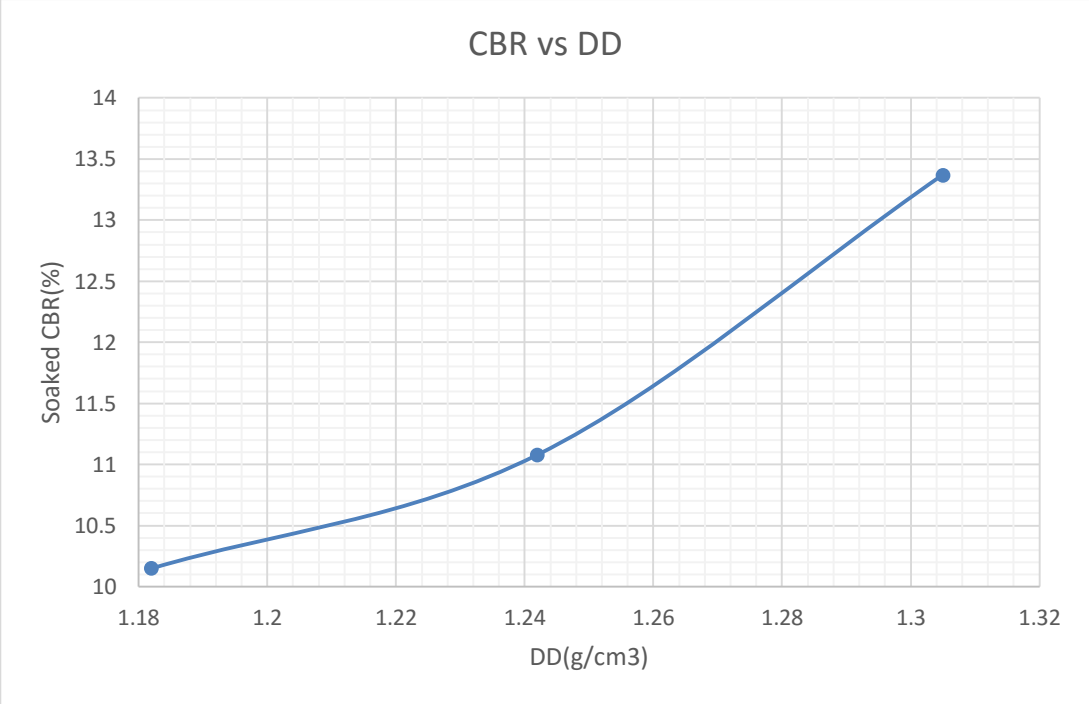

MDD (gm/cc) Proctor	1.30
95 % of MDD	1.23
C.B.R.at 95%of MDD	**11.04**

APENDIX B

Laboratory Test Result of KK Soil sample

1 ATERBERG LIMIT

Determination		***Liquid Limit***			***Plastic Limit***	
Number of blows		*35*	*27*	*20*		
Test	No	1	2	3	1	2
Container	No	A12	B14	C4	p65	X
Wt. of container + wet soil,	(g)	58.38	49.80	60.70	28.60	24.30
Wt. of container + dry soil,	(g)	48.48	38.52	49.95	24.92	22.48
Wt. of container,	(g)	37.80	26.90	39.20	14.60	17.78
Wt. of water,	(g)	9.90	11.28	10.75	3.68	1.82
Wt. of dry soil,	(g)	10.68	11.62	10.75	10.32	4.70
Moisture container,	(%)	*92.7*	*97.1*	*100.0*	*35.7*	*38.7*
Average	(%)	96.59			**37.2**	

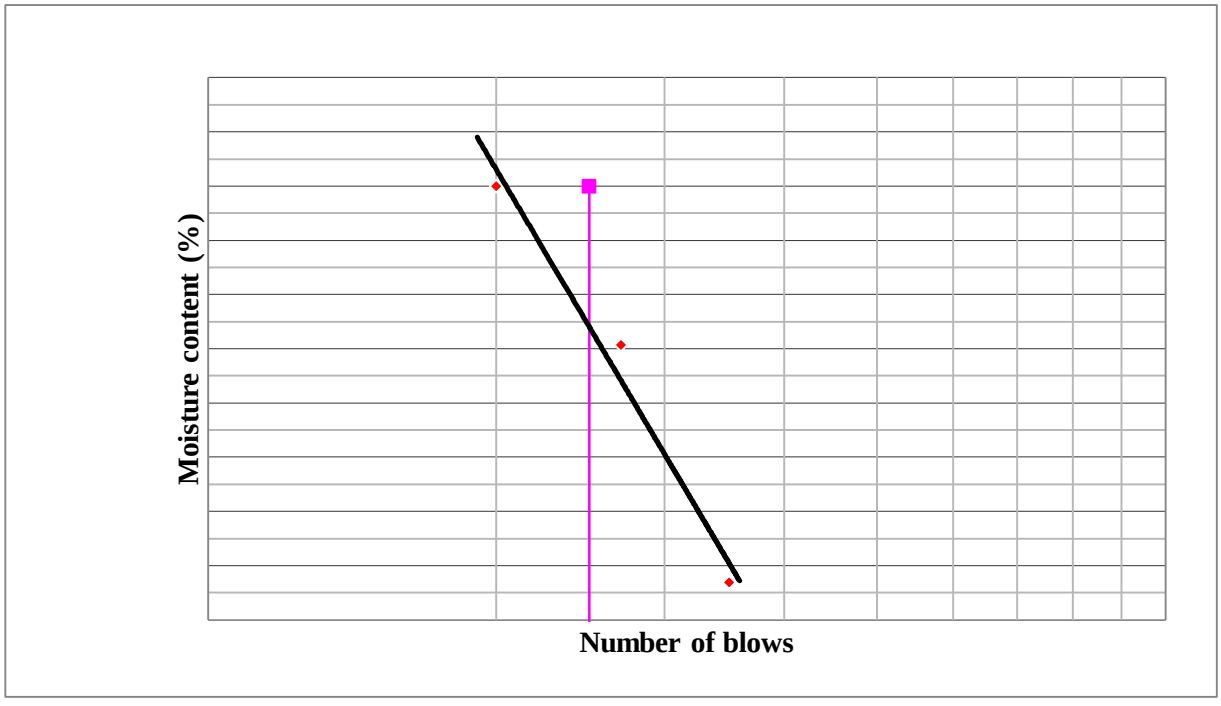

Liquid and plastic limit for natural soil

Determination	***Liquid Limit***				***Plastic Limit***	
Test	No	1	2	3	1	2
Container	No	A	E	D	qd	x
Wt. of container + wet soil,	(g)	40.80	37.76	32.00	32.14	29.80
Wt. of container + dry soil,	(g)	32.68	30.42	24.10	28.85	27.19
Wt. of container,	(g)	23.50	22.80	16.20	21.80	20.88
Wt. of water,	(g)	8.12	7.34	7.90	3.29	2.61
Wt. of dry soil,	(g)	9.18	7.62	7.90	7.05	6.31
Moisture container,	(%)	*88.5*	*96.3*	*100.0*	*46.7*	*41.4*
Average	(%)	94.93			**44.0**	

liquid and plastic limit 4% ash 0% Lime

Determination	***Liquid Limit***				***Plastic Limit***	
Number of blows		*33*	*20*	*15*		
Test	No	1	2	3	1	2
Container	No	A12	B14	C4	p65	X
Wt. of container + wet soil,	(g)	31.41	30.29	24.80	20.98	24.09
Wt. of container + dry soil,	(g)	24.12	23.85	17.97	18.37	20.84
Wt. of container,	(g)	15.94	16.78	10.89	13.29	14.73
Wt. of water,	(g)	7.29	6.44	6.83	2.61	3.25
Wt. of dry soil,	(g)	8.18	7.07	7.08	5.08	6.11
Moisture container,	(%)	*89.1*	*91.1*	*96.5*	*51.4*	*53.2*
Average	(%)	92.23			**52.3**	

liquid and plastic limit 4% ash 1% Lime

Determination	***Liquid Limit***				***Plastic Limit***	
Number of blows		*34*	*26*	*17*		
Test	No	1	2	3	1	2
Container	No	A12	B14	C4	p65	A
Wt. of container + wet soil,	(g)	35.14	34.58	35.40	20.59	22.3
Wt. of container + dry soil,	(g)	26.15	25.98	26.88	17.63	18.23
Wt. of container,	(g)	15.67	16.28	17.85	13.33	11.78
Wt. of water,	(g)	8.99	8.60	8.52	2.96	4.07
Wt. of dry soil,	(g)	10.48	9.70	9.03	4.30	6.45
Moisture container,	(%)	*85.8*	*88.7*	*94.4*	*68.8*	63.10078
Average	(%)	89.60			**66.0**	

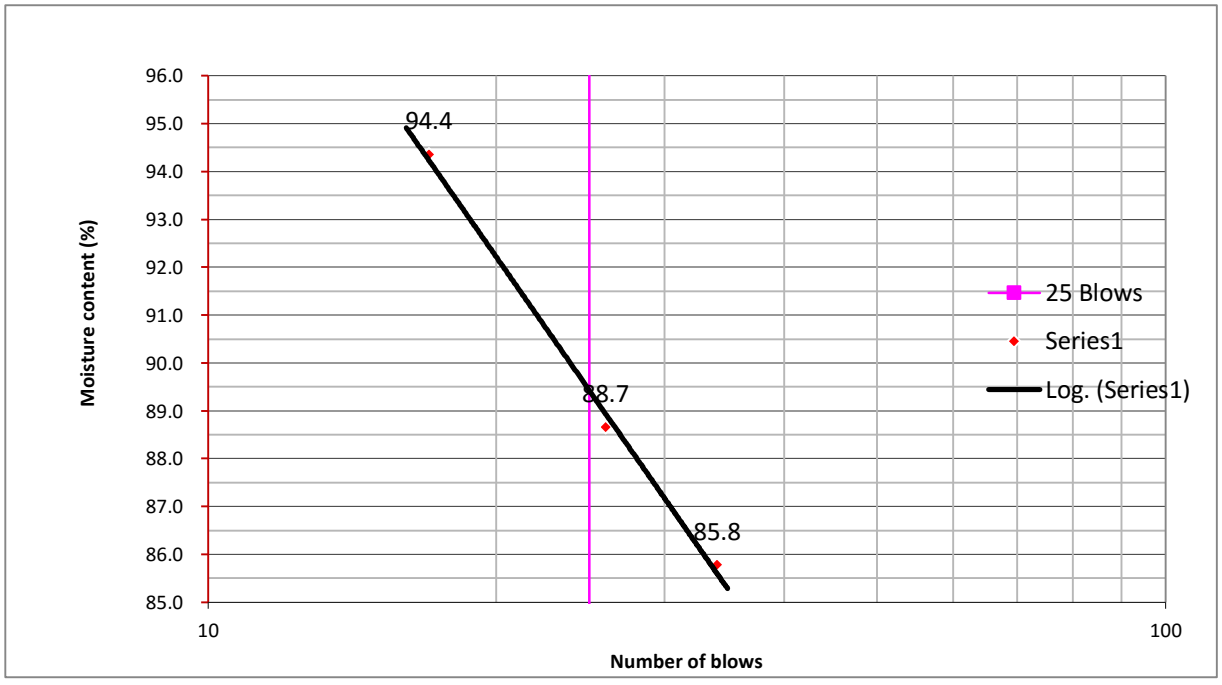

Liquid and plastic limit 3% ash 2% Lime

Determination	***Liquid Limit***				***Plastic Limit***	
Number of blows		*35*	*25*	*18*		
Test	No	1	2	3	1	2
Container	No	C12	A6	13	21	C7
Wt. of container + wet soil,	(g)	40.60	36.98	43.70	19.83	18.76
Wt. of container + dry soil,	(g)	31.33	27.74	33.03	15.41	15.22
Wt. of container,	(g)	19.56	16.97	20.85	8.96	9.9
Wt. of water,	(g)	9.27	9.24	10.67	4.42	3.54
Wt. of dry soil,	(g)	11.77	10.77	12.18	6.45	5.32
Moisture container,	(%)	*78.8*	*85.8*	*87.6*	*68.52*	*66.54*
Average	(%)	84.05			**67.53**	

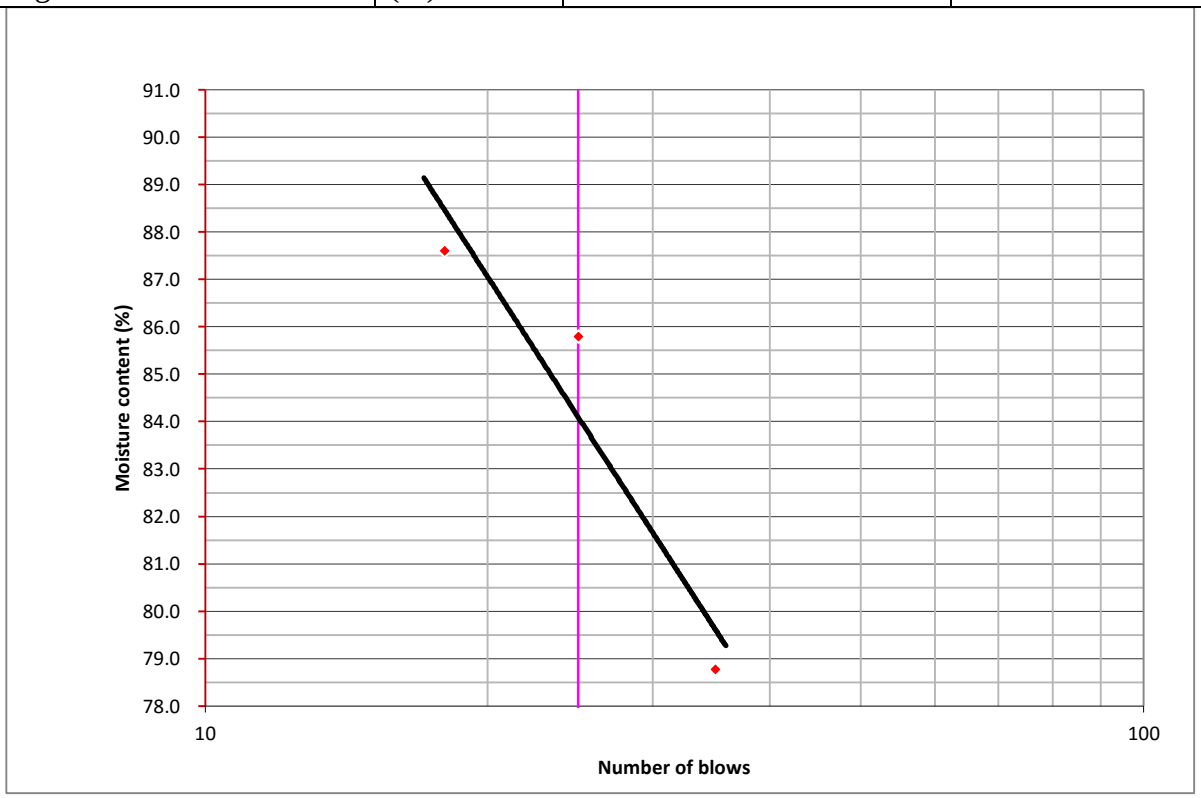

Liquid and plastic limit 2% ash 3% Lime

Determination	*Liquid Limit*				*Plastic Limit*	
Number of blows		*35*	*25*	*18*		
Test	No	1	2	3	1	2
Container	No	C12	A6	13	21	C7
Wt. of container + wet soil	(g)	24.28	30.18	31.75	19.90	21.99
Wt. of container + dry soil,	(g)	16.81	20.19	20.69	14.11	15.42
Wt. of container,	(g)	7.04	7.49	7.68	5.62	6.06
Wt. of water,	(g)	7.47	9.99	11.06	5.79	6.57
Wt. of dry soil,	(g)	9.77	12.70	13.01	8.49	9.36
Moisture container,	(%)	*76.5*	*78.7*	*85.0*	*68.2*	*70.2*
Average	(%)	80.04			69.02	

Liquid and plastic limit 1% ash 4% Lime

2 Compaction test result for KK Soil sample

Test No.	1	2	3	4
Mass of sample (gm)	4200	4200	4200	4200
Mass of Mold+Wet soil(gm)(A)	6424	6576	6480	6432
Mass of Mold(gm)(B)	2719.8	2725.5	2719.8	2715.8
Mass of Wet Soil(gm)A-B=C	3704.2	3850.5	3760.2	3716.2
Volume of Mold cm^3(D)	2124	2124	2124	2124
Bulk Density gm/cm^3 C/D=(E)	1.74	1.81	1.77	1.74

Container Code .	p66	p62	c81	11	p67	2	3	c160
Mass of Wet soil+Container(gm)(F)	164.9	154.5	100.89	98.94	129.4	132.3	87.45	93.21
Mass of dry soil+container(gm)(G)	139.1	129.8	84.55	85.82	107.4	108.47	69.46	73.78
Mass of container(gm)(H)	37.28	37.37	33.43	34.43	39.46	37.62	5.61	5.81
Mass of moisture(gm)F-G=(I)	25.8	24.7	16.34	13.12	22	23.83	17.99	19.43
Mass of Dry soil(gm)G-H=(J)	101.82	92.43	51.12	51.39	67.94	70.85	51.47	54.35
Moisture content % (I/J)*100=K	25.34	26.72	31.96	25.53	32.38	33.63	34.95	35.75
Avg. Moisture Content % (L)	26.03		28.75		33.01		35.35	
Dry Density gm/cm^3 E/(100+L)*100	1.38		1.41		1.33		1.29	

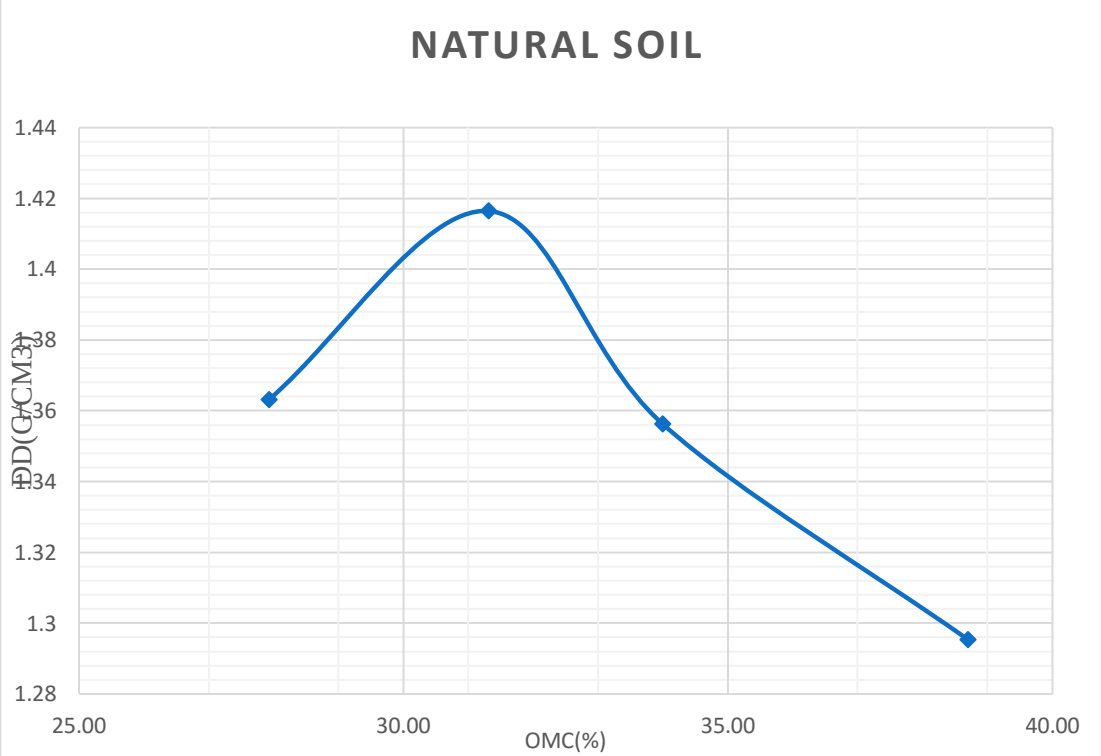

Compaction test result for KK natural soil sample

Test No.	1	2	3	4
Mass of sample (gm)	4200	4200	4200	4200
Mass of Mold+Wet soil(gm)(A)	6260	6460	6410	6372
Mass of Mold(gm)(B)	2719.8	2725.5	2719.8	2715.8
Mass of Wet Soil(gm)A-B=C	3540.2	3734.5	3690.2	3656.2
Volume of Mold cm^3(D)	2124	2124	2124	2124
Bulk Density gm/cm^3 C/D=(E)	1.67	1.76	1.74	1.721375

Container Code .	3b	e3	t1	b12	q1	k-4	30b	a6
Mass of Wet soil+Container(gm)(F)	96.54	102.63	103.33	105.76	115.27	98.75	96.73	98.71
Mass of dry soil+container(gm)(G)	77.94	83.13	81.68	82.15	89.42	78.3	76.01	77.14
Mass of container(gm)(H)	7.36	6.08	5.03	5.34	17.37	18.36	5.61	5.81
Mass of moisture(gm)F-G=(I)	18.6	19.5	21.65	23.61	25.85	20.45	20.72	21.57
Mass of Dry soil(gm)G-H=(J)	70.58	77.05	76.65	76.81	72.05	59.94	55.29	55.57
Moisture content % (I/J)*100=K	26.35	25.31	28.25	30.74	35.88	34.12	37.48	38.82
Avg. Moisture Content % (L)	25.83		29.49		35.00		38.15	
Dry Density gm/cm^3 E/(100+L)*100	1.32		1.36		1.29		1.246059	

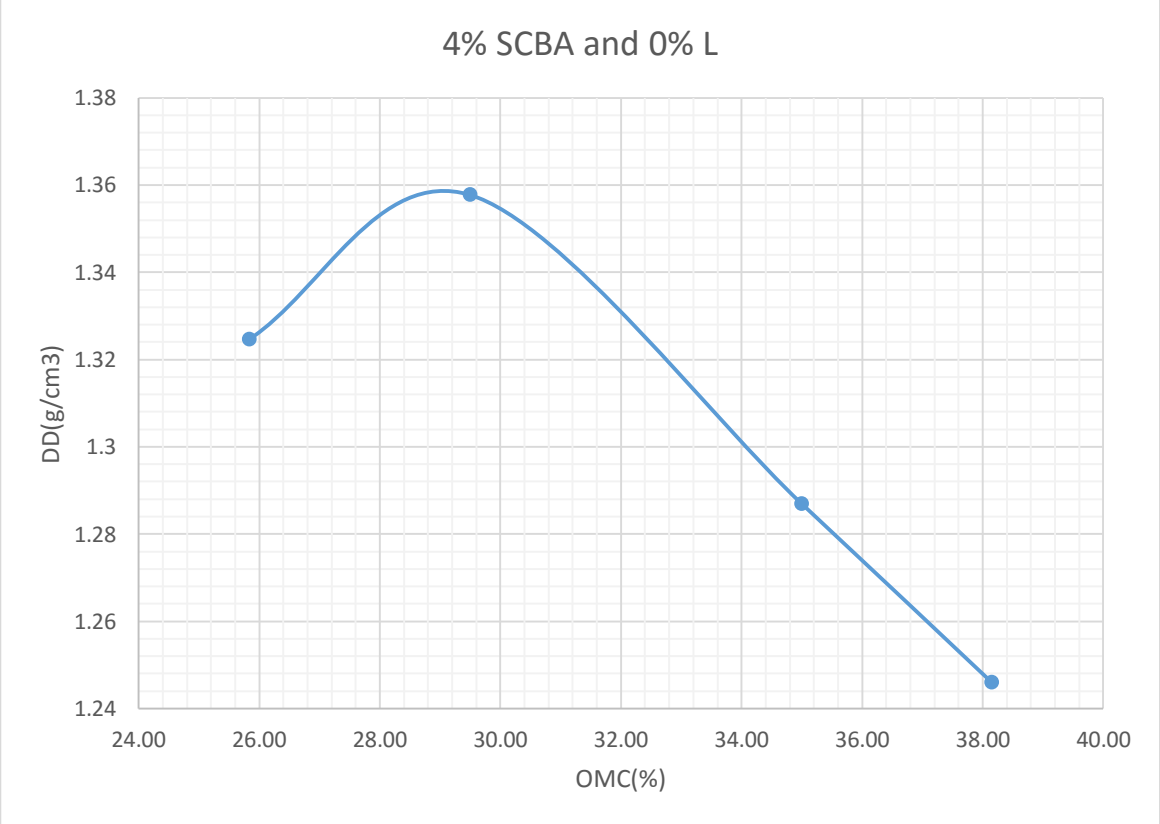

Test No.	1	2	3	4

Mass of sample (gm)	4200	4200	4200	4200
Mass of Mold+Wet soil(gm)(A)	6276.7	6441	6427.7	6411.2
Mass of Mold(gm)(B)	2719.8	2725.5	2719.8	2715.8
Mass of Wet Soil(gm)A-B=C	3556.9	3715.5	3707.9	3695.4
Volume of Mold cm^3(D)	2124	2124	2124	2124
Bulk Density gm/cm^3 C/D=(E)	1.67	1.75	1.75	1.739831

Container Code .	g19	t3	t1	t2	p66	cd	tg	c12
Mass of Wet soil+Container(gm)(F)	150.38	154.64	110	115.37	164.9	132.3	97.54	107.56
Mass of dry soil+container(gm)(G)	129.75	131.8	89.84	95.72	138.8	107.5	75.82	86.06
Mass of container(gm)(H)	37.8	37.5	14.8	17.5	37.6	37.62	7.35	14.81
Mass of moisture(gm)F-G=(I)	20.63	22.84	20.16	19.65	26.1	24.8	21.72	21.5
Mass of Dry soil(gm)G-H=(J)	91.95	94.3	75.04	78.22	101.2	69.88	54.1	64.56
Moisture content % (I/J)*100=K	22.44	24.22	26.87	25.12	25.79	35.49	40.15	33.30
Avg. Moisture Content % (L)	23.33		25.99		30.64		36.73	
Dry Density gm/cm^3 E/(100+L)*100	1.36		1.39		1.34		1.272503	

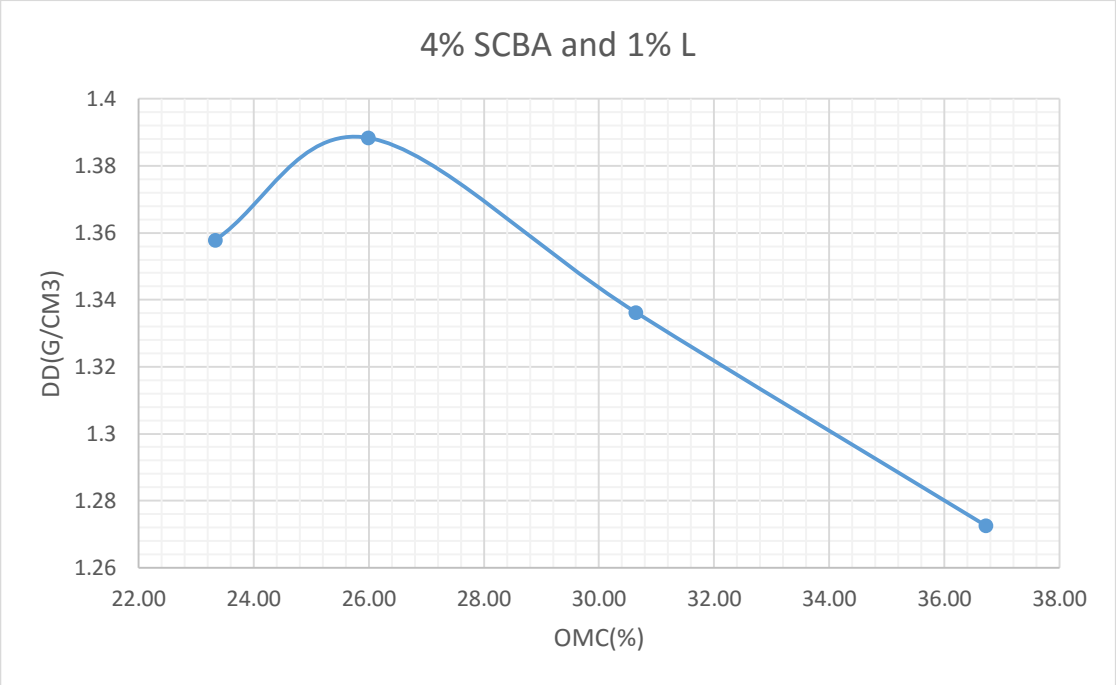

Test No.	1	2	3	4
Mass of sample (gm)	4200	4200	4200	4200
Mass of Mold+Wet soil(gm)(A)	6243	6408	6428	6383
Mass of Mold(gm)(B)	2715.8	2719.8	2723	2719.7
Mass of Wet Soil(gm)A-B=C	3527.2	3688.2	3705	3663.3
Volume of Mold cm^3(D)	2124	2124	2124	2124
Bulk Density gm/cm^3 C/D=(E)	1.66	1.74	1.74	1.724718

Container Code .	B12	A14	CA1	1G	30B	P66	T1	T13
Mass of Wet soil+Container(gm)(F)	128.74	145.68	98.65	122.76	146.9	127.8	112.33	124.77
Mass of dry soil+container(gm)(G)	107.44	123.8	81.55	101.59	123.28	107.05	84.88	106.27
Mass of container(gm)(H)	17.35	19.5	14.8	17.45	37.05	37.43	6.5	6.05

Mass of moisture(gm)F-G=(I)	21.3	21.88	17.1	21.17	23.62	20.75	27.45	18.5
Mass of Dry soil(gm)G-H=(J)	90.09	104.3	66.75	84.14	86.23	69.62	57.43	87.77
Moisture content % (I/J)*100=K	23.64	20.98	25.62	25.16	27.39	29.80	47.80	21.08
Avg. Moisture Content % (L)	22.31		25.39		28.60		34.44	
Dry Density gm/cm^3 E/(100+L)*100	1.36		1.38		1.36		1.282913	

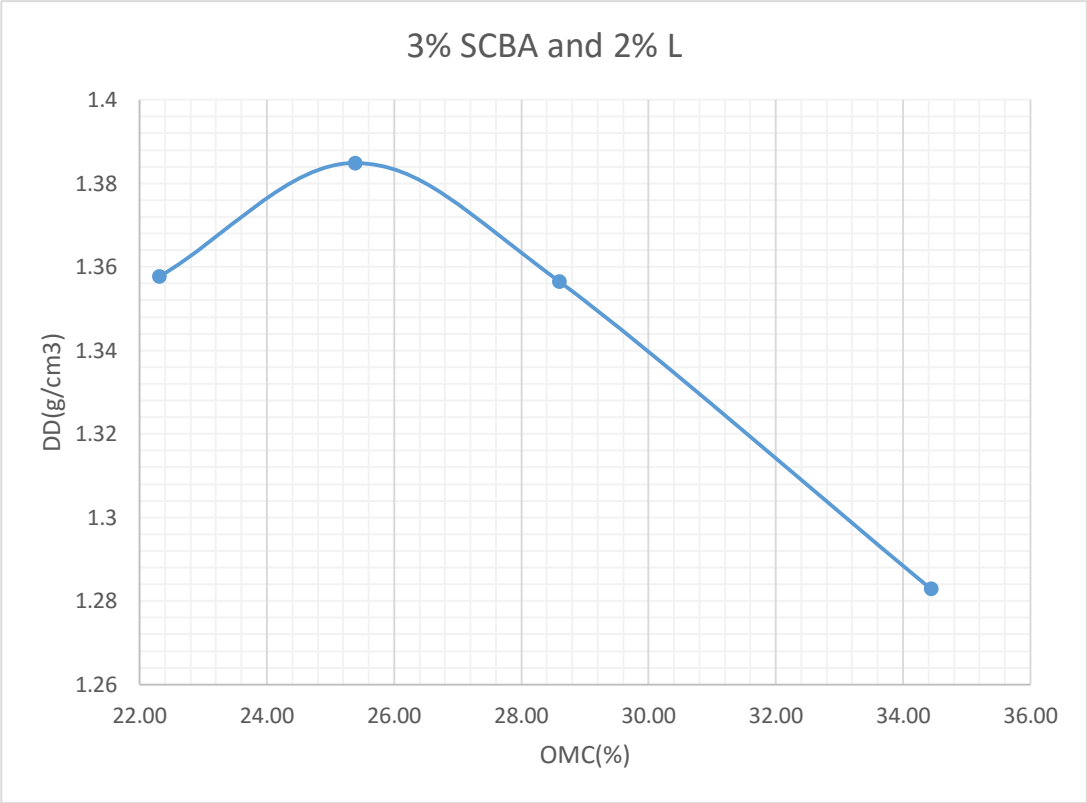

Test No.	1	2	3	4
Mass of sample (gm)	4200	4200	4200	4200
Mass of Mold+Wet soil(gm)(A)	6285.5	6502.4	6441	6370.7
Mass of Mold(gm)(B)	2715.8	2719.8	2723	2719.7

Mass of Wet Soil(gm)A-B=C	3569.7	3782.6	3718	3651
Volume of Mold cm^3(D)	2124	2124	2124	2124
Bulk Density gm/cm^3 C/D=(E)	1.68	1.78	1.75	1.718927

Container Code .	G1	G10	12	A2	C12	K-4	AC	B
Mass of Wet soil+Container(gm)(F)	154.5	144.3	131.1	164.9	95.41	90.88	86.45	103.7
Mass of dry soil+container(gm)(G)	134.2	125.15	110.4	141.1	77.41	75.88	69.46	82.7
Mass of container(gm)(H)	34.76	36.45	35.41	37.6	18.17	17.35	14.43	6.05
Mass of moisture(gm)F-G=(I)	20.3	19.15	20.7	23.8	18	15	16.99	21
Mass of Dry soil(gm)G-H=(J)	99.44	88.7	74.99	103.5	59.24	58.53	52.47	61.7
Moisture content % (I/J)*100=K	20.41	21.59	27.60	23.00	30.38	25.63	32.38	34.04
Avg. Moisture Content % (L)	21.00		25.30		28.01		33.21	
Dry Density gm/cm^3 E/(100+L)*100	1.39		1.42		1.37		1.290408	

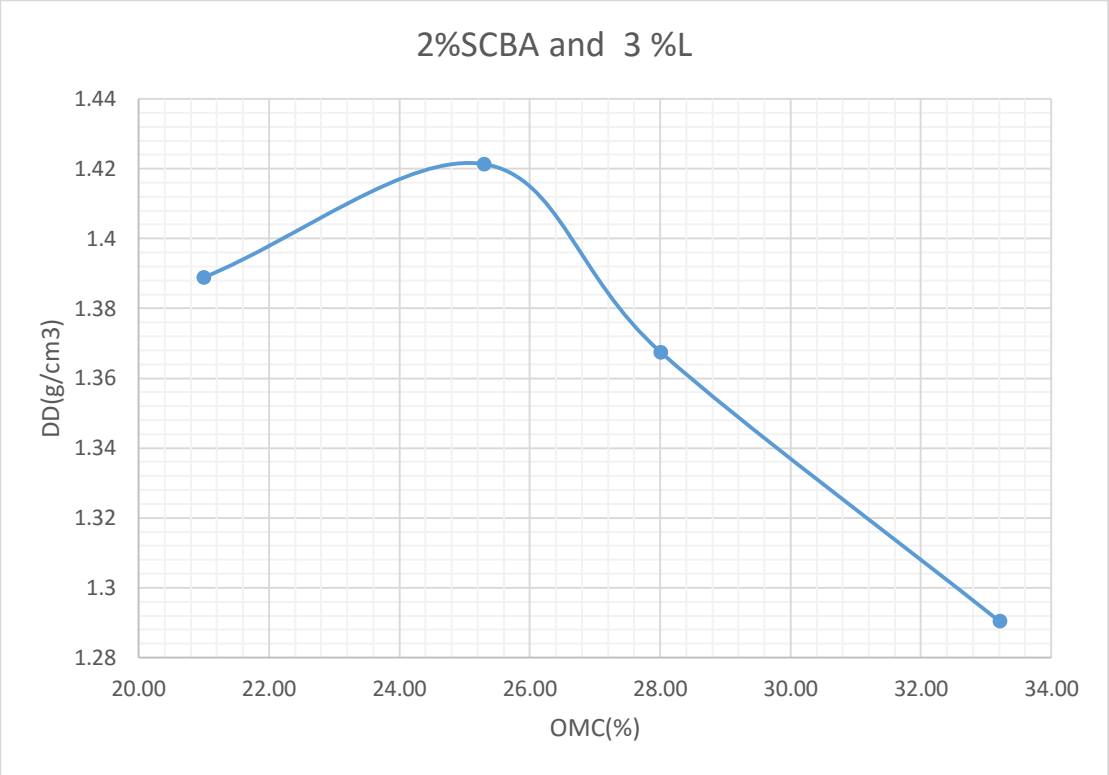

Test No.	1	2	3	4
Mass of sample (gm)	4200	4200	4200	4200
Water Added(cc)	300	480	660	
Mass of Mold+Wet soil(gm)(A)	6355.12	6586	6542	6370.7
Mass of Mold(gm)(B)	2715.8	2719.8	2723	2719.7
Mass of Wet Soil(gm)A-B=C	3639.32	3866.2	3819	3651
Volume of Mold cm^3(D)	2124	2124	2124	2124
Bulk Density gm/cm^3 C/D=(E)	1.71	1.82	1.80	1.718927

Container Code .	p66	p62	c81	11	p67	2
Mass of Wet soil+Container(gm)(F)	115.36	120.22	109.68	94.44	104.75	102.33
Mass of dry soil+container(gm)(G)	96.05	103.34	90.97	77.84	84.82	80.77
Mass of container(gm)(H)	17.4	18.02	17.25	17.62	18.4	17.18
Mass of moisture(gm)F-G=(I)	19.31	16.88	18.71	16.6	19.93	21.56
Mass of Dry soil(gm)G-H=(J)	78.65	85.32	73.72	60.22	66.42	63.59
Moisture content % (I/J)*100=K	24.55	19.78	25.38	27.57	30.01	33.90
Avg. Moisture Content % (L)	22.17		26.47		31.96	
Dry Density gm/cm^3 E/(100+L)*100	1.40		1.44		1.36	

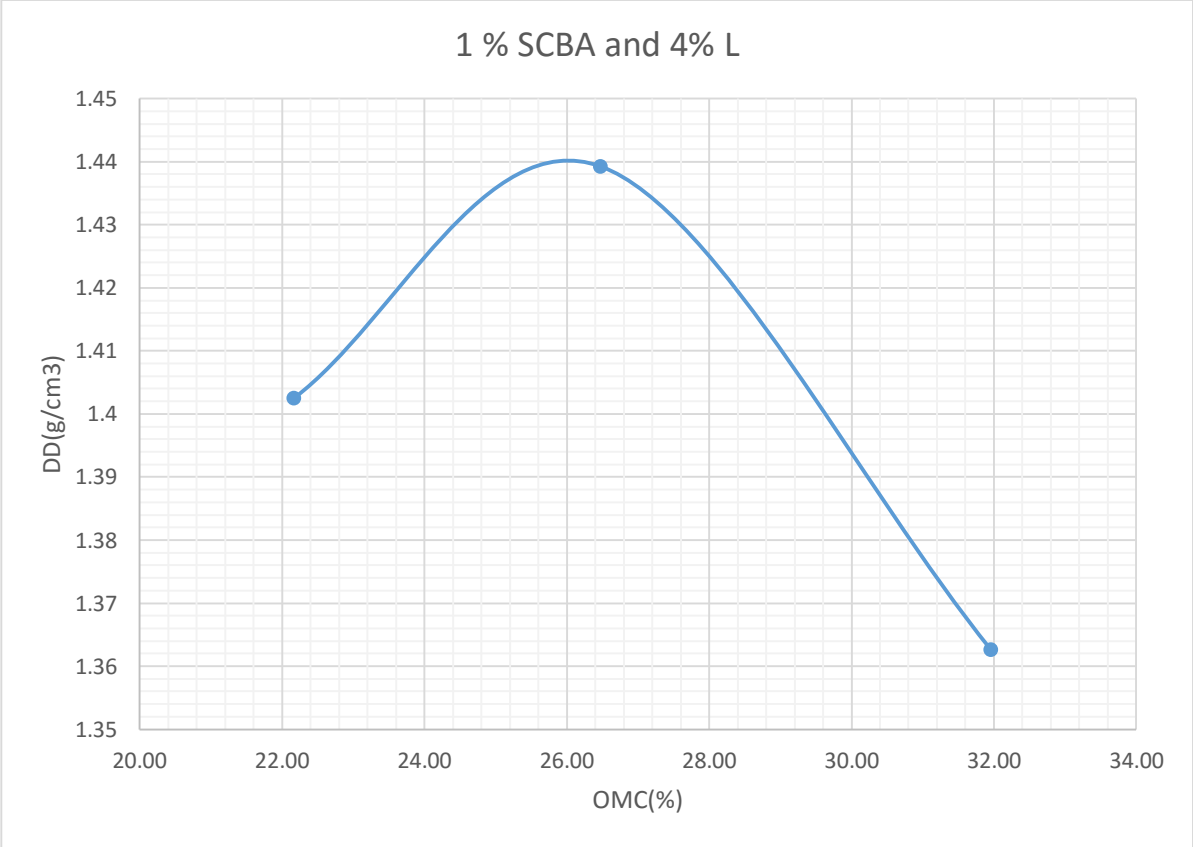

Test No.	1	2	3
Mass of sample (gm)	4200	4200	4200
Mass of Mold+Wet soil(gm)(A)	6055.12	6286	6142
Mass of Mold(gm)(B)	2719.8	2725.5	2719.8
Mass of Wet Soil(gm)A-B=C	3335.32	3560.5	3422.2
Volume of Mold cm^3(D)	2124	2124	2124
Bulk Density gm/cm^3 C/D=(E)	1.57	1.68	1.61

Container Code	p66	p62	c81	11	p67	2
Mass of Wet soil+Container(gm)(F)	115.36	120.22	109.68	94.44	104.75	102.33
Mass of dry soil+container(gm)(G)	95.05	101.34	89.97	76.84	83.82	80.77
Mass of container(gm)(H)	17.4	18.02	17.25	17.62	18.4	17.18
Mass of moisture(gm)F-G=(I)	20.31	18.88	19.71	17.6	20.93	21.56
Mass of Dry soil(gm)G-H=(J)	77.65	83.32	72.72	59.22	65.42	63.59
Moisture content % (I/J)*100=K	26.16	22.66	27.10	29.72	31.99	33.90
Avg. Moisture Content % (L)	24.41		28.41		32.95	
Dry Density gm/cm^3 E/(100+L)*100	1.26		1.31		1.21	

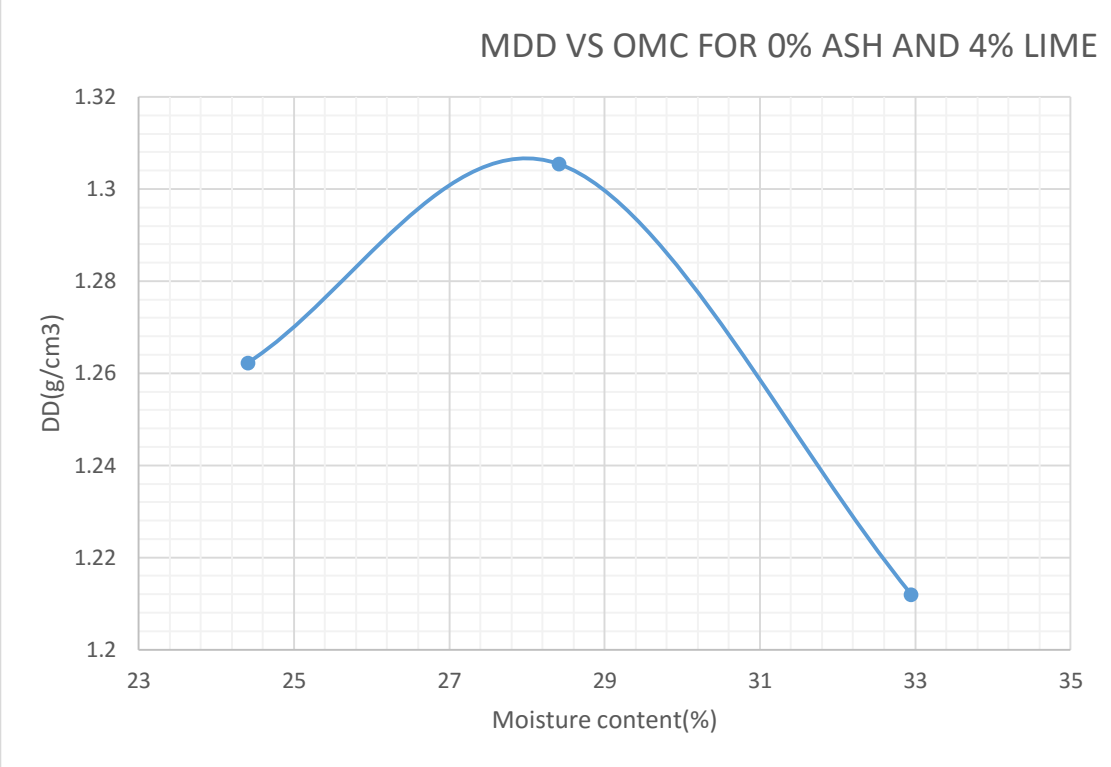
MDD VS OMC FOR 0% ASH AND 4% LIME
1.32
1.3
1.28
1.26
1.24
1.22
1.2
DD(g/cm3)
23
25
27
29
31
33
35
Moisture content(%)

3 CBR DETERMINATION FOR KK SOIL SAMPLE

BLOWS	LOAD (KN)		CBR(%)		DRY DENSITY Vs SOCKED CBR.			
	2.54mm	5.08mm	2.54mm	5.08mm				
10	0.19	0.22	1.44	1.10	**NO # OF BLOWS**	**65**	**30**	**10**
30	0.21	0.22	1.57	1.40	**DRY DENSITY**	1.360	1.338	1.310
65	0.250	0.35	1.87	1.74	**SOAKED CBR**	1.87	1.57	1.44

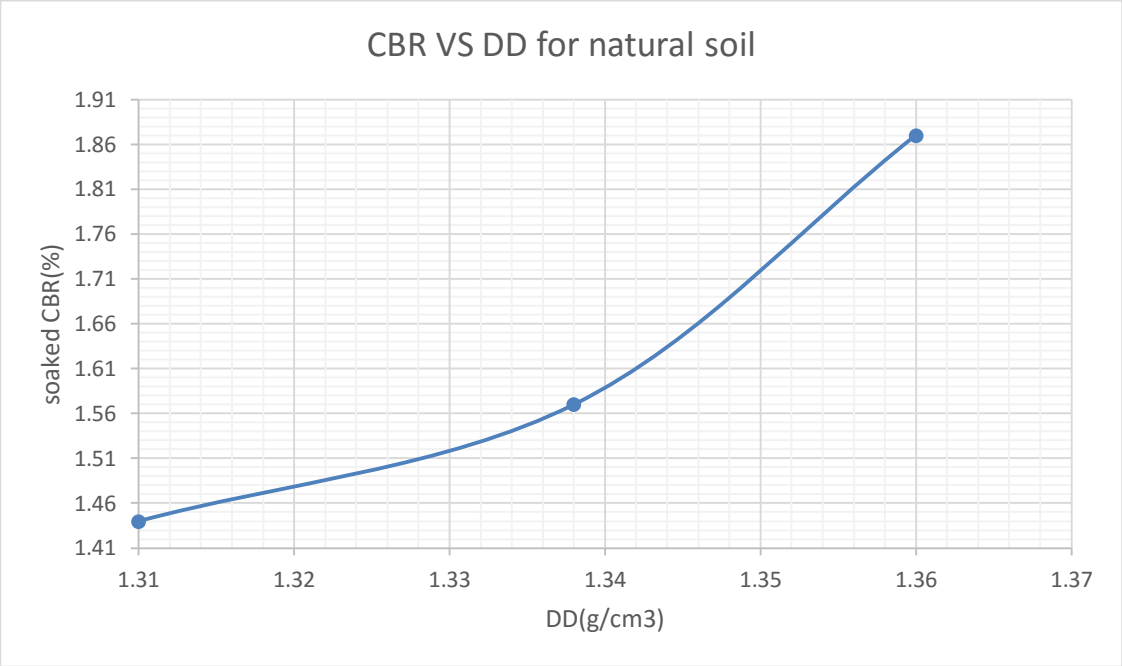

MDD (gm/cc) Proctor	1.41
95 % of MDD	1.33
C.B.R.at 95%of MDD	**1.58**

BLOWS	LOAD (KN)		CBR(%)		DRY DENSITY Vs SOCKED CBR.			
	2.54mm	5.08mm	2.54mm	5.08mm				
10	0.36	0.39	2.70	1.96	**No # OF BLOWS**	**65**	**30**	**10**
30	0.37	0.46	2.77	2.32	**DRY DENSITY**	1.340	1.308	1.230
65	0.40	0.49	2.98	2.43	**SOAKED C.B.R.**	2.98	2.77	2.32

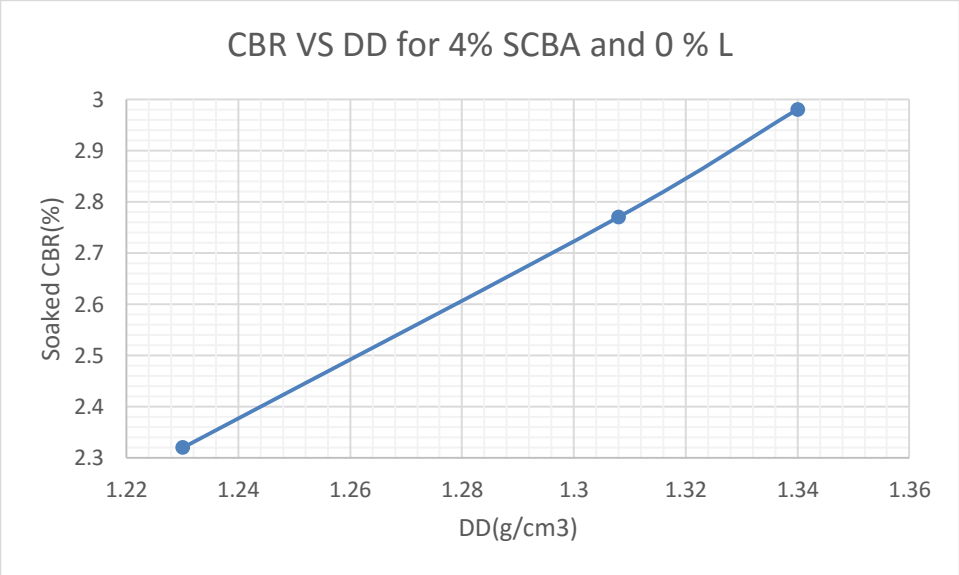

MDD (gm/cc) Proctor	1.39
95 % of MDD	1.32
C.B.R.at 95%of MDD	**2.78**

BLOWS	LOAD (KN)		CBR(%)		DRY DENSITY Vs SOCKED CBR.			
	2.54mm	5.08mm	2.54mm	5.08mm				
10	0.42	0.62	3.16	3.09	**No # OF BLOWS**	**65**	**30**	**10**
30	0.52	0.66	3.90	3.32	**DRY DENSITY**	1.313	1.278	1.210
65	0.55	0.79	4.12	3.97	**SOAKED C.B.R.**	4.12	3.90	3.16

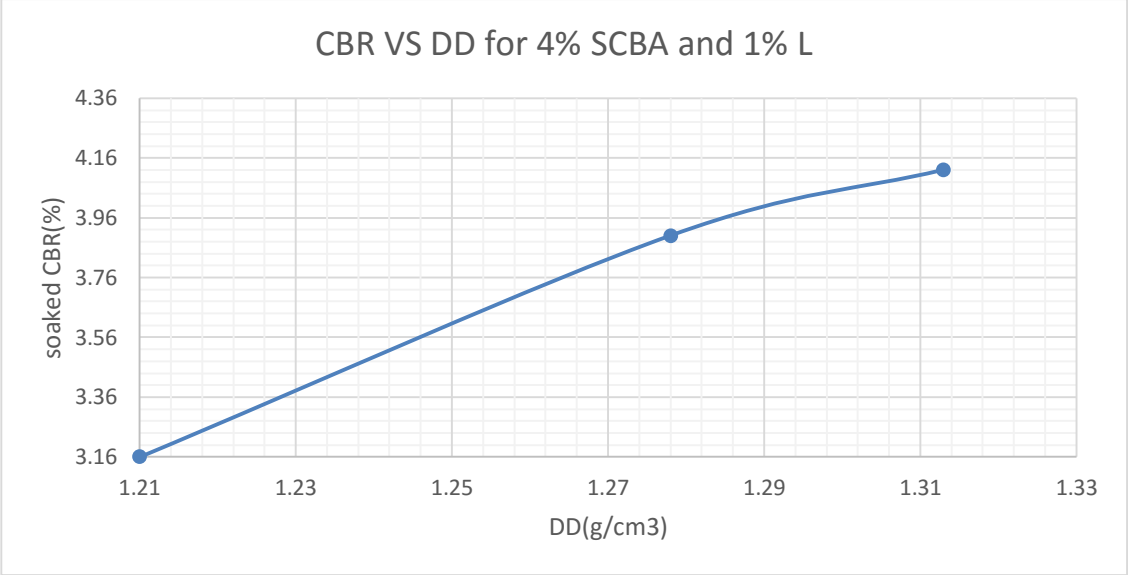

MDD (gm/cc) Proctor	1.31
95 % of MDD	1.24
C.B.R.at 95%of MDD	**3.82**

BLOWS	LOAD (KN)		CBR(%)		DRY DENSITY Vs SOCKED CBR.			
	2.54mm	5.08mm	2.54mm	5.08mm				
10	0.98	1.01	7.38	5.05	**No # OF BLOWS**	**65**	**30**	**10**
30	1.04	1.22	7.80	6.10	**DRY DENSITY**	1.291	1.254	1.193
65	1.08	1.25	8.13	6.24	**SOAKED C.B.R.**	8.13	7.80	7.38

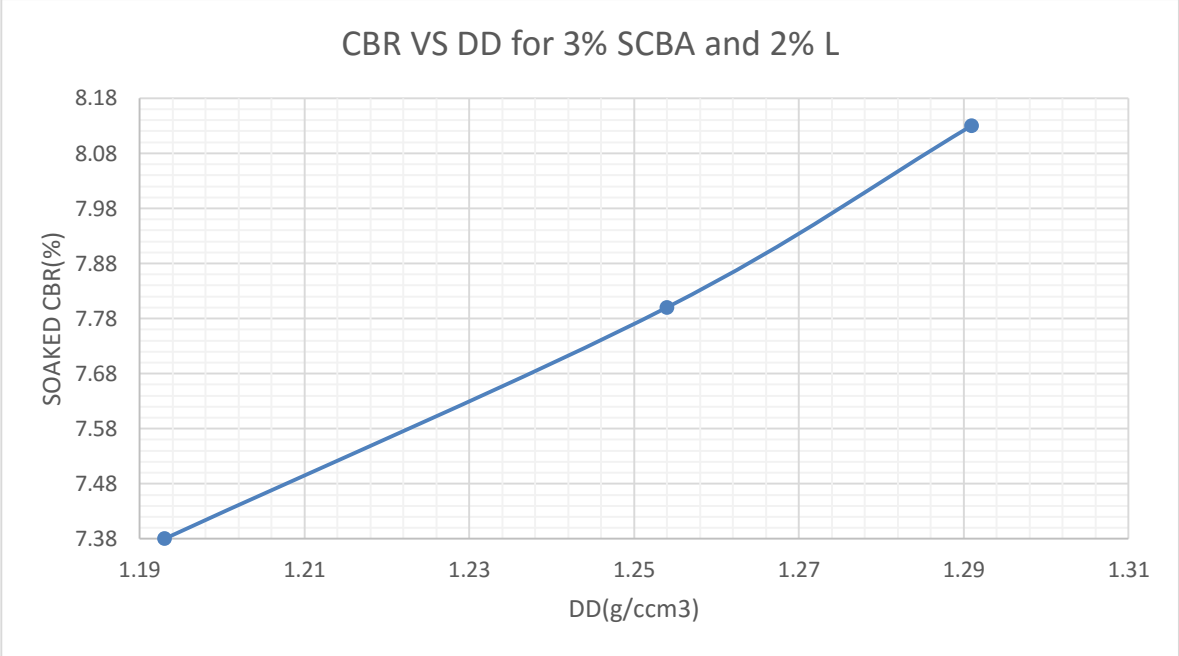

MDD (gm/cc) Proctor	1.39
95 % of MDD	1.33
C.B.R.at 95%of MDD	**7.79**

BLOWS	LOAD (KN)		CBR(%)		DRY DENSITY Vs SOCKED CBR.			
	2.54mm	5.08mm	2.54mm	5.08mm				
10	1.10	1.32	8.25	6.60	**No # OF BLOWS**	**65**	**30**	**10**
30	1.12	1.44	8.40	7.20	**DRY DENSITY**	1.18	1.11	1.09
65	1.20	1.59	8.97	7.95	**SOAKED C.B.R.**	10.08	9.15	8.10

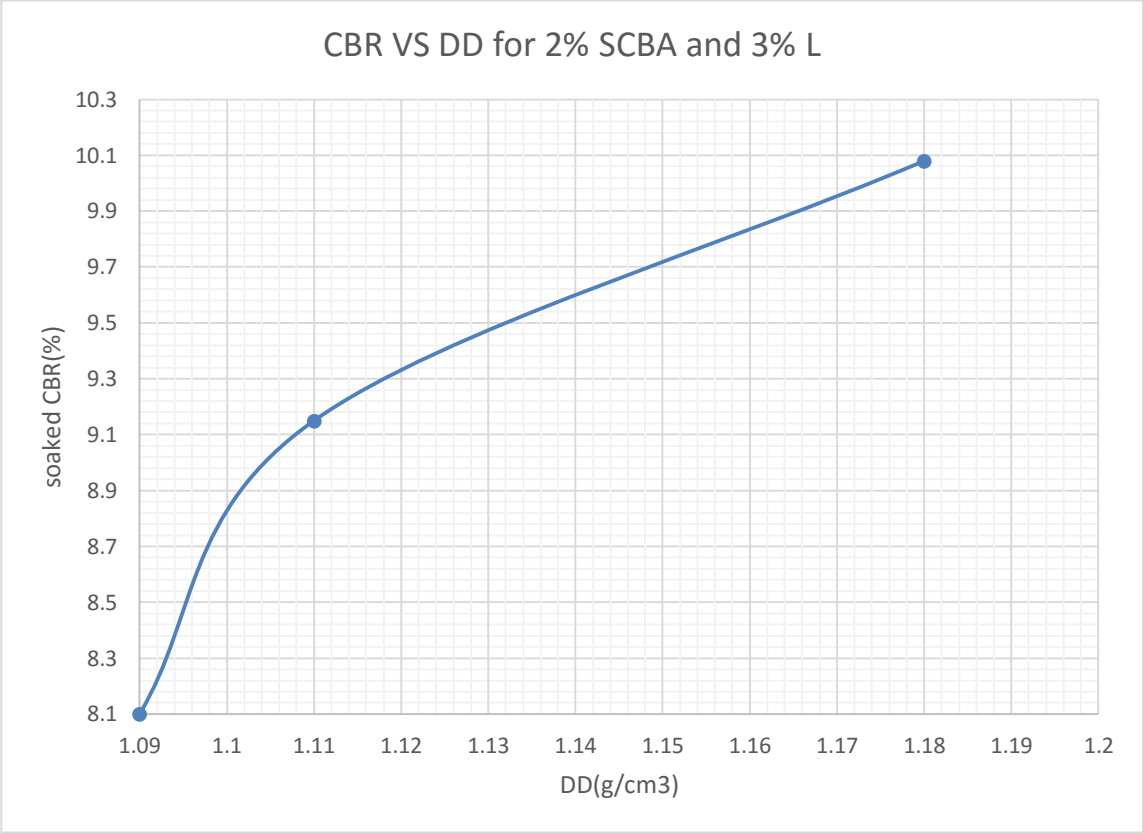

MDD (gm/cc) Proctor	1.36
95 % of MDD	1.29
C.B.R.at 95%of MDD	**9 .35**

BLOWS	LOAD (KN)		CBR(%)		DRY DENSITY Vs SOCKED CBR.			
	2.54mm	5.08mm	2.54mm	5.08mm				
10	1.30	1.79	9.72	8.94	**No # OF BLOWS**	**65**	**30**	**10**
30	1.35	1.84	10.10	9.22	**DRY DENSITY**	1.284	1.213	1.171
65	1.55	2	11.59	10	**SOAKED C.B.R.**	11.59	10.10	9.72

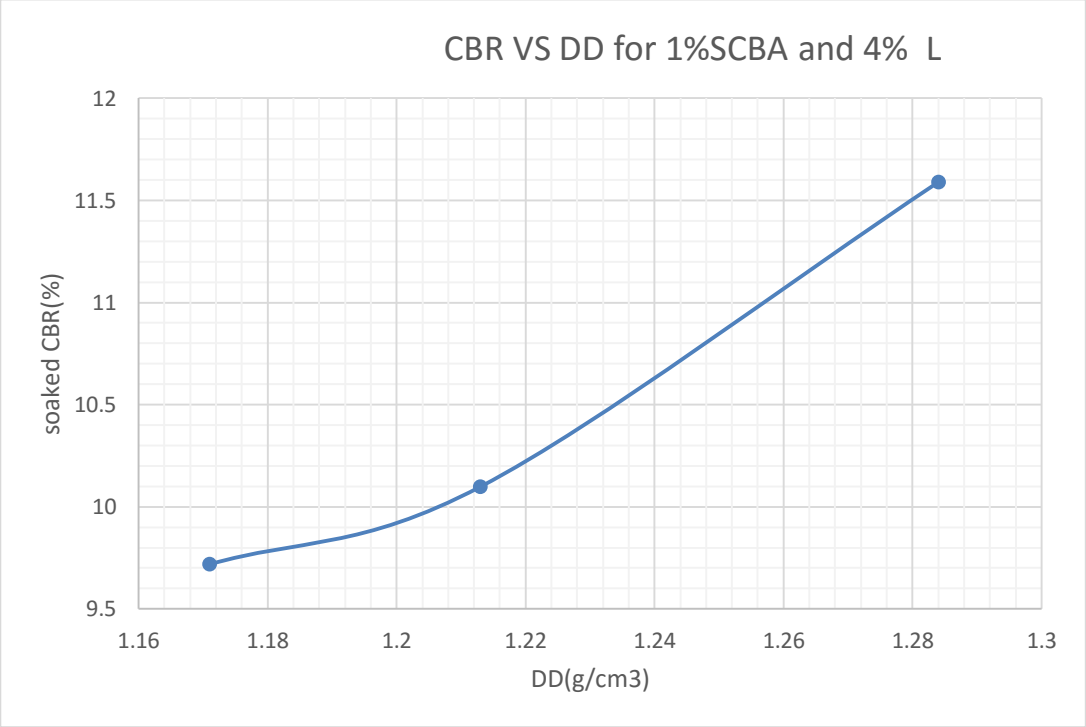

MDD (gm/cc) Proctor	1.38
95 % of MDD	1.31
C.B.R.at 95%of MDD	**10.4**

APENDEIX C

SIMULATION RESULT

Visualization of Different Responses from FEM

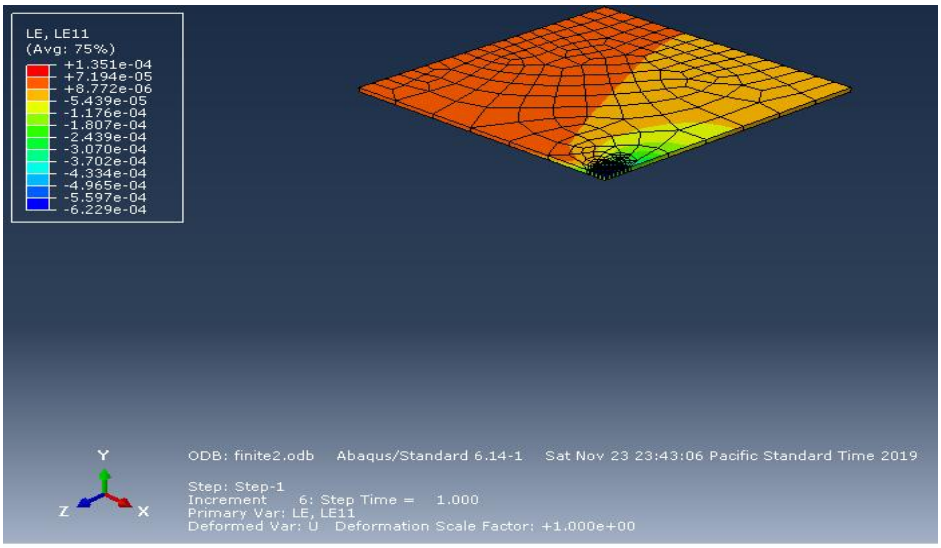

Figure C.1 Horizontal tensile strain visualization from finite element analysis with treatment of subgrade

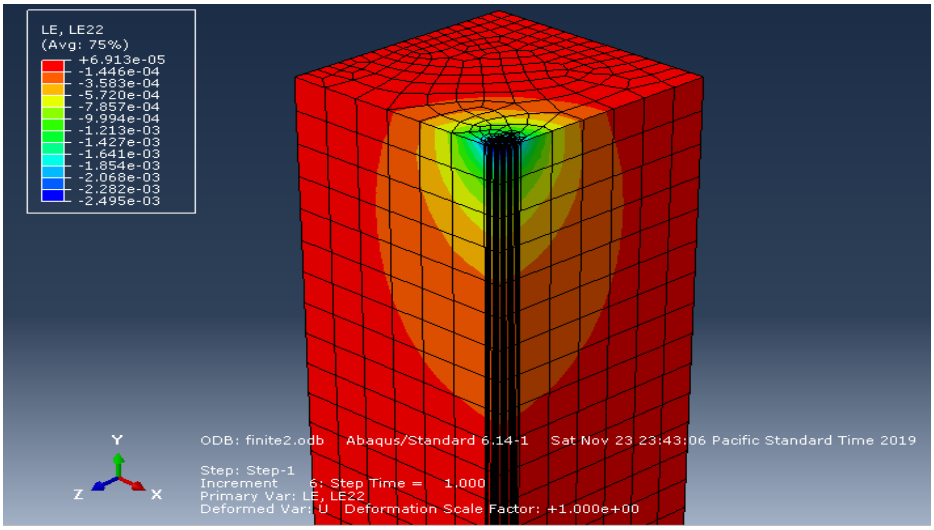

Figure C. 2 Vertical compressive strain visualization from finite element analysis. With treatment of subgrade

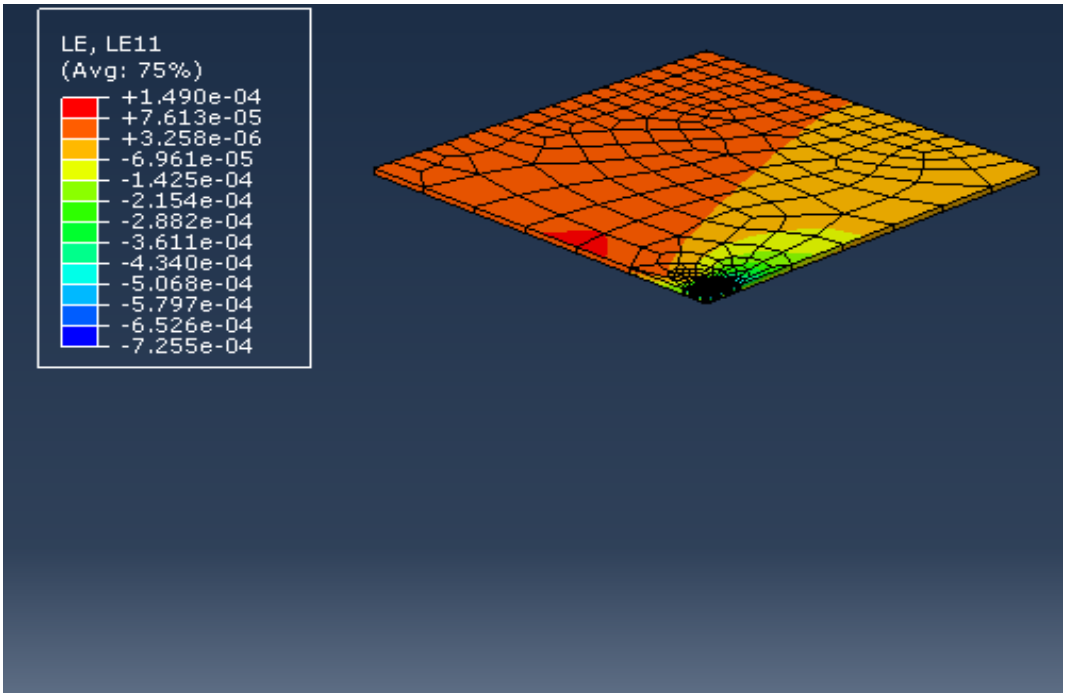

Figure C. 3 Horizontal tensile strain visualization from finite element analysis. Without treatment of subgrade

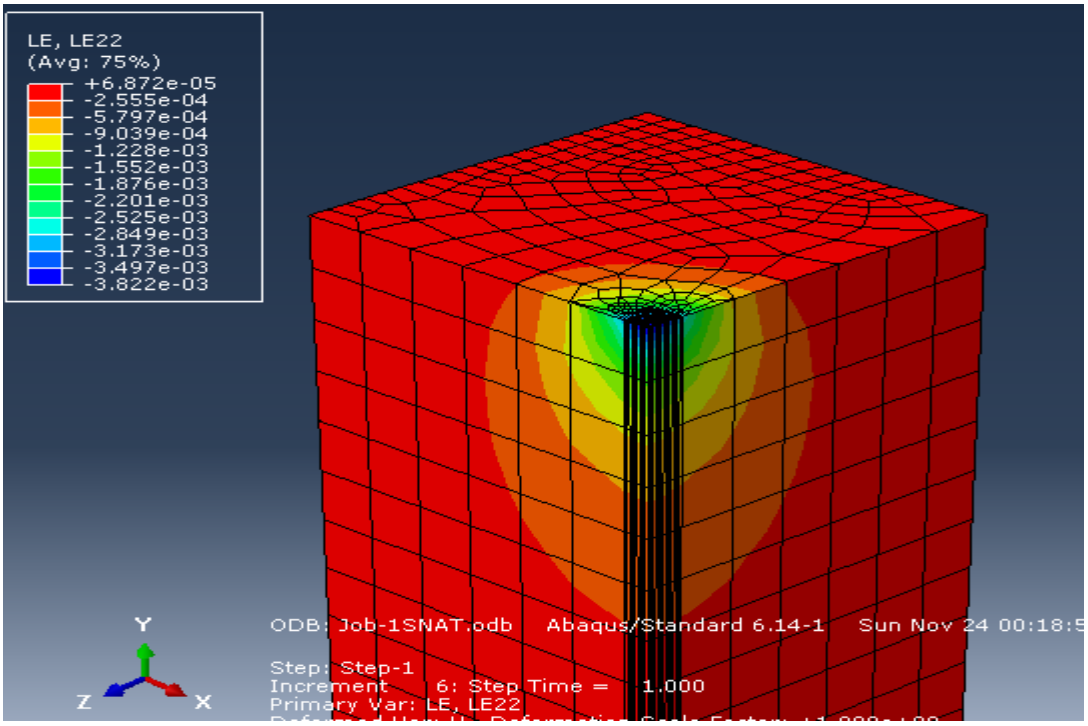

Figure C. 4 Vertical compressive strain visualization from finite element analysis. Without treatment of subgrade

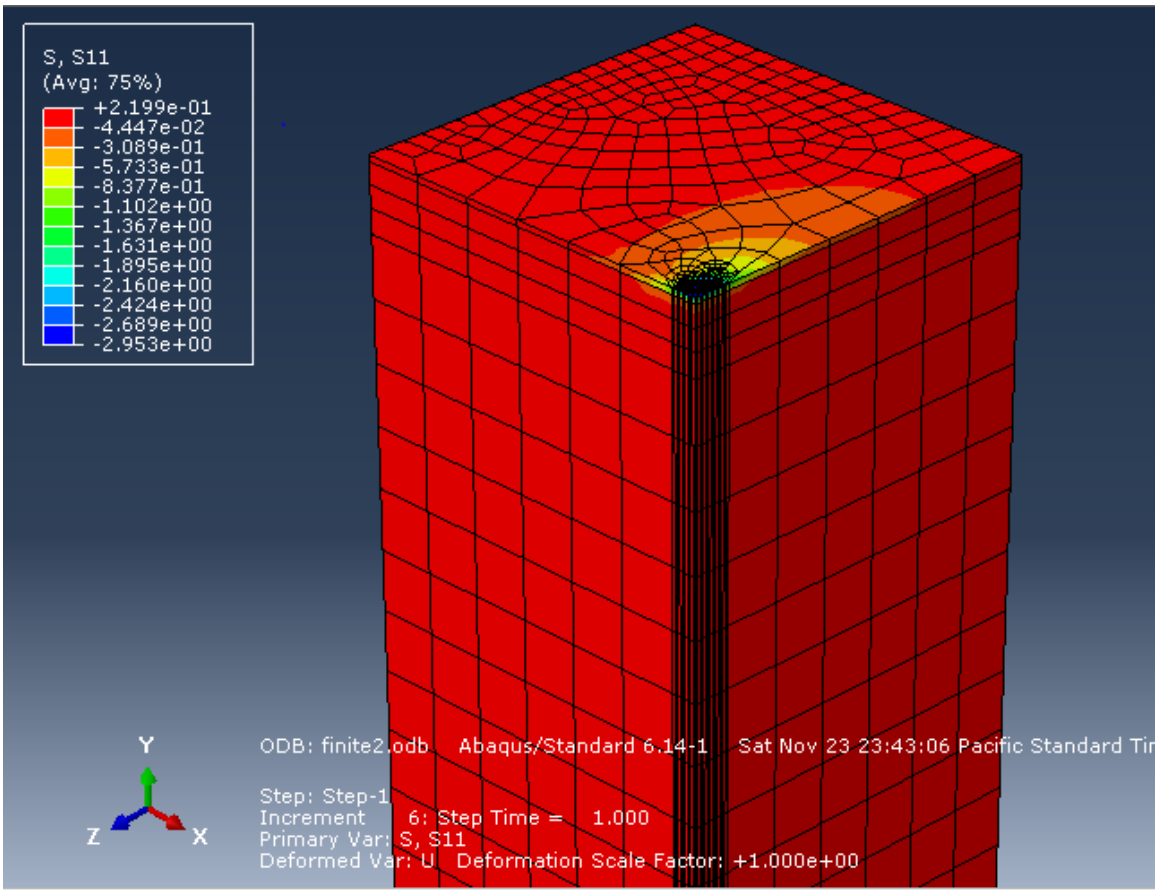

Fig C 5. Contour plot for horizontal stress with treatment of subgrade

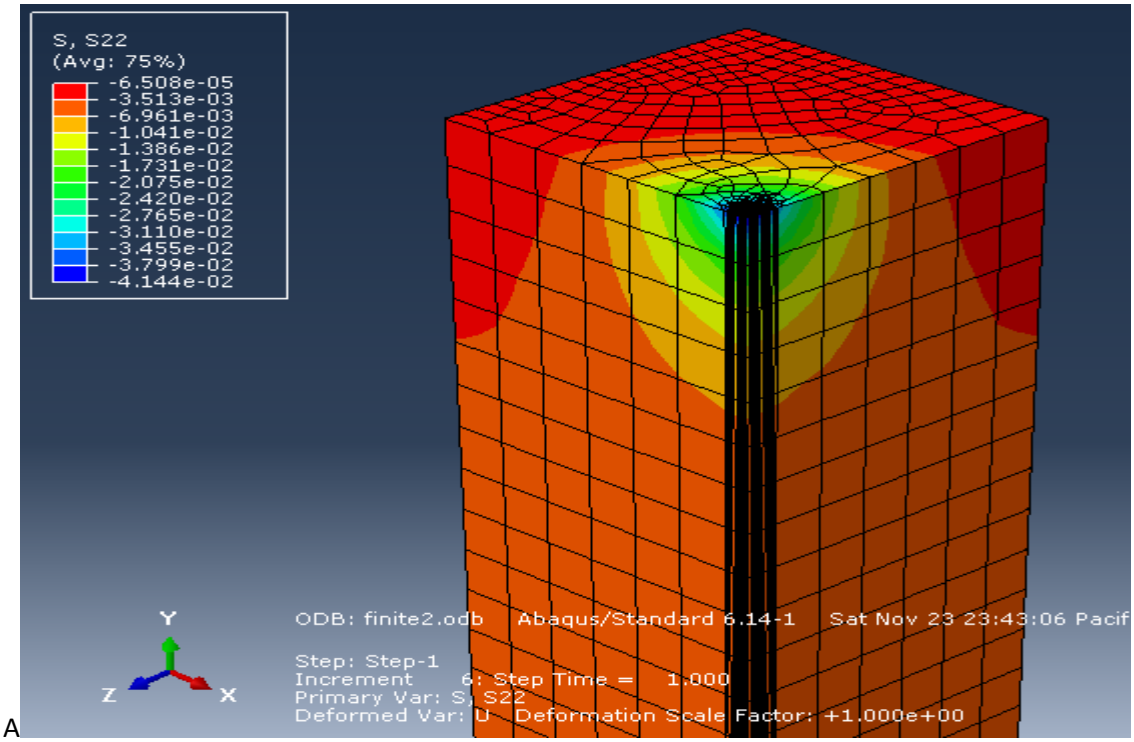

A

Fig C6. Contour plot for vertical compressive stress with treatment of subgrade

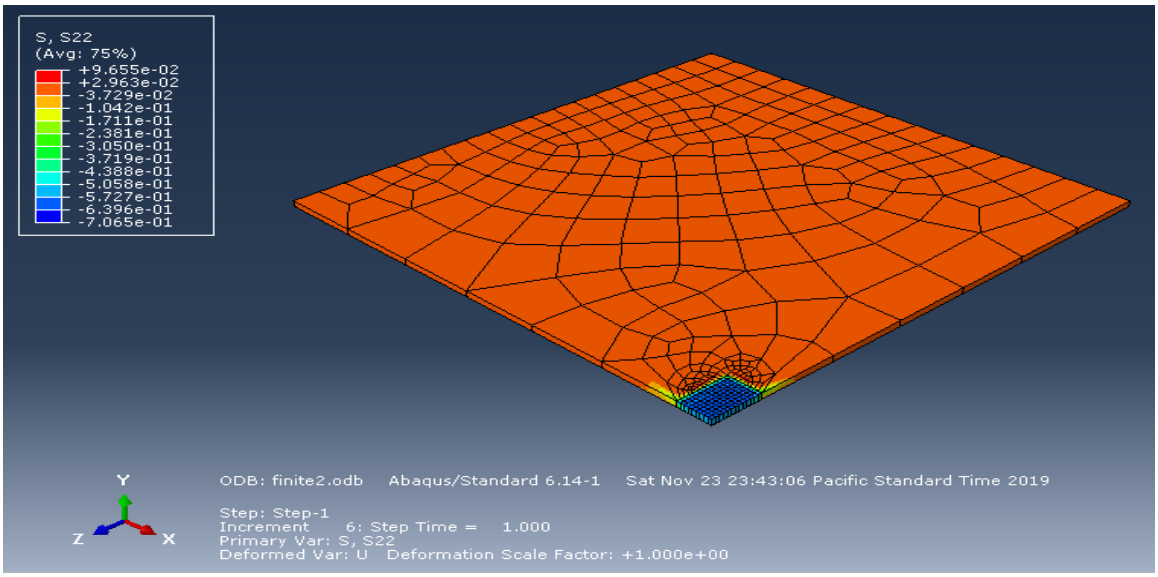

Fig C7. Contour plot for vertical compressive stress with treatment of subgrade

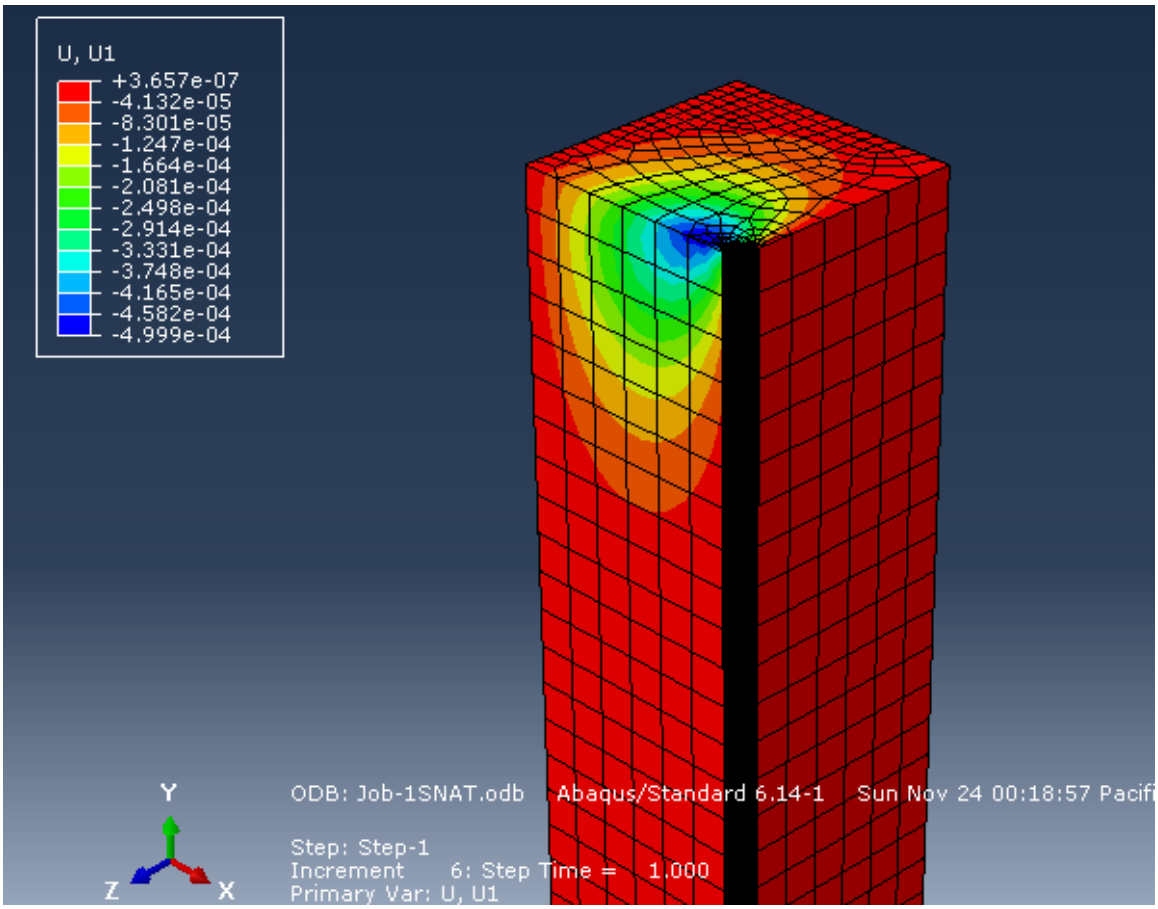

Figure C8. Horizontal displacement contour plot without treatment of subgrade

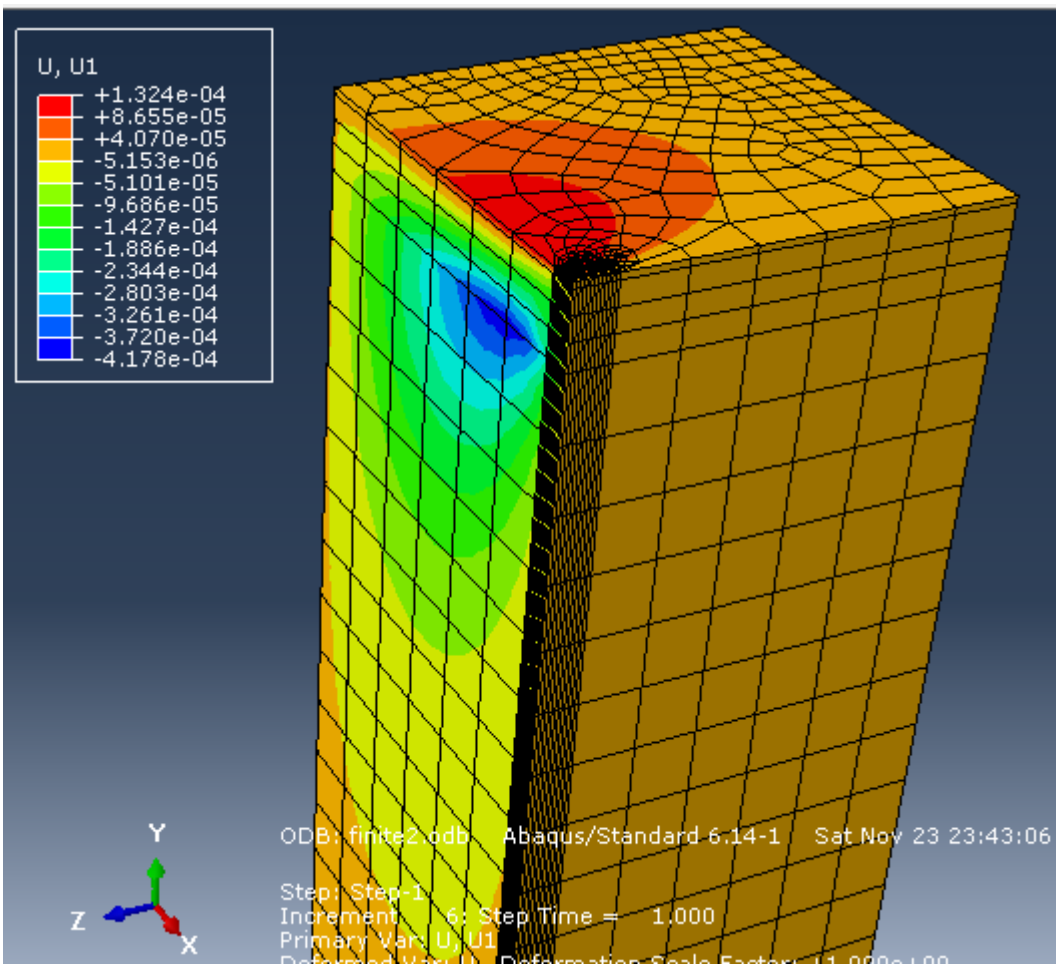

Figure C9. Horizontal displacement contour plot with treatment of subgrade

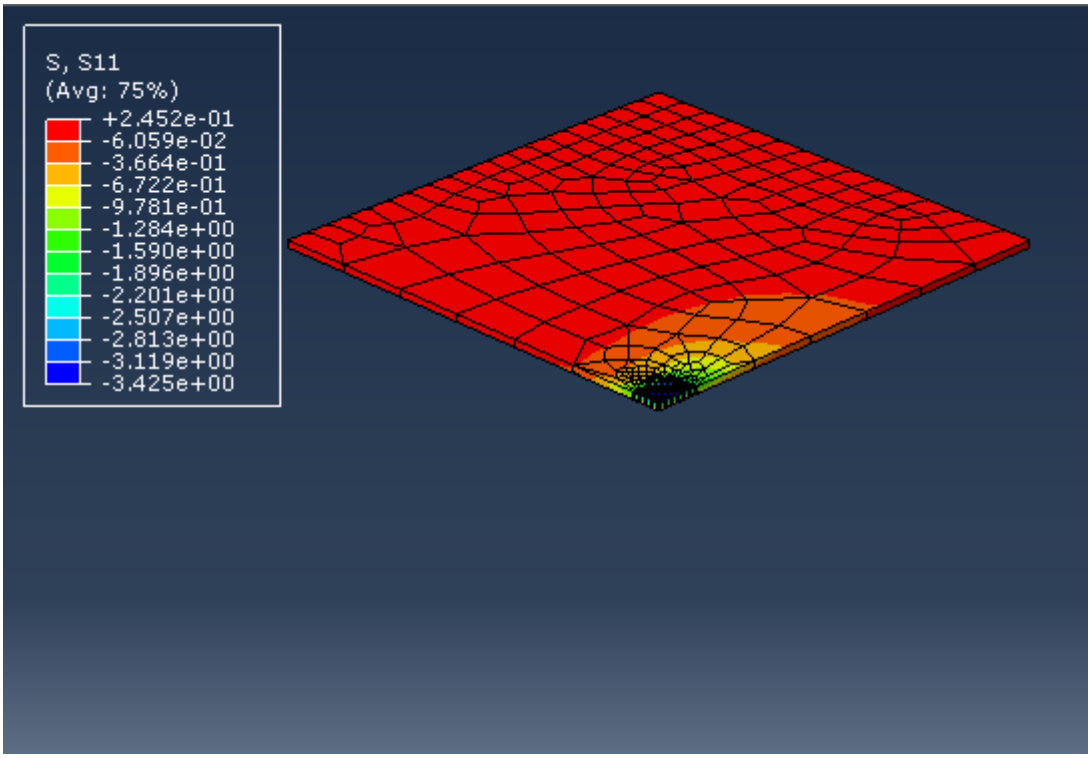

Figure C10. Contour plot for horizontal stress at the bottom of HMA layer without subgrade treatment.

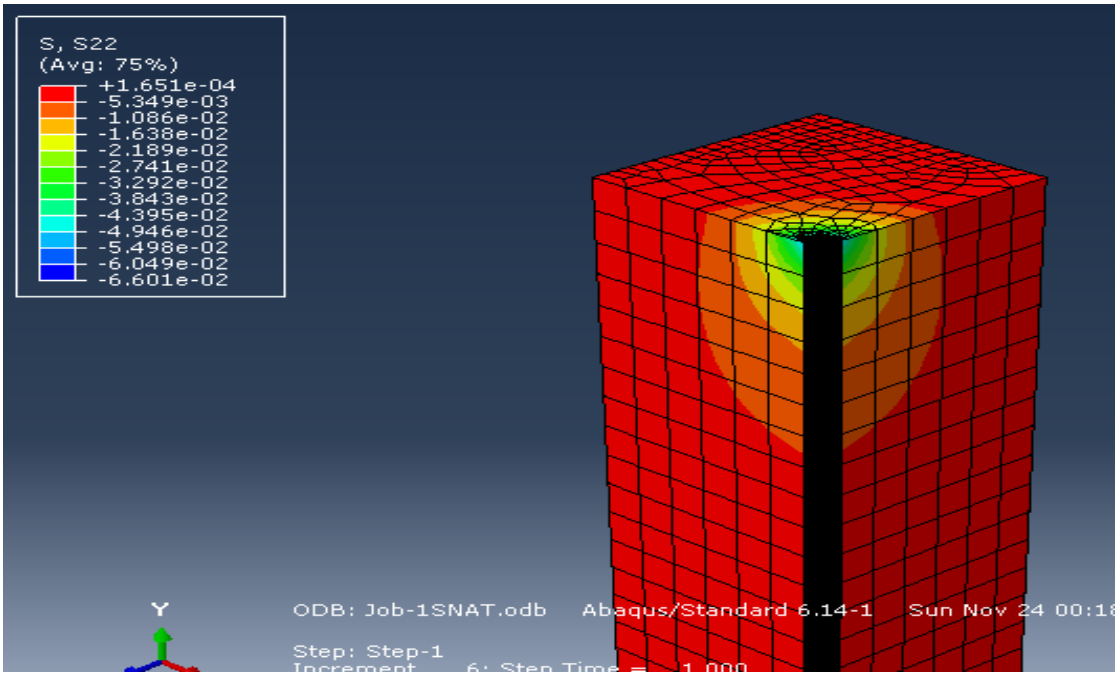

Figure C11. contour float for vertical stress at the top of subgrade layer without subgrade treatment.